EXPERIMENTAL AND MODELLING STUDY OF A GEODESIC DOME SOLAR GREENHOUSE SYSTEM IN OTTAWA

by

Paula A. Claudino, B.Eng. & Mgmt., Mechanical Engineering and Management

McMaster University, 2006

A thesis submitted to the

Faculty of Graduate and Postdoctoral Affairs

in partial fulfillment of the requirements for the degree of

Master of Applied Science in Sustainable Energy Engineering and Policy

Department of Mechanical and Aerospace Engineering

Carleton University

Ottawa, Ontario

January, 2016

Abstract

A building model was created in TRNSYS 17 to determine whether appropriate growing conditions can be maintained in a geodesic dome greenhouse in Ottawa, Canada, without the use of auxiliary power or heating. A microcontroller, the Arduino UNO, is used as the data collection device. In order to test the effects of ventilation, thermal mass, and solar panel shading on both the modelled and the measured results, combinations of these variables were used to create five operating scenarios. The model was calibrated and run under each of these scenarios, using actual 2015 weather data, and was also run for a full year using the CWEC weather data to compare the performance of each scenario for a typical weather year. The results indicate that air temperatures are expected to exceed acceptable ranges during a typical weather year, which indicates that further efforts will be required to heat and cool the Biodome.

Acknowledgements

This thesis would not have been possible without the help of many dedicated volunteers from the Brewer Park Community Garden. Thank you to everyone who helped to plan, build, and maintain the Biodome. I look forward to continuing to work with you on this project, even after my thesis is complete.

Thank you to my supervisor, Professor Cynthia Cruickshank, for her patience and support during several false starts, delays, and bursts of work over the course of this thesis. Her understanding and eternally positive attitude made all the difference in the world.

Thank you to Professor David Mears in the Department of Plant Biology and Pathology at Rutgers School of Environmental and Biological Sciences, who provided a wealth of research materials as well as much appreciated advice on how to heat a greenhouse in a northern climate.

Finally, thank you to my family for their on-going support, especially my husband, Stéphane Gagnon, who helped me tremendously, especially when I was trying to learn how to use the Arduino and set up the data acquisition system. I could not have done this work without his encouragement.

Table of Contents

List of Tables

List of Figures

List of Symbols

A	surface area, m^2
N	number of air changes per hour, h^{-1}
q_c	conduction, W
q_i	infiltration, W
q_t	total peak heating requirements, W
r	sample correlation coefficient
r^2	Pearson coefficient of determination
T_A	temperature of the device, or the cold-junction, ^oC
t_i	inside temperature, ^oC
t_o	outside temperature, ^oC
T_R	temperature of the remote thermocouple junction, or hot-junction, ^oC
U	overall heat loss coefficient, $W/(m^2 K)$
V	greenhouse internal volume, m^3
v	geodesic dome frequency
V_{OUT}	thermocouple output voltage, µV
X	greenhouse floor area, m^2
x_1	deviation of observed data from the sample means
x_2	deviation of the simulated data from the sample means
Y_r	heat capacity of rock storage, $kJ/^oC$
Y_w	volume of water storage, kL

List of Abbreviations

ASABE	American Society of Agricultural and Biological Engineers
BPCG	Brewer Park Community Garden
IC	Integrated circuit
CO_2	Carbon dioxide
CWEC	Canadian weather for energy calculations
EAHE	Earth-to-air heat exchanger
EPS	Expanded polystyrene
PCSS	Polycarbonate structured sheet

List of Appendices

Chapter 1

Introduction

1.1 Background

There is increased interest in locally-grown food in Canada, and specifically in Ontario, as evidenced by the passage of the Ontario Local Food Act (Bill C-36, 2013). The purpose of this legislation, the first of its kind in Canada, is to promote local food awareness and increase sales of Ontario produce by setting local food goals and targets. An Ipsos-Reid survey (2006) found that Canadians believe the benefits of buying locally-grown produce include:

- Help their local economy (71%)
- Support family farmers (70%)
- Taste better (53%)
- Are Cheaper (50%)
- Not genetically modified (48%)
- Healthier (46%)
- No chemical / Synthetic pesticides (45%)
- Safer (44%)
- Environmentally friendly (43%)

The increased interest in locally grown food is also evident from the growing number of community gardens, which are enjoying increased popularity in many Canadian urban centres, such as Montreal, Ottawa, Toronto, and Vancouver.

In 2006, Vancouver City Council issued a community challenge to “create 2010

new garden plots by 2010, as an Olympic legacy" (Reichel, 2012). This challenge was exceeded by the beginning of 2010 (Reichel, 2012) and was replaced by the mayor's goal to reach 5000 garden plots in the City of Vancouver by 2020, as part of Vancouver's Greenest City Action Plan (Vancouver, 2012).

This increased interest in community gardening is also being seen in Ottawa, Ontario, where, according to the Ottawa Deputy City Manager's report (Ottawa, 2009), "each year, interest in and demand for community gardens increase, influenced by rising food costs and gas prices, concerns about food security, interest in growing and eating locally-produced food, urban greening projects and urban agriculture." As of July 2015, the city of Ottawa had 48 community gardens, including one city-run allotment garden (Just Food, 2015), an increase of 153 percent from 2008, when there were 19 community gardens in Ottawa (Ottawa, 2009).

In more temperate climates, such as that of Vancouver, some community gardens are maintained year-round (Reichel, 2012) but in Ottawa, community gardens are typically open for only six months a year, from mid-May to mid-October, as the temperature is prohibitively low for gardening during the remainder of the year. In order to extend the growing season, some community garden organizations have started to construct community greenhouse gardens.

For example, the Banff Greenhouse Gardening Society (BGGS) operates two community greenhouses in Banff, Alberta. The first greenhouse, built in 2011, is 6.1 m by 14.6 m and houses 34 individual 1.5 m^2 plots. The second greenhouse, built in 2013, is 6.1 m by 9.1 m and houses 20 individual 1.4 m^2 plots (BGGS, 2013).

Greenhouses allow farmers and gardeners to extend the growing season by providing a controlled growing space, leading to increased yields due to the longer growing season, optimized growing conditions, and the ability to grow plants that would otherwise not survive in a given climate. One of the trade-offs, however, is that greenhouses can be more energy intensive than other forms of agriculture, especially if energy is required to ventilate or heat the space and if supplemental lighting is provided.

According to Statistics Canada (2015), the total area of fruit and vegetable greenhouses in Canada has increased steadily over the past five years, increasing by over 1.7 km^2 or 14.7 percent between 2010 and 2015. Similarly, in Ontario the total area of vegetable greenhouses increased by 20.8 percent between 2010 and 2015, increasing from 7.8 km^2 in 2010 to 9.4 km^2 in 2015 (Statistics Canada, 2015). This trend in increased greenhouse area in Canada is illustrated in Figure 1.

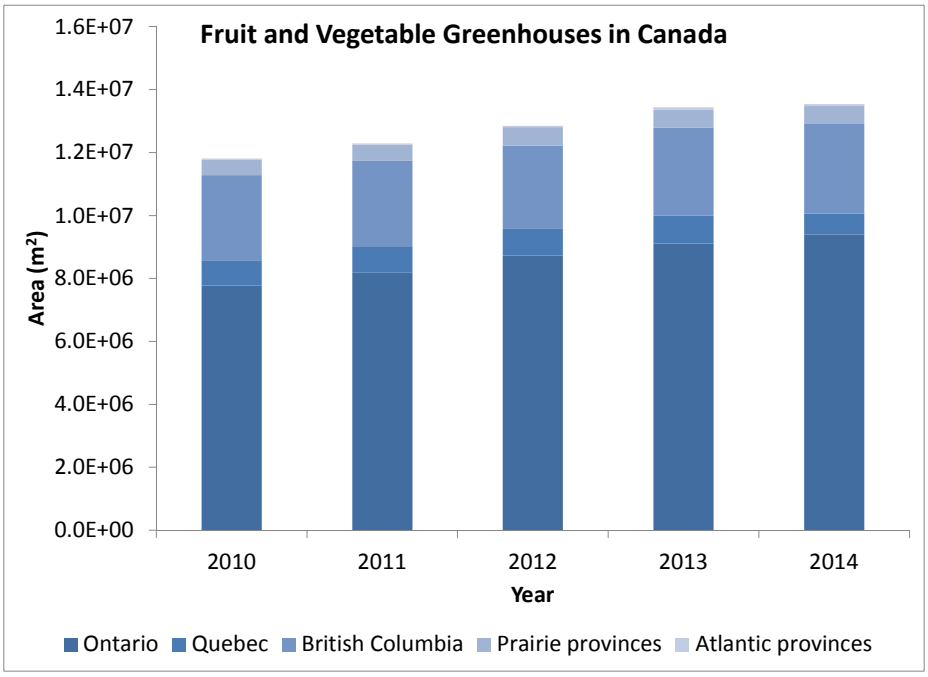

Figure 1: Area of fruit and vegetable greenhouses in Canada, by Province from 2010 to 2015. (Statistics Canada. CANSIM Table 001-0047)

Greenhouses are also being considered in more and more extreme environments, such as in Canada's far north. In August 2014, Prime Minister Stephen Harper announced measures to promote northern agriculture, including the launch of the Northern Greenhouse Initiative, aimed at "advancing the commercialization and enhancing the productivity of greenhouse projects across Canada's North" (Prime Minister of Canada Stephen Harper, 2014). The construction of commercial or community greenhouses in the north would contribute to improved health of the local population due to the increased availability of better quality food, increased food security, and to science education and skills training (Exner-Pirot, 2012).

One of the challenges for community greenhouses, especially in cold climates, is the availability of and access to supplementary energy that is typically necessary to maintain year-round operation. A greenhouse design that is able to minimize or eliminate the need for supplementary energy would greatly contribute to the potential for the successful implantation of greenhouse operations in northern community gardens.

In addition to providing the conditions necessary to grow plants, greenhouses can also be used to grow animal protein, in the form of fish. The combination of hydroponics (the cultivation of plants in nutrient-rich water instead of soil) and aquaculture (raising aquatic animals in tanks) has been termed Aquaponics (Diver, 2006). Some of the benefits of including an Aquaponics system in a greenhouse are that the water tanks act as thermal energy storage for the greenhouse and the fish can provide more CO_2 for the plants. The greenhouse also acts as a passive solar collector, reducing the amount of additional energy needed for heat.

1.2 Brewer Park Community Garden Biodome Project

Brewer Park Community Garden (BPCG) is a registered non-profit organization that operates a community garden located in Brewer Park, in the area of Old Ottawa South, in Ottawa, Ontario. Membership in BPCG is open to people who live, work, or study in Old Ottawa South and neighbouring areas. The garden is currently composed of some 50 raised garden beds that are used by members to grow food.

One of the goals of the BPCG is to contribute to local food security and community development (BPCG, 2013). As such, one of the key projects undertaken by BPGC beginning in 2013 was the design, construction, and operation of a geodesic dome-shaped community garden greenhouse, referred to hereafter as the Biodome. The purpose of the Biodome is to showcase different growing methods and support member-driven educational projects that benefit the Garden's members and the local community. The Biodome is located on the same site as the community garden, as shown in Figure 2 and Figure 3.

The Biodome is located in Brewer Park, a municipal park in Ottawa, Ontario, Canada, across from Carleton University. Located at 45°N, 75°W, Ottawa has a humid continental, or Dfb classification, climate according to the widely used Köppen-Geiger climate classification system (Rubel, 2010). The temperature in Ottawa can range from an extreme minimum of -38.9°C in winter to an extreme maximum of 37.8°C in summer (Environment Canada, 2015). These wide temperature swings make it exceptionally challenging to maintain a consistent internal operating temperature, with both heating and cooling being required throughout the year.

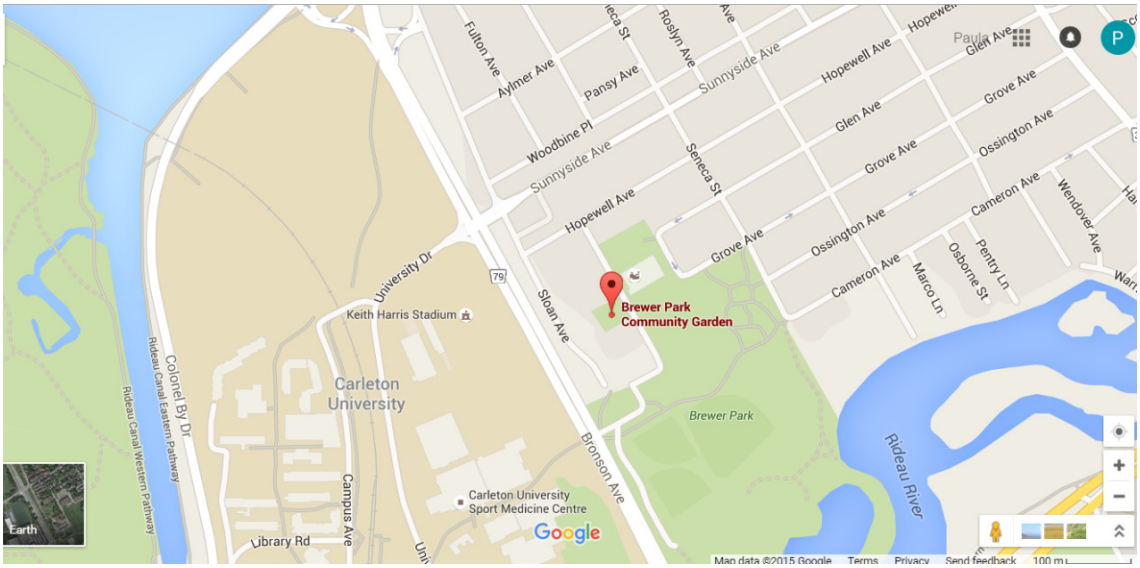

Figure 2: Map of location of BPCG in Ottawa (Google maps, 2015)

Figure 3: Aerial view of Biodome (Google maps, 2015b)

It is the hope of those involved in this project that if the prototype proves successful, it could result in the construction of other dome greenhouses, providing local food and creating green jobs for those that build these greenhouses. An aquaponics

system is planned for the Biodome, but this study will not focus on the design or operation of the aquaponics system, other than the temperature of the tanks and their use as thermal energy storage.

Planning for this project began in 2011 and the goal was to build the Biodome in 2013, but construction was delayed by planning and permitting issues. The author of this thesis joined the Biodome team in March 2013, in the role of Energy Lead, and provided guidance and support during the design, public consultation, construction, and implementation phases of this project. Construction began in April 2014 and the Biodome's grand-opening was held on August 17, 2014.

The Biodome received funding from the following organizations:

- The City of Ottawa Better Neighbourhoods Program;
- TD Friends of the Environment Foundation; and
- Just Food and the Community Garden Network.

The Biodome was built by Future Food Bio-dome Systems; the Ottawa architecture firm, Christopher Simmonds Architect Inc., created architectural drawings for the building and provided guidance in applying for building permits; structural engineering services were provided by Cleland Jardine Engineering Ltd.; and geotechnical engineering services, including soil bearing and frost protection analysis, were provided by Peterson Group Consulting Engineers. Project management and on-going operations are provided by a group of volunteers composed of local community members.

As the Biodome is located in a municipal public park and is in a floodplain, there were certain restrictions to the design of the structure, including the following:

- No excavation of the site, beyond the removal of the sod and top layer of soil;
- No installation of any permanent structure, including a building foundation;
- No electricity grid connection;
- All mechanical and electrical equipment must be installed above 59.63 m geodetic elevation, or 1.63 m above grade, in accordance with flood safety standards; and
- No open flames or the use of any kind of heating fuel.

During a public consultation that was held on June 2, 2013, local members of the community also expressed their concerns regarding the private use of public space, adequate public consultation, and building accessibility. There were no objections to the preferred location and strong support for a larger dome, measuring approximately 26 ft (7.9 m) in diameter, versus the sizes that were initially considered, which were 22 ft to 24 ft (6.7 m to 7.3 m) in diameter.

During the early stages of this project, many different dome frequency and size options were considered, including the three dome variations shown in Figure 4, which are, from left to right: 3v, 4/9 dome with a base wall height of approximately 0.9 m; 4v half dome, with a base wall height of approximately 0.6 m; and a 4v, 4/12 dome, with a base wall height between 0.96 m and 1.07 m. An explanation of dome frequency is given in Section 2.3. Drawings of each of these options were created by the author of this thesis in order to facilitate the selection of the most appropriate design by the Biodome team.

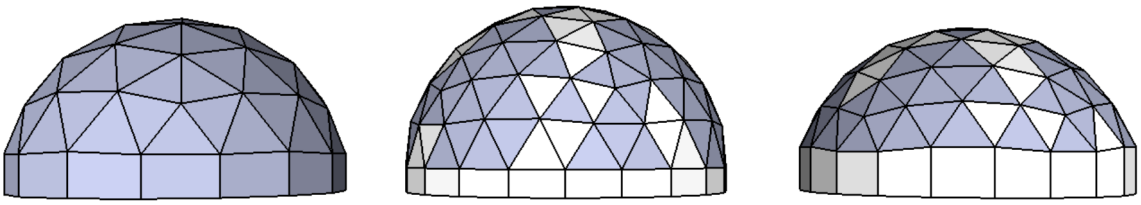

3v 4/9 4v 6/12 (half) 4v 4/12

Figure 4: Three different geodesic dome shapes that were considered.

Ultimately, the shape on the far left in Figure 4, the 3v 4/9 dome, was chosen because it provided the least variation in base wall height, and the best balance of base wall height to overall dome height.

Accessibility was also a major consideration, so the Biodome was designed to comply with the requirements for barrier-free design. All walkways are designed to have a minimum width of 3'7" (1.09 m), as shown in Figure 5, and the curbs in front of the Biodome were cut to accommodate accessible entry from the roadway via a ramp.

In order to comply with the restrictions listed earlier, the Biodome is designed as a demountable structure, which can be disassembled and removed, should the need arise. In place of a foundation to which to anchor the structure to the ground, the weight of the soil in the interior and exterior plant beds on "dead men anchors" and the weight of the structure itself were deemed to provide sufficient uplift resistance. The dead men anchors are 4" by 4" (0.1 m by 0.1 m) hemlock beams passing through the main walls and connecting the inner and outer walls.

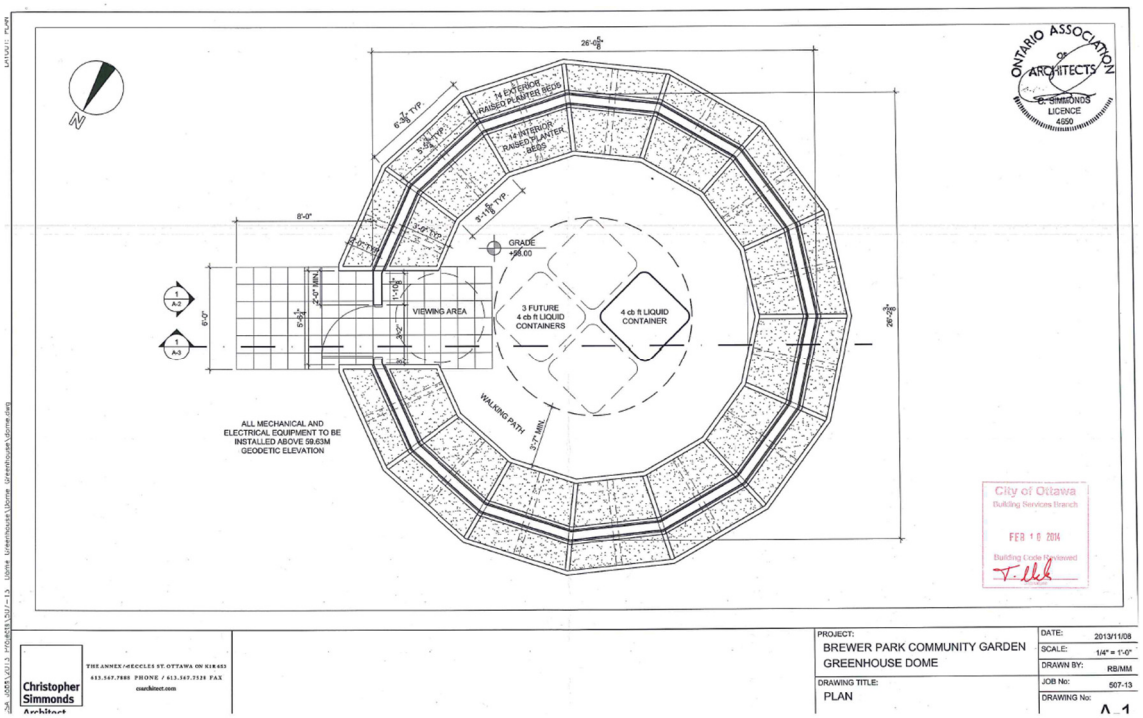

Figure 5: Architectural drawing of proposed Biodome layout (Christopher Simmonds Architect Inc., 2014). Adapted with permission.

Several locations within Brewer Park were considered, but ultimately the specific location for the Biodome was chosen in order to fulfill the following criteria, which were recommended by the author of this thesis:

- Minimal overhead shading from nearby structures and trees;
- Accessibility from the road (Brewer Way);
- Proximity to the rest of the community garden; and
- Proximity to outdoor lighting to reduce the potential for graffiti.

The final location of the Biodome, in relation to surrounding roads and buildings, is shown in Figure 6.

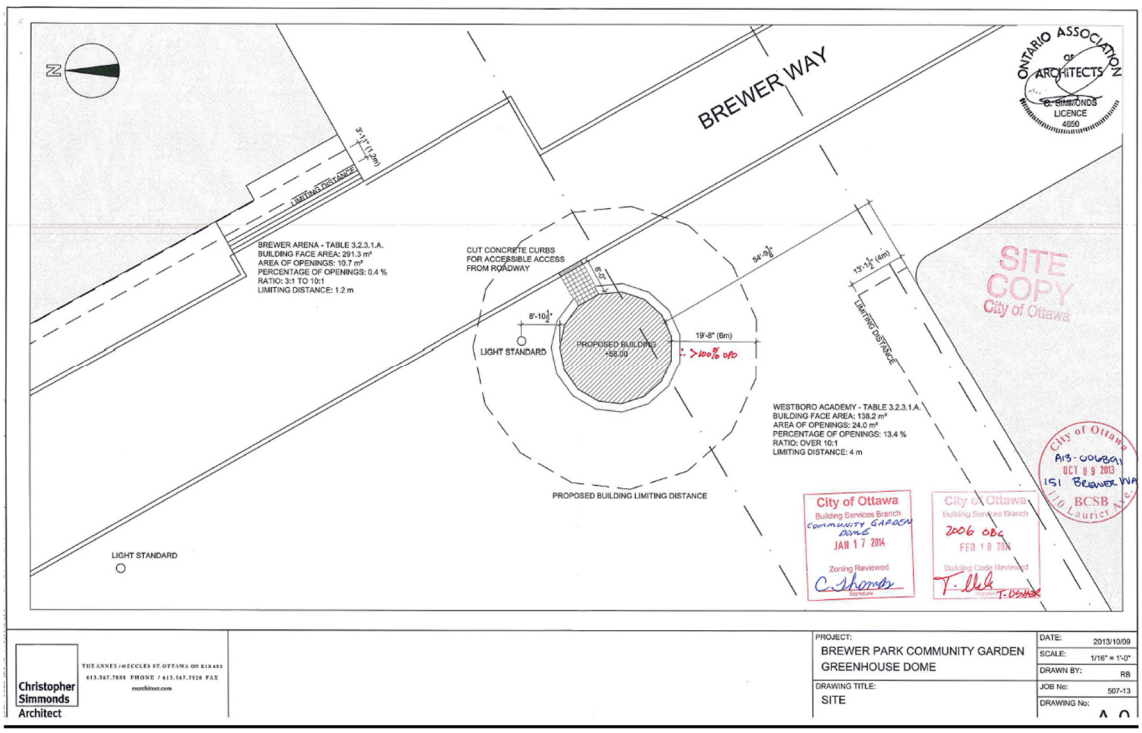

Figure 6: Architectural drawing of Biodome location (Christopher Simmonds Architect Inc., 2014). Adapted with permission.

Frost protection was specified in the form of 2” (5.08 cm) expanded polystyrene (EPS) insulation installed 8” (0.2 m) below grade and extending 3’3¼” (1 m) from both sides of each of the dome wall centrelines, as shown in Figure 7.

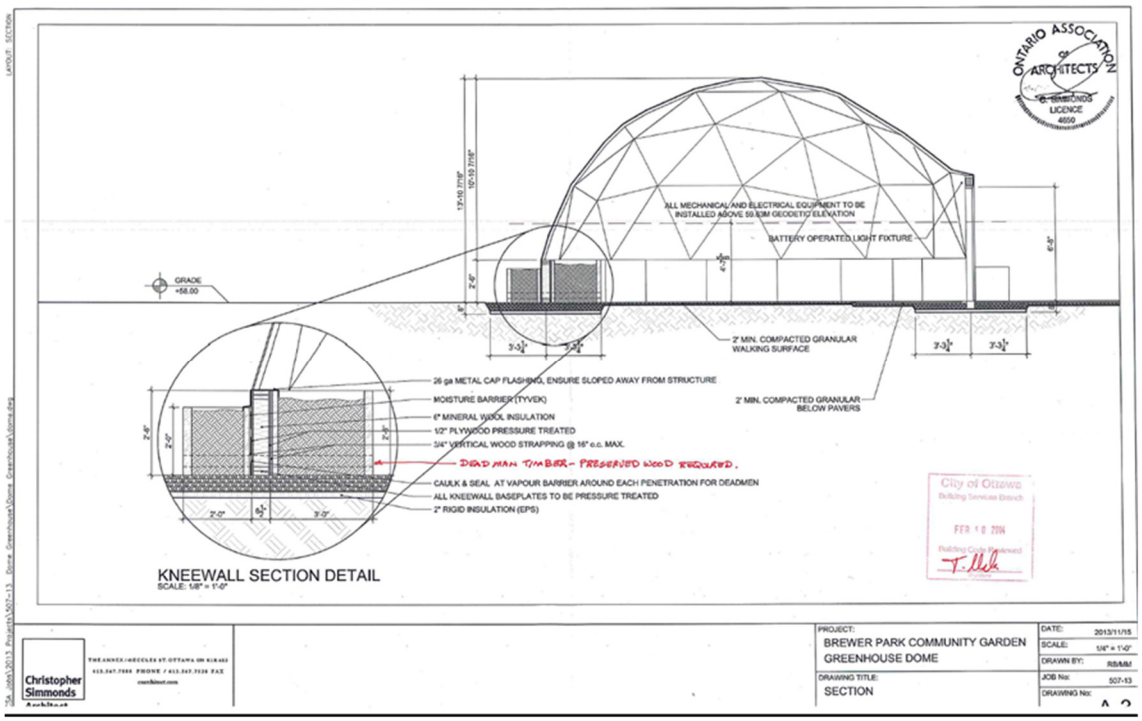

Figure 7: Architectural drawing of Biodome structure and wall detail (Christopher Simmonds Architect Inc., 2014). Adapted with permission.

Prior to installation, the EPS boards were laid out and pre-cut in the public hockey arena across from the build site, as shown in Figure 8. This planning step allowed the actual on-site installation to go more smoothly and more quickly.

Figure 8: Layout of insulation before installation (E. Kucerak, personal photograph, April 26, 2014). Adapted with permission.

The Biodome building site was excavated to a depth of 8” (0.2 m) and the pre-cut EPS insulation was placed in the hole, taped together along all of its seams, and covered with 2” (0.05 m) of compacted granular ‘A’, as shown in Figure 9.

Figure 9: Installation of EPS insulation on site (E. Kucerak, personal photograph, May 2, 2014). Adapted with permission.

In preparation for the future installation of an earth-to-air heat exchanger (EAHE) system, a series of six 4” (0.1 m) corrugated drainage pipes were installed under the area of the internal planter boxes, as shown in Figure 10. An EAHE provides a method of storing thermal energy by using fans to circulate warm air through underground pipes in order to transfer the heat from the air to the underground thermal mass. A further description of EAHEs is provided in Section 2.4.3, as part of the literature review.

The entire area was then covered with an additional 4” (0.1 m) of compacted granular ‘A’, as shown in Figure 11. Also shown in Figure 11 is plastic tubing that is criss-crossing the centre of the Biodome. This tubing was installed in order to facilitate the possibility of installing radiant heating in the future, but it is not currently in use.

Figure 10: Layout of earth to air heat exchanger piping (E. Kucerak, personal photograph, May 3, 2014). Adapted with permission.

Figure 11: Installation of earth to air heat exchanger piping (E. Kucerak, personal photograph, May 3, 2014). Adapted with permission.

Top-view and cross-sectional schematics of the arrangement of the EAHE pipes are shown in Figure 12 and Figure 13, respectively. This pipe placement was selected so that the heat transfer area around each pipe would not overlap with the adjacent pipe and so that the pipes would be safely out of the way of gardeners working in the plant grow beds. The two sets of pipe sections situated under the interior planter boxes (pipes 1, 2, 5, and 6), as shown in Figure 16, are intended to provide heat to the soil in the planter boxes, while the set of pipes situated just beyond the planter box wall (pipes 3 and 4) are intended to provide heat to the rock bed thermal storage. The air intake for the pipes is located opposite from the Biodome entrance and the outlets are located on either side of the entrance.

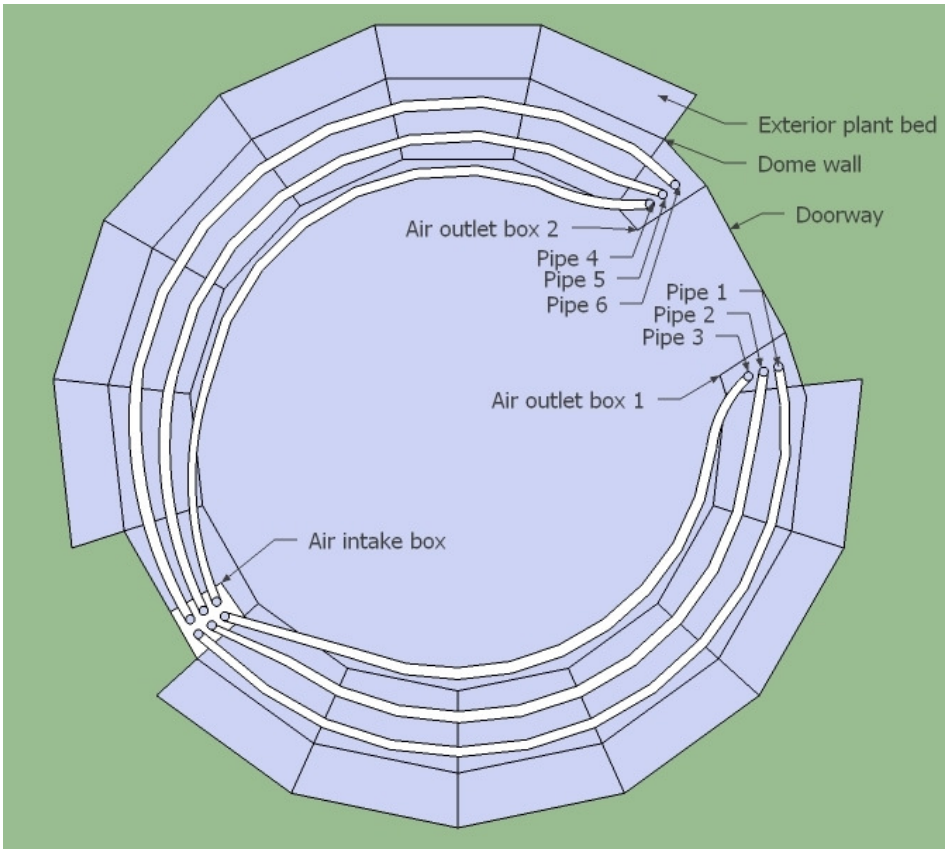

Figure 12: Top view of placement of underground pipes in the Biodome.

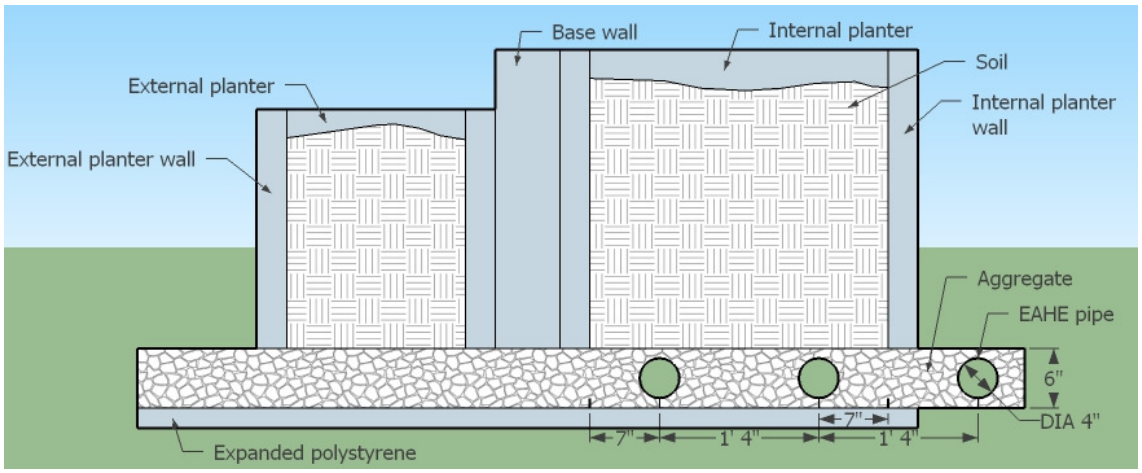

Figure 13: Cross-sectional view of placement of underground pipes.

All of the EAHE pipes share a common air intake box, located opposite the Biodome entrance, and terminate in one of two air outlet boxes on either side of the Biodome entrance. The EAHE air intake box, an air outlet box, and an air outlet box vent are pictured in Figure 14.

Figure 14: Earth-to-air heat exchanger air intake box (left), air outlet box 1 (middle), and air outlet box 1 vent (right).

Four 120 mm, 12 V, 0.66 A, high-reliability computer cooling fans rated at 102 CFM (0.048 m^3/s) each are installed in the lid of the EAHE air intake box for a total air moving capacity of 408 CFM (0.19 m^3/s) into the EAHE tubes.

Each of the components of the Biodome structure was cut and partially assembled off-site in order to facilitate on-site assembly. Construction of the Biodome structure was completed in four main stages: installation of base plates, as shown in Figure 15; installation of base walls, also known as knee walls, as shown in Figure 16; installation of the trusses, as shown in Figure 16; and installation and sealing of the glazing. Once the main structure was assembled, the growing beds were assembled and filled.

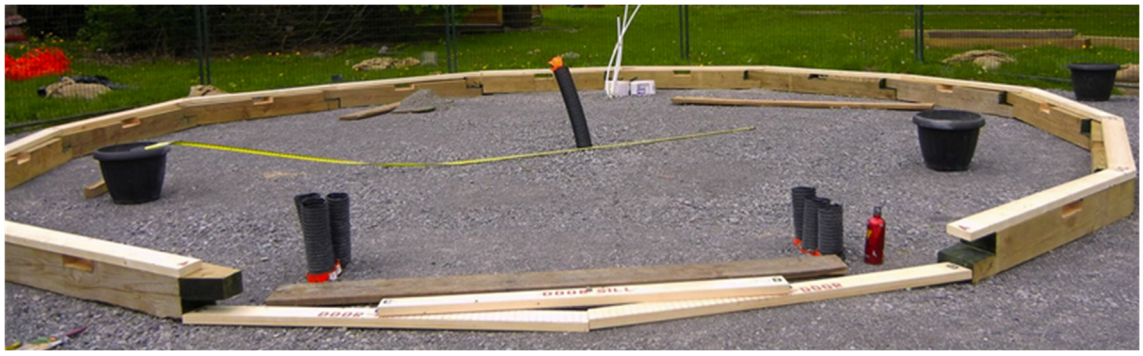

Figure 15: Installation of base plates (E. Kucerak, personal photograph, May 25, 2014). Adapted with permission.

Figure 16: Installation of base walls (left) (E. Kucerak, personal photograph, May 26, 2014) and trusses (right) (E. Kucerak, personal photograph, May 29, 2014). Adapted with permission.

The dome glazing material is a triple-wall co-extruded polycarbonate with UV protection on the inner surface to reduce solar degradation of the polycarbonate. This material provides good performance, in terms of light transmission and insulation, and is significantly lighter than glass (Moretti, Zinzi, and Belloni, 2013). Polycarbonate has the added advantage that, unlike glass, it is virtually shatterproof; with an impact resistance of over 200 times that of tempered glass, which is an added benefit in a public space.

The main sources of ventilation in the Biodome are two manually-operated hinged square vents with bug screens, one located on the south-west side of the dome, and the other located on the north-west side of the dome, which are both visible in Figure 17.

Figure 17: Completed Biodome structure (E. Kucerak, personal photograph, September 19, 2014). Adapted with permission.

There is also a sliding screened window in the door to the Biodome. An EcoSmart solar-powered exhaust vent, located on top of the dome just above the door, on the

north-east side, with an integrated solar panel mounted facing south provides forced ventilation. The exhaust vent has a maximum rated capacity of 500 CFM (0.24 m^3/s), depending on available solar radiation and intake ventilation area (GAF, 2015).

1.3 Research Objectives

The main question to be answered by this research is whether appropriate growing conditions (to be defined in Chapter 2) can be maintained in the Biodome year-round without the use of auxiliary power, such as grid-supplied electricity, and without the use of a supplementary heating source, such as propane, natural gas, or biomass.

The main topics to be included in the scope of work of this project are:

- The effects of solar gain, thermal mass, and insulation on greenhouse air and soil temperatures;
- The effect of shading by solar photovoltaic panels mounted on the roof of the Biodome; and
- The measurement and regulation of internal temperature.

Some constraints that will be considered, but not assessed directly include:

- The overall design of greenhouse dome structure and foundation, including compliance with local building codes;
- The internal design of the greenhouse, including placement of benches, displays, etc.; and
- Water drainage.

Topics to be specifically excluded from this analysis include:

- The design and maintenance of the aquaculture system, including plant and fish

selection and maintenance;

- The design and maintenance of the growing beds, including plant selection, maintenance, yields, etc.;
- Construction methods; and
- Water supply.

1.4 Organization of Research and Thesis Document

This document is organized as follows:

- Chapter 2 provides a review of literature that is relevant to the research topic.
- Chapter 3 describes the experimental approach and instrumentation including the development of a TRNSYS model and a data acquisition system.
- Chapter 4 describes the results of the modelled and measured scenarios.
- Chapter 5 provides a comparison and discussion of the scenarios.
- Chapter 6 describes the contributions of this thesis work.
- Chapter 7 provides conclusions on the experimental results as well as recommendations for future research and possible improvements to both the Biodome TRNSYS model and the Biodome design and operation.

Chapter 2

Literature Review

2.1 Introduction

To inform the current research and provide guidance to the Biodome team on design aspects to include in the construction of the dome, a literature review was conducted and is presented here. The review begins with a description of greenhouses, including the optimal growing conditions and the effects of greenhouse shape and orientation on performance. Geodesic dome greenhouses, in particular, are discussed next, followed by a description of thermal energy storage systems and their applicability to greenhouse environmental control.

2.2 Greenhouses

Greenhouses can be considered to be large solar thermal collectors. The transparent glazing on a greenhouse allows short-wave radiation into the greenhouse where it is absorbed by surfaces within the dome and re-radiated as long-wave radiation, such as heat and infrared radiation, that cannot pass back through the glazing. The accumulation of energy through this greenhouse effect increases the temperature inside the greenhouse.

2.2.1 Temperature

The optimal temperature inside a greenhouse is heavily dependent on the nature of the crop being grown. For example, cold-season crops, such as spinach and kale, are more

tolerant of low temperatures and may even tolerate brief periods of freezing temperatures, while tropical, or warm-season crops, such as tomatoes and cucumbers, would be killed by the same low temperatures. Therefore, it is important to consider the target crops when designing a greenhouse and, if possible, rotate the crops so that they align with the growing season.

Cool-season crops tend to do best when grown in the range of 5 to 15.5^{o}C and will tolerate an occasional drop near 0^{o}C or an increase to 32^{o}C. Warm-season crops tend to do best when grown in the range of 15.5 to 27^{o}C and will tolerate an occasional drop to 10^{o}C or an increase to 38^{o}C. For most vegetables, very little growth will occur below 5^{o}C or above 30^{o}C (McCullagh, 1978).

In climates with extreme temperatures in both the summer and winter, both heating and cooling may be required in order to operate a greenhouse year-round. A composite system that can be used for both heating and cooling greenhouses is the EAHE, which is described in further detail in Section 2.4.

According to the American Society of Agricultural and Biological Engineers (ASABE), most heat loss from a greenhouse is lost through long-wave (thermal) radiation, conduction, convection, and infiltration (ASABE, 2008), so each of these modes of heat loss should be addressed in order to maintain an optimum temperature and reduce the amount of supplementary heat required. An additional heat loss mechanism was proposed by Rempel et al. (2013) who theorized that glazing cooling due to rain can draw energy from a greenhouse's mass, as well as air, through radiative exchange.

The density and type of crop being grown in the greenhouse will also affect the

amount of solar energy that is converted to heat. The American Society of Heating, Refrigeration and Air-Conditioning Engineers (ASHRAE) estimates that in a greenhouse with a mature crop of plants, one-half of the incoming solar energy is converted to latent heat, one-quarter to one-third, to sensible heat, and the remainder is either reflected out of the greenhouse or absorbed by the plants and used in photosynthesis (2011). A diagram of the major energy flow pathways in a greenhouse is shown in Figure 18.

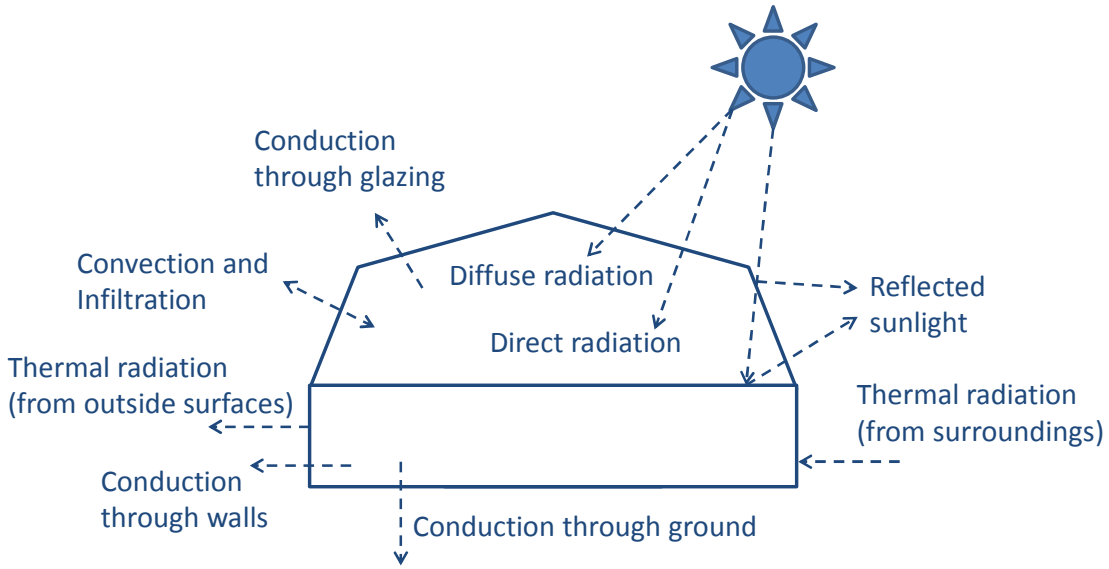

Figure 18: Energy flow pathways in a greenhouse.

An estimate of the peak heating requirements q_t for a greenhouse can be calculated by considering only the conduction q_c and infiltration q_i (ASHRAE, 2011), as shown in Equations 1, 2, and 3.

$$q_t = q_c + q_i \quad (1)$$

$$q_c = UA(t_i - t_o) \quad (2)$$

$$q_i = 0.5VN(t_i - t_o) \quad (3)$$

where: U = overall heat loss coefficient, W/(m^2 K)

A = surface area, m^2

t_i = inside temperature, ^oC

t_o = outside temperature, ^oC

V = greenhouse internal volume, m^3

N = number of air changes per hour, h^{-1}

The overall heat loss coefficient U can be estimated based on the type of construction and the heat transfer coefficient of the glazing material.

Although Equation 1 provides a good estimate of the peak heating load for a greenhouse, it does not take into account the effect of thermal energy storage, which is discussed in Section 2.4.

Conduction heat loss occurs mainly between the greenhouse floor and the soil below, and through the greenhouse glazing (Vadiee, 2011), so this form of heat loss can be reduced through the use of improved ground insulation and glazing materials with a high U factor. Unfortunately, a material's thermal performance is normally inversely related to its light transmissivity, so the relative importance of these two properties must be considered for a given climate and growing conditions. It should also be noted that water condensation on the inside surface of glazing increases the thermal resistance of the glazing (Zhu et al., 1998).

2.2.2 Lighting

Solar radiation that enters a greenhouse can be categorized as ultraviolet radiation, photosynthetically active radiation, and near-infrared radiation. Of these three types of

solar radiation, only photosynthetically active radiation, which has light wavelengths of 400 to 700 nm, contributes to photosynthesis (Lamnatou and Chemisan, 2012). Light intensity is also important to plant growth. For example, light saturation (the maximum level of light intensity a plant is capable of absorbing) of lettuce occurs at 11 MJ/m^2 d, and growth is inhibited at 19 MJ/m^2 d (Lamnatou and Chemisan, 2012). Samples of recommended ranges of radiant energy intensity, duration, and time of day for supplemental lighting in greenhouses in order to promote optimal plant growth are shown in Table 1.

Table 1: Suggested radiant energy, duration, and time of day for supplemental lighting in greenhouses (adapted from 2011 ASHRAE Handbook, Table 10).

Plant	Stage of Growth	Radiant Energy (W/m^2)	Duration (hr)	Duration (time)
Cucumber	rapid growth and early-flowering	12 to 24	24	
Eggplant	early-fruiting	12 to 48	24	
Lettuce	rapid growth	12 to 48	24	
Salvia	early-flowering	12 to 48	24	
Tomato	rapid growth and early-flowering	12 to 24	16	0800-2400

The glazing, or window material, used on a greenhouse affects both the greenhouse's level of insulation as well as the level of transmittance of solar radiation. Some of the glazing materials commonly used to cover greenhouses include glass, polycarbonate, acrylic, fibreglass, and plastic films. Combinations of these materials, including glass-film-combinations have been investigated (Max et al., 2012) and have been found to combine the advantages of the individual materials, such as durability and

low weight, and of single and double-layer systems, such as light transmission and insulation properties. Polycarbonate panels also provide good thermal and optical performance with a much lower weight than glass, at a similar price (Moretti et al., 2014).

2.2.3 Ventilation and Humidity

Ventilation affects three main variables in a greenhouse: humidity; temperature; and concentration of CO_2. The relative humidity in a greenhouse should be maintained above 40 percent to prevent plant wilt (McCullagh, 1978), but should not be kept higher than 85 percent in order to reduce the risk of the crop developing fungal diseases (Campen et al., 2003).

Plants require CO_2 for photosynthesis and grow best in high CO_2 environments. Ambient air contains about 300 ppm of CO_2, while the level of CO_2 in a closed greenhouse may reach 500 ppm at dawn and can quickly drop to less than 200 ppm on a sunny day if there is insufficient ventilation available, which can lead to reduced growth rates (Agriculture Canada, 1987).

Ventilation can either be natural or forced. Natural ventilation is accomplished through the use of strategically placed vent openings in the greenhouse and is dependent on wind speed and direction, as well as on the temperature differential between the greenhouse air and ambient air. Forced ventilation involves the use of fans or blowers to mechanically move air. Fuchs et al. (1997) found that external wind speed has no significant effects on forced ventilation.

The most effective vent configuration is a combination of roof and side vents, followed by side vents only, which have a 46% reduction in ventilation, while the least

effective vent configuration uses only roof vents and results in a 71% reduction in ventilation (Katsoulas et al., 2006).

In order to ensure sufficient natural ventilation Agriculture Canada's (1987) general guideline is to provide a total ventilation area of at least one-sixth of the greenhouse floor area, with the total upper area representing about 55% of the total ventilation area. As noted by Sethi and Sharma (2007) a vent opening area of 15 to 30 percent of greenhouse floor area is recommended, as the effect of additional ventilation area on the temperature difference is very small above this range.

The use of insect screens in vent openings causes a reduction in natural greenhouse ventilation rate. Katsoulas et al. (2006) estimated this decrease to be about 33 percent. Decreased screen porosity is associated with decreased ventilation rate and increased vertical temperature gradients (Sethi and Sharma, 2007). The effect of insect screens must be taken into consideration when calculating the required ventilation area.

If an aquaculture system is included in the greenhouse, the surface evaporation of the water in the fish tanks and plant grow beds will also contribute to the relative humidity and further increase the ventilation requirements, and therefore the overall energy requirements. To reduce this effect, it is recommended that tank surface openings be covered at night (Fuller, 2007).

2.2.4 Effects of Greenhouse Shape and Orientation on Performance

Five of the most commonly used single span greenhouse shapes are even-span, uneven-span, vinery, modified arch, and quonset type (Sethi, 2009). Sethi (2009) modelled and compared the level of solar radiation, and the resulting inside air temperature, for each

of these greenhouse shapes in both an east-west orientation and in a north-west orientation. Assuming greenhouses of the same size (i.e., same height, width, and length), Sethi found that the shape and orientation of the greenhouse affected the total solar radiation incident upon it. Sethi concluded that at altitudes of 31^{o}N, where ambient air temperatures are low in winter but high in summer, resulting in harsh summers and winters, a greenhouse shape that receives less radiation in summer (e.g., Quonset shape) but more in winters (e.g., Uneven-span) would be ideal and an east-west orientation would be preferred, as it would provide more radiation in winter and less in summer.

As it is not feasible to use two different shapes in one year, Sethi suggested that a greenhouse that neither receives highest solar radiation in summer nor least solar radiation in winter would be preferred, such as a modified arch or even-span greenhouse. In areas where the ambient air temperature remains low during most of the year, Sethi suggested that a greenhouse shape that received the highest solar radiation throughout the year, such as the uneven-span greenhouse, should be selected. Unfortunately, no scientific studies on the relative effectiveness of a geodesic dome greenhouse were found during the literature review.

2.3 Geodesic Dome Greenhouses

Dome-shaped buildings were made popular in the 1950s by Buckminster “Bucky” Fuller who named these structures “geodesic domes”, inspired by the term “geodesic line”, which refers to the shortest distance between two points on a curved surface (Chandler, 2015).

Geodesic domes are typically based on icosahedrons, which are roughly spherical shapes with 20 identical equilateral triangle faces, as shown in Figure 19.

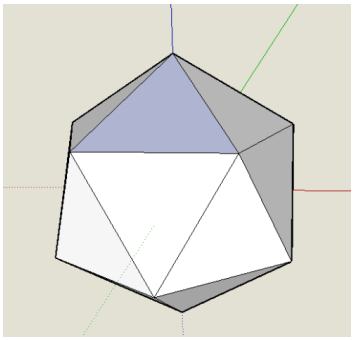

Figure 19: Icosahedron centred at the origin.

Geodesic domes are classified according to their frequency (v), which is the number of triangle subdivisions that were used to create the dome shape. An icosahedron can be classified as a 1v geodesic sphere, as there are no subdivisions of each face. The Relationship between icosahedron equilateral triangle face subdivisions and geodesic dome frequency is shown in Figure 7. By subdividing each face of an icosahedron into more equilateral triangles and projecting out the vertices of each triangle so that they are all the same distance from the centre of the icosahedron, a shape approaching a sphere can be created.

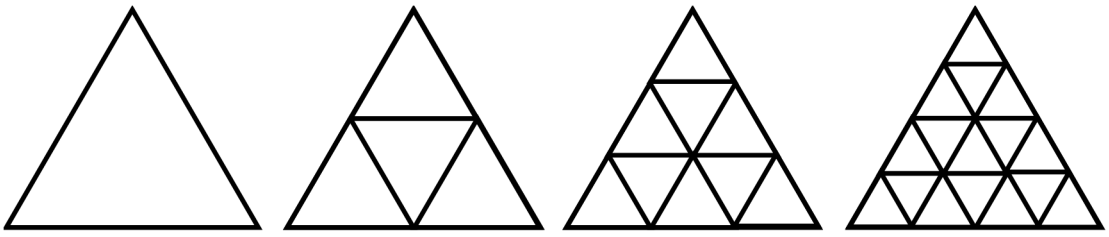

Figure 20: Relationship between icosahedron equilateral triangle face subdivisions and geodesic dome frequency.

Mathematically, a sphere has the largest volume to surface area ratio, so a structure approaching this shape, such as a geodesic dome, is able to maximize the internal space, while minimizing the surface area, and therefore construction material, of a structure. A reduced total surface area also results in reduced surface conduction area, which may reduce the amount of heat lost through conduction. The challenge of using this building shape is that it can be more complicated to construct due to the many angles and connections points, which may also make it more difficult to achieve a tightly-sealed building envelope, increasing the possibility of air and water infiltration.

According to the Buckminster Fuller Institute (2015), geodesic domes are energy efficient for the following reasons:

- "The concave interior creates a natural airflow that allows the hot or cool air to flow evenly throughout the dome with the help of return air ducts;
- Extreme wind turbulence is lessened because the winds that contribute to heat loss flow smoothly around the dome; and
- It acts like a type of giant down-pointing headlight reflector and reflects and concentrates interior heat. This helps prevent radiant heat loss."

Two of the most famous geodesic dome greenhouses, the Rainforest Biome and the Mediterranean Biome, are part of the Eden Project, in Cornwall, United Kingdom. The Rainforest Biome, which houses the world's largest rainforest in captivity, covers about 16,000 m^2 and is 50 m tall, while the adjacent Mediterranean Biome is comparatively small, with an area of 6540 m^2 and is 30 m tall (Eden Project, 2015). Another iconic geodesic dome greenhouse, the Climatron located at the Missouri Botanical Garden, was

built in 1960 as the first geodesic dome to be used as a conservatory (Missouri Botanical Garden, 2015). The Climatron covers more than 2000 m^2, has a centre height of over 21 m, and spans over 53 m at its base. Individual and community-sized dome greenhouses are also becoming increasingly popular, with several manufacturers and individuals constructing domes all over the world.

Although there is a lot of anecdotal evidence available on the internet on the effectiveness of geodesic domes as greenhouses, very little scientific data on this topic was found through a search of scholarly sources. Various attempts were made to contact owners, operators, and builders of other geodesic dome greenhouses, but no useful information was collected. A representative at Growing Spaces indicated that over the years they had collected a "decent amount of data" but that it was not well organized (U. Parsons, personal communication, June 12, 2015).

The only reference to a geodesic dome greenhouse in the literature was by Provenzano and Winfield (1987) who used a geodesic dome greenhouse with polyethylene glazing to cover a tilapia growth tank measuring 10.7 m^3 and reported that the fish tank water temperatures generally remained between 24 and 36^oC between May and September in Virginia, USA, with an average daily fresh water make-up rate of 4 percent of tank volume.

2.4 Thermal Energy Storage

In a typical commercial greenhouse, air temperature is primarily controlled using a combination of shading, misting, and ventilation for cooling, and some form of auxiliary heater for heating. Solar greenhouses are instead designed to maximize the capture and

storage of solar energy in thermal mass and minimize heat loss through insulation, resulting in reduced daily temperature fluctuations and reduced heating and cooling requirements. Thermal energy that is captured, stored, and later released without the use of any outside energy, such as electricity to drive fan or pump, is considered to have undergone passive thermal storage. If at any point during the process outside energy is used to capture, store, or release the thermal energy, then that portion of the system is considered to involve active thermal storage. Santamouris et al. (1994) identified five main categories of passive solar greenhouse, according to the characteristics of the heat storage system, namely, water, latent heat material, rock bed, buried pipes, and other.

The suitability of a thermal storage medium depends largely on its capacity to store energy, or thermal mass, its cost, and its availability. The density and volumetric heat capacity of several common thermal storage media are presented in Table 2, for reference.

Table 2: Heat capacity of materials used for heat storage (Adapted from Table 4 of Energy-Conserving Urban Greenhouses for Canada, Agriculture Canada, 1987).

Material	**Density (kg/m^3)**	**Volumetric Heat Capacity ($MJ/m^3\ ^oC$)**
Water	1000	4.19
Rock	2200	1.60
Clay Brick	2000	1.65
Concrete	2200	1.60
Soil (medium moisture)	1600	1.80
Mud (saturated soil)	1900	3.00
Glauber's salt solution	1460	374

Sethi and Sharma (2008) compiled a comprehensive survey and evaluation of greenhouse heating energy storage technologies, including water storage, rock bed storage, phase change material storage, and earth-to-air heat exchanger systems. The benefits and challenges of each of these types of thermal storage system and guidelines on the quantity of storage material required are discussed in the following four sections.

2.4.1 Water Thermal Energy Storage

As was shown in Table 2, water has a volumetric heat capacity that is almost three times greater than that of rock, clay brick, and concrete at about half the density, making it an effective thermal storage material. Water is also relatively inexpensive and is generally readily available. One challenge of using water as a thermal energy storage medium is that it has the potential to freeze when exposed to prolonged sub-zero temperatures and upon freezing it may expand enough to damage its storage container, which may lead to water leaks that can be very destructive, depending on the environment they are in. Water tanks placed in a greenhouse also occupy precious floor space that could instead be using for cultivation.

Gupta and Tiwari (2002) created a model for predicting the thermal storage effect of water mass in a greenhouse. Their transient model predicted room air temperature, storage water temperature, and the thermal energy storage effect of a water mass in a passive greenhouse. Their conclusions are that there is a significant thermal energy storage effect of a large water mass on the internal greenhouse air temperature, as evidenced by the decrease in thermal load leveling that is associated with an increase in the mass of storage water. Similarly, Zhu et al. (1998) modelled the thermal

characteristics of greenhouse pond systems in TRNSYS and found that the night time air temperature in a greenhouse with a pond remains a few degrees higher than in a similar greenhouse.

Sethi and Sharma (2008) developed empirical relationships between the volume of water storage and greenhouse floor area, listed in Table 3, to provide greenhouse designers with a method of estimating the approximate volume of water storage required for a given application.

Table 3: Empirical relationships between water storage volumes used for given greenhouse ground areas using different cover materials and storage material (Adapted from Table 2 in Sethi and Sharma, 2008).

Type	Empirical relationship [a]	r^2	(r_{xy})
Greenhouse ground area versus volume of water storage used (overall)	$Y_w = 0.0362X + 1.1005$	0.7731	0.879
Polyethylene as cover material	$Y_w = 0.037X + 0.6071$	0.827	0.909
Glass as cover material	$Y_w = 0.0699X - 1.5449$	0.6048	0.777
Ground tubes as storage material	$Y_w = 0.0232X + 1.8865$	0.4175	0.646
Water tanks/barrels as storage material	$Y_w = 0.0369X + 1.9042$	0.8875	0.942

[a] Y_w represents the volume of water storage in kl, X represents the greenhouse floor area in m^2.

It should be noted that these relationships were developed based on other researchers' reported water volumes and greenhouse floor areas, but these volumes were not necessarily optimized for the given situations and may not reflect best practices. These equations also ignore the effects of greenhouse location, volume, crop, etc. Nonetheless, these equations can provide a starting point for future work.

2.4.2 Rock Bed Thermal Energy Storage

Heat can be stored in a rock bed thermal energy storage system either passively or actively. In passive systems, heat is stored in the rock bed during the day through direct incident solar radiation and is released at night through convection, once the indoor air temperature falls below that of the rock bed. In active systems, fans are used to blow air through the rock bed. During the day, warm air is pushed through the rock bed to remove excess heat from the air and charge the rock bed and at night the cooler indoor air is pushed in reverse through the rock bed to be reheated. Although a very large quantity of rock is required for an effective rock bed storage system, it does not have to occupy internal floor space, as the rock bed can be built underneath or adjacent to the greenhouse.

Sethi and Sharma (2008) developed empirical relationships between the heat capacity of rock bed storage and greenhouse ground areas using different cover materials and storage material, listed in Table 4, to provide greenhouse designers with a method of estimating the approximate heat storage capacity required for a given greenhouse application. They found that rock beds are typically composed of 2 to 10 cm diameter gravel with a depth of 40 to 50 cm and can satisfy 20 to 70 percent of a greenhouse's annual heating needs, with inside temperatures ranging from 4 to 10^{o}C higher than minimum ambient air temperatures.

Table 4: Empirical relationships between heat capacity of rock bed storage and greenhouse ground areas using different cover materials and storage material (Adapted from Table 4 in Sethi and Sharma, 2008).

Type	Empirical relationship [a]	r^2	(r_{xy})
Greenhouse ground area versus heat capacity of rock storage used (overall)	$Y_r = 0.0362X + 1.1005$	0.7731	0.879
Polyethylene as cover material	$Y_r = 0.037X + 0.6071$	0.827	0.909
Glass as cover material	$Y_r = 0.0699X - 1.5449$	0.6048	0.777
Gravel as storage material	$Y_r = 0.0232X + 1.8865$	0.4175	0.646

[a] Y_r = heat capacity of rock storage in kJ/^{o}C, X = greenhouse floor area in m^2

2.4.3 Earth-to-Air Heat Exchangers

Earth-to-air heat exchangers (EAHE) provide another method of storing energy in the ground under or adjacent to a greenhouse or other building. In these systems fans are used to circulate the naturally warm, moist air of the greenhouse underground through pipes in order to transfer the heat to the underground thermal mass, which can include sand, soil, rocks, or a combination of these materials. In the case of the Biodome, fans located at the air intake box will be used to push warm greenhouse air through the pipes buried under the internal garden beds and out through the two air outlet boxes located within the Biodome, as described in Section 1.2. The warm air will heat the soil surrounding the pipes in the EAHE system.

Ghosal and Tiwari (2006) reported that the use of an EAHE was found to result in greenhouse air temperatures that were on average 7 to 8^{o}C higher in the winter and 5 to 6^{o}C lower in the summer than in the same greenhouse without an EAHE. They also found that the EAHE was increasingly effective with increasing pipe length, decreasing pipe

diameter, decreasing mass flow rate of flowing air and increasing depths up to 4 m. Unfortunately, no optimization of the combination of these variables was performed and no upper limits were stated, other than the limit of 4 m of depth.

A survey of the application of EAHE systems to agricultural greenhouses was performed by Sethi and Sharma (2007, 2008), and is shown in Table 5. As shown in Table 5, EAHEs have been used in greenhouses all over the world and in greenhouses of various sizes and with different glazing types. From this data it can also be seen that there does not appear to be any agreement between these systems on the optimal pipe number, depth, size, spacing, or material used, or on the air flow rate through the pipes.

Bansal et al. (2012) found that the affected heat transfer distance from the EAHE pipes depends on the thermal conductivity of the soil and the distance beyond which no significant temperature change is observed is equal to the pipe diameter.

2.5 Summary

The results of the literature review provided the Biodome team with a good understanding of the optimal growing conditions in a greenhouse as well as the design aspects to include in the construction of the Biodome, which is described in Chapter 3.

Table 5: Summary of the performance of various agricultural greenhouses using an earth-to-air heat exchanger system (Adapted from: Table 7 from Sethi and Sharma, 2008).

Area (m^2)	Location and Coordinates	Cover Material	Pipe Material	System Specifications					Flow rate ($m^3 h^{-1}$)	Remarks	Reference
				N	d (cm)	L (m)	D1 (cm)	D2 (cm)			
58	Valencienne, France 50.21 °N, 3.32 °E	Double PE	Plastic	2			80	210		62% cover	Santamouris et al. (1994b)
1736	Yokohama, Japan 35.27 °N, 139.28 °E	Glass	Plastic	44	10	587	50	90	25,920	28% oil reduction	Kozai (1989)
139	Athens, Greece 37.90 °N, 23.70 °E	PE	Aluminum	6	20	90	200			3°C higher	Mavrogianopoulos and Kyritsis (1985)
30	Bukhara, USSR 39.48 °N, 64.25 °E	Glass	Plastic	1	4		40		21.6	4°C higher	Immakoulov (1986)
835	Adana, Tunisia 37.00 °N, 35.40 °E	PE	Plastic		10		50		10,000	5°C higher	Bascetincelik (1987)
100	Montreal, Canada 45.50 °N, 73.50 °W	Glass	Plastic	16	10.2	192	45	75	3240	35% heatings	Bernier (1987)
100	Japan	Glass	Plastic	9	11.4	70.2	50			4°C higher	Yoshioka (1989)
176	Avignon, France 43.57 °N, 4.50 °E	Polycarbonate	Plastic	10	12.5	200	40	80	5800	7-9°C higher	Boulard (1989)
1000	Agrinion, Greece 38.5 °N	Fiberglass	Plastic	4	25	100	150			30% heating cover	Santamouris et al. (1996)
1000	Agrinion, Greece	Polycarbonate	Plastic	4	25	130	150			48% heating cover	Santamouris et al. (1994b)
72	Quebec, Canada 46.80 °N, 71.38 °W	Fiberglass	Plastic	2	10		30	30		10°C higher	Cofflin (1985)
79	Montreal, Canada 45.50 °N, 73.50 °W	Polycarbonate	Corrugated plastic	26	10.2	312	45	75	3270	33% heating cover	Bernier et al. (1991)
2500	Volos, Greece 39.21 °N, 22.37 °E	Polycarbonate	Plastic		25		120	180			Santamouris et al. (1994b)
58	Athens, Greece 37.90 °N, 23.70 °E	Double PE	Plastic	1	10.2		200	210		62% heating cover	Mihalakakou et al. (1994a)
79.65	Quebec, Canada 46.80 °N, 71.38 °W	Polycarbonate	Plastic	26	10.2	273	45	75	3276	5-7°C higher	Gauthier et al. (1997)

Chapter 3

Modelling and Experimental Approach and Instrumentation

3.1 Introduction

This section describes: the experimental approach that was taken to evaluate the effects of ventilation, water thank thermal storage, and solar panel shading on the Biodome operating conditions, the modelling approach used to simulate the performance of the Biodome, the design and implementation of the instrumentation and control system, including a detailed description of the system so that this system can be used in future projects, the instrumentation plan, and the model calibration approach.

3.2 Experimental Approach

In order to test the effects of ventilation, water tank thermal mass, and solar panel shading on both the modelled and the measured results, different combinations of these variables were used to create five Biodome operating scenarios, A through E, as listed in Table 6.

Table 6: Biodome operating scenarios

Variable	Biodome Operating Scenario				
	A	B	C	D	E
Ventilation Rate (1/h)	0	0	4	4	4
Water Tank (L)	No	2592	No	2592	2592
Solar Panel Shading	No	No	No	No	Yes
Actual Measurement Start (h)	1951	1626	2505	3883	4261
Actual Measurement End (h)	2302	1705	3388	4094	4353

The ventilation rate could not be modulated, due to the nature of the ventilation system, so the effects of ventilation were studied by turning the ventilation on and off.

The appropriate volume of water thermal storage to be used in the Biodome was calculated using Equation 4, from Table 3 of the literature review, shown below, which results in a recommended total tank volume of 3,377 L.

$$Y_w = 0.0369X + 1.9042 \qquad (4)$$

where: Y_w represents the volume of water storage (kL)

X represents the greenhouse floor area (m^2)

Two intermediate bulk containers (IBCs), such as the one shown in Figure 21, each with a capacity of 1,440 L, for a total capacity of 2,880 L of water, were placed in the centre of the Biodome.

Figure 21: Intermediate bulk container to be used as a water storage tank (E. Kucerak, personal photograph, October 25, 2014). Adapted with permission.

One IBC will be used as a fish tank in the future aquaponics system. The other IBC will be used to supply water for irrigation of the plants grown in the Biodome. Approximately 400 L of additional water will be added to the Biodome in sump tanks and grow beds, once the Aquaponics system is complete. Although this total volume of water is approximately 97 L less than the recommended volume resulting from Equation 4, it is the maximum amount of water that could reasonably be fit in the Biodome while maintaining sufficiently wide pathways.

In order to meet the electrical power requirements of the pumps in the aquaponics system and the fans in the EAHE, two 0.22 kW solar panels were mounted on the roof of the Biodome and will be used to charge a battery bank. Three possible mounting configurations were considered, as shown in Figure 22.

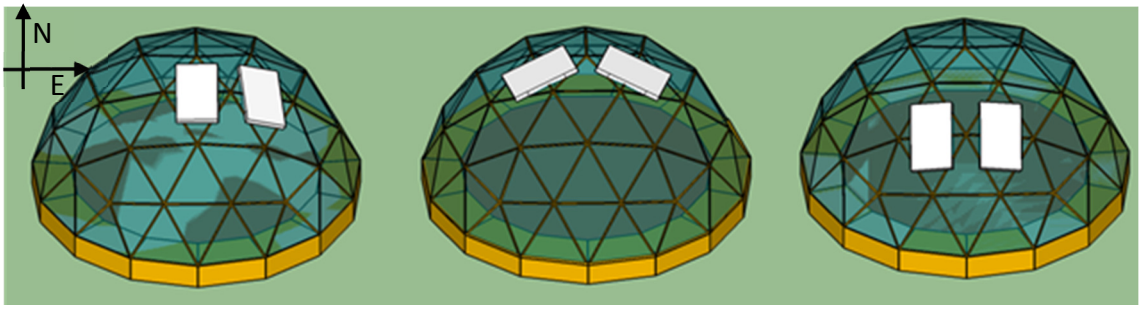

Figure 22: Three possible solar panel mounting configurations, 1, 2, and 3, from left to right.

To evaluate which of the three possible solar mounting configurations would be most suitable; an estimate of electricity generation from each setup was calculated using the online calculator, PVWatts version 1, offered by the US National Renewable Energy Laboratory. A derate factor of 0.7 was used and the location selected was Ottawa, Ontario.

As shown in Table 7, Solar Setup 3 would result in not only the largest total annual electricity generation, but also the largest minimum monthly generation, which would occur in November. Solar Setup 3 was selected and the solar panels were installed in June 2015, as shown in Figure 23.

Table 7: Evaluation of three possible solar panel mounting configurations.

Solar Setup	Panel	Azimuth Angle	Tilt Angle	Estimated Electricity Generation (kWh)		
				Annual	Maximum Monthly	Minimum Monthly
1	1	180.0	18.7	4055	480	143
	2	166.5	17.8	4023	480	139
2	1	162.0	19.6	4048	479	142
	2	198.0	19.6	4031	477	142
3	1	187.3	37.5	4242	447	174
	2	172.7	37.5	4256	450	174

Figure 23: Installed solar panels (E. Kucerak, personal photograph, June 25, 2015). Adapted with permission.

3.3 Modelling Approach

The modelling approach of this thesis relies on the development and use of a TRNSYS model. The TRNSYS software package is a transient system simulation program that can be used to evaluate many different types of transient systems, such as solar thermal systems, multizone buildings, cogeneration systems, etc. A TRNSYS project is composed of connected components, known as Types, which are each described by a mathematical model in the TRNSYS simulation engine (TRNSYS, 2012). An additional tool, TRNBuild, is used to enter input data for multizone buildings, such building structure details, window optical properties, heating and cooling schedules, etc. (TRNSYS, 2012).

The TRNSYS modelling platform was used because it has a proven record for accurately modelling greenhouses. It has been used by many researchers to create greenhouse models (Fuller et al., 1987; Willits et al., 1985; Fuller, 2007; Vadiee, 2011; Hollmuller and Lachal, 1998; Hoes and Desmedt, 2008; Wong et al., 2011).

The main components of the Biodome TRNSYS model are: Type 15-5, weather data reading and processing; Type 56, multi-zone building model; calculators, specifically Wizard Settings, Azimuth Angles, and Radiation calculators; and printers, specifically the Irradiation, Temperature, and System printers.

Each of these components is shown in the TRNSYS model in Figure 24 and is described in the sections below. The complete TRNSYS input file is provided in Appendix A and the TRNSYS deck file is provided in Appendix B.

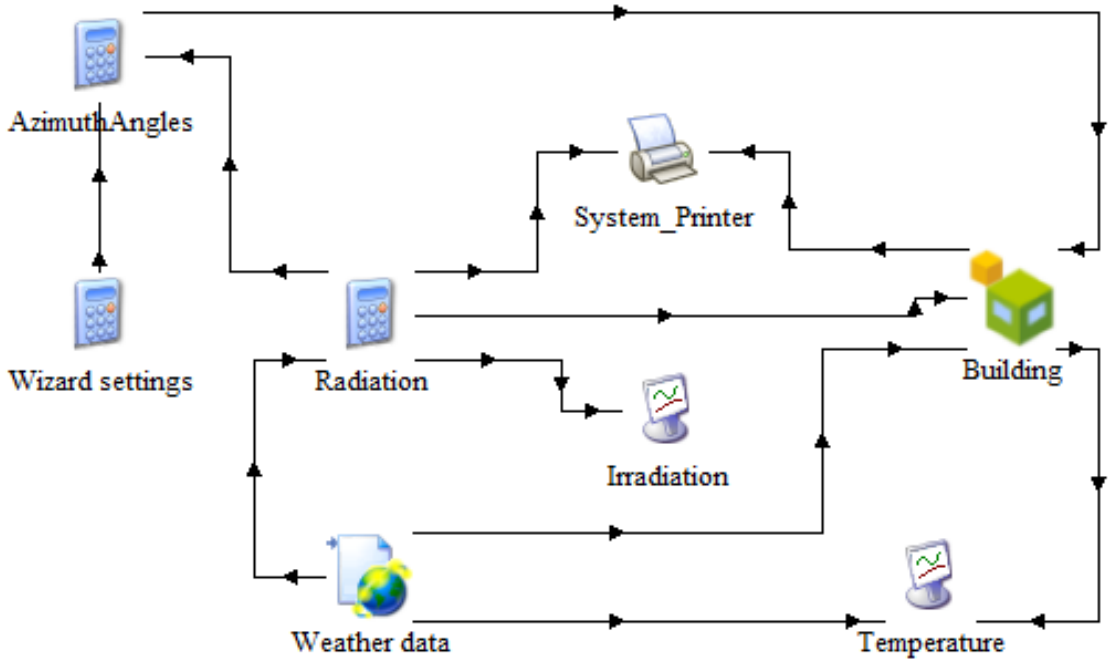

Figure 24: Biodome TRNSYS model.

3.3.1 Type 15-5 Weather Data Reading and Processing

The Type 15-5 component in TRNSYS is used to import weather data from a specified external file and interpolate this data, as required, for use by other TRNSYS components (TRNSYS, 2012). The version of the module used in this model is Type 15-5, which was selected as it is able to read data in the Canadian Weather for Energy Calculations (CWEC) format (TRNSYS, 2012). The CWEC dataset contains hourly weather observations for an artificial one-year period composed of twelve Typical Meteorological Months selected from the Canadian Weather Energy and Engineering Datasets for the period from 1953 to 1995 (Environment Canada, 2015). The CWEC files were produced by Numerical Logics in collaboration with Environment Canada and the National Research Council of Canada, specifically for use in building energy calculations, and is available from Environment

Canada (2015). The CWEC files follow the ASHRAE Weather Year for Energy Calculation 2 format. The CWEC file used for the simulations in this project is composed of data from the following weather station (Environment Canada, 2015):

- Station Name: Ottawa International Airport
- Latitude: 45.32
- Longitude: -75.67
- Elevation: 114 m
- World Meteorological Organization Identifier: 716280

In order to develop a file of actual weather data to be used for model comparison and calibration, the CWEC file described above was used as the starting point and actual data for 2015 was substituted, where applicable and available, as described below.

Carleton University is host to a Campbell Scientific Weather Station, which is mounted on the roof of the Mackenzie Building and automatically measures and logs data every 5 minutes. For the period from January 1, 2015 to July 1, 2015, the CWEC data was replaced with weather data collected by this weather station for the following fields: dry bulb temperature (^{o}C); relative humidity (%); global horizontal radiation (Wh/m^2); wind direction (degrees); and wind speed (m/s).

All atmospheric pressure data for this time period was taken from the Ottawa CDA RCS (Canada Department of Agriculture Reference Climate Station) weather station, available online from Environment Canada (2015). The details of this weather station are as follows (Environment Canada, 2015):

- Station Name: OTTAWA CDA RCS
- Latitude: 45.38
- Longitude: -75.72
- Elevation: 79.2 m
- Climate Reference Identifier: 6105978
- World Meteorological Organization Identifier: 71063
- International Air Transport Association/ Transport Canada Identifier: XOA

The Carleton weather station was not functional from February 13, 2015 to February 25, 2015, so the data for this period is taken from the Ottawa CDA RCS weather station (Environment Canada, 2015) instead. For the period from July 1 to December 31, CWEC data is used as a placeholder for all fields.

Weather variables that were not used in calculations affecting the models were left unchanged, including extraterrestrial horizontal radiation (Wh/m^2), extraterrestrial direct normal radiation (Wh/m^2), direct normal radiation, diffuse horizontal radiation, global horizontal, direct normal, and diffuse horizontal illuminance (lux), zenith luminance (Cd/m^2), total sky cover (0.1), and opaque sky cover (0.1).

Minor data cleaning was done to prevent calculation errors, including removing all non-zero values from the global horizontal radiation field for periods before or after sunrise or sunset, respectively and removing all zero atmospheric pressure readings and replacing these values with the values from the previous non-zero pressure reading.

3.3.2 Type 56 Multi-Zone Building

The Type 56 multi-zone component in TRNSYS is used to import the description of a multi-zone building from a set of specified external files having the extensions *.bui, *.bld, and *.trn (TRNSYS, 2012). These external files are generated using the TRNBuild preprocessor application (TRNSYS, 2012). The Type 56 component was selected because there are several zones of interest within the Biodome, namely the air zone, the soil zones, and the water tank zone, which can each be modelled separately within this one component. A simplified 3D model of the main structure of the Biodome was created in SketchUp, using a TRNSYS plugin for SketchUp (TRNSYS, 2012), and imported into TRNSYS using the Type56 wizard, which generates all of the necessary TRNBuild files.

Each building zone to be modelled in a Type 56 component must be created separately in SketchUp. For this project, the first zone to be modelled was the geodesic dome zone, which was created using a SketchUp visual tutorial (Goch, 2013). Starting with an icosahedron centred on the origin, one face of the icosahedron was subdivided into 9 identical equilateral triangles. Lines were drawn from the origin through each vertex of the subdivided face to a distance of 13 ft (3.96 m) and the ends of these lines were connected to form triangles. All other construction lines were deleted and only the new triangles were copied, pasted, and rotated about the origin to form a geodesic sphere. The bottom 5/9 of the geodesic sphere was deleted, leaving only a 4/9 dome. The dome was shifted vertically along the z-axis until the distance between the lowest triangle's edge and the x-y plane was 2 ft (0.61 m). A window was drawn onto each of the dome's triangular faces.

Each interior and exterior planter box was then drawn as a separate zone, and the area below the dome and between the interior planter boxes was split into five zones, as shown in Figure 25.

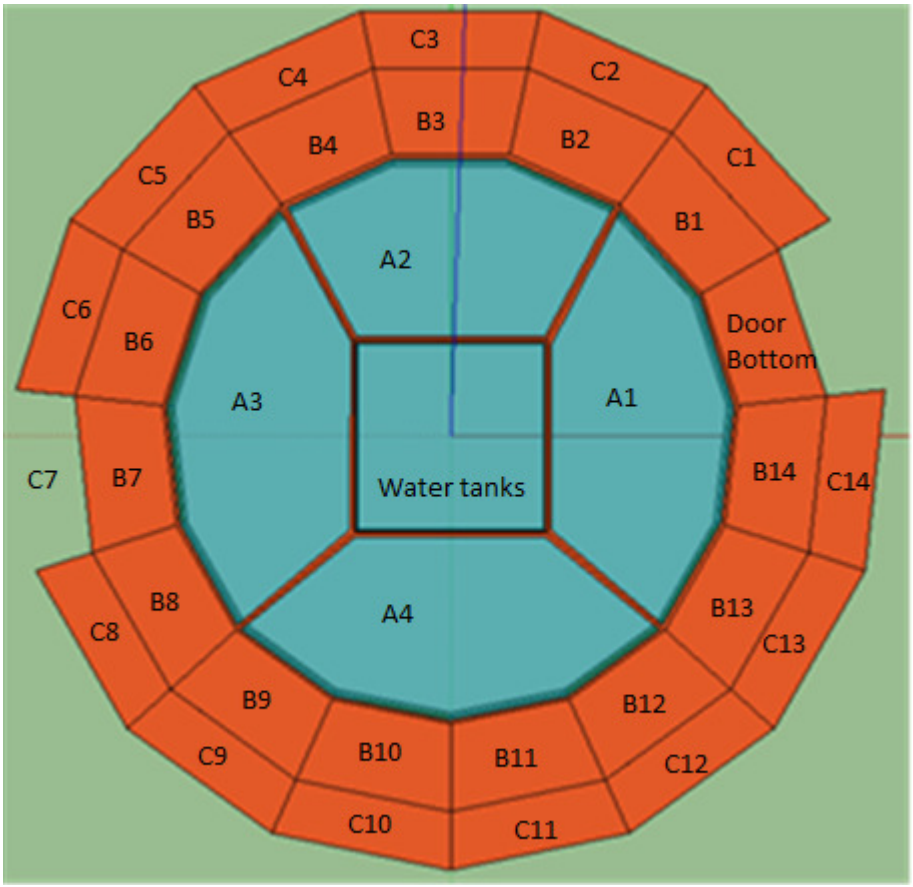

Figure 25: Top-view and identification of planter bed zones, air spaces, and water storage tank area.

The square zone in the middle of the area beneath the dome was created in order to model the effects of adding a water storage tank to the centre of the Biodome, as the properties of this zone can be modified independently from the properties of the zones surrounding it. The effects of direct solar radiation on the water tanks is not considered in this model as the water tanks in the Biodome are all shaded by surrounding structures and do not receive direct sunlight. The final 3D model of the Biodome in SketchUp is

shown in Figure 26.

The physical properties and starting conditions assigned to each of the dome zones in the TRNBuild software are shown in Table 8.

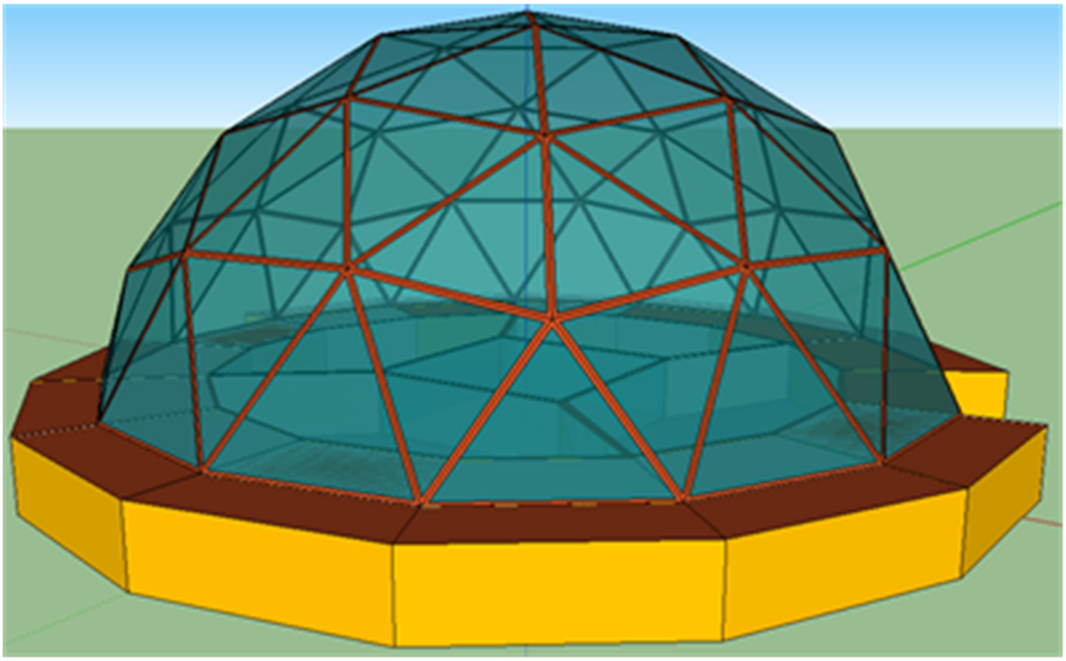

Figure 26: 3D Model of Biodome in SketchUp.

Table 8: Initial properties of modelled Biodome zones.

Zone	Volume (m^3)	Density (kg/m^3)	Specific Heat Capacity (c_p) [kJ/(kg·K)]	Capacitance (kJ/K)
Dome	90.330	1.2	1.005	108.4
Internal Plant Beds (B1-B6, B8-B14)	0.786	1600.0	1.800	2263.7
EAHE Air Intake Box (B7)	0.786	1.2	1.005	0.9
External Plant Beds (C1-C14)	0.635	1600.0	1.800	1843.2
Door Bottom	0.770	1.2	1.005	0.9
Water Tanks	2.438	999.8	1.005	2.9
Internal Air (A1-A4)	16.573	1.2	1.005	20.0

The volumes for most of the zones were read from the SketchUp file, except for the water tank volume, which was calculated based on the size of the two intermediate bulk containers used, assuming they are filled to 90 percent of their total capacity. The volumes of the internal plant beds were all made equal in order to facilitate manual changes to capacitance values in future model runs. The density and specific heat capacity of each zone was based on the properties of the material in each zone. For example, it was assumed that the internal and external plant beds would be filled with soil and the water tank would be filled with water. The capacitance of each zone was calculated by multiplying the volume, density, and specific heat capacity. The specific heat capacity of the Water Tank zone was set to that of air in order to represent an empty water tank. The starting temperature and humidity of each zone was set to 0^{o}C and 95 percent relative humidity, respectively.

The dome glazing is 16 mm triple-wall polycarbonate structured sheet (PCSS), produced by Polygal. The relevant technical data for the PCSS provided by Polygal (2011) is as follows:

- Gauge: 16 mm (5/8”)
- Light Transmission: 70% (according to ASTM D1003)
- U-Factor: 0.41 $Btu \cdot h^{-1} \cdot ft^{-2} \cdot F^{-1}$ (0.71 $W \cdot m^{-2} \cdot K^{-1}$)
- R-Factor: 2.439 $Btu \cdot h^{-1} \cdot ft^{-1} \cdot F^{-1}$ (4.221 $W \cdot m^{-1} \cdot K^{-1}$)
- Shading Coefficient: 0.790
- Solar Heat Gain Coefficient (SHGC): 0.680
- Solar Reflection: 0.223

As this glazing material is not included in the TRNSYS window library, a window modelling software, WINDOW 6.3, developed by Lawrence Berkeley National Labs (LBNL, 2013), was used to create a new glazing system with these properties, which was then imported into TRNSYS for use with Type 56. This software is a database program, so users have the option to create a new window that is assembled from component pieces that are either found in pre-existing libraries of window component properties (i.e., frame, glazing, coating, properties) or are created specifically for a given project (LBNL, 2013).

Triple-wall PCSS is not in the glass library, so a new glass type with the properties listed above was created. As no detailed spectral data is available for this material, the spectral data for another glass type in the Window library, Makrolon 15 clear polycarbonate (NFRC_ID 9005), was used, as an approximation (LBNL, 2013).

To account for the inner support triangles within each of the Biodome windows, an estimate of the window to frame surface area was created, as shown in Figure 27, and was used to adjust the width of the window frames in the Window application.

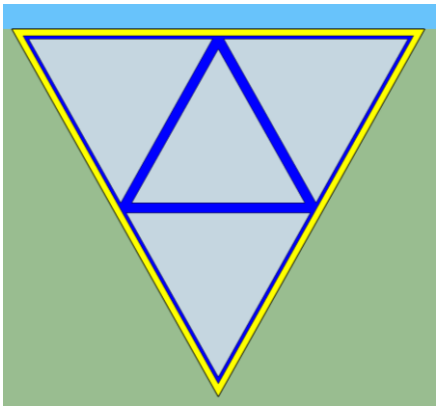

Legend

Colour	Description	Area (m^2)	%
Yellow	Wood frames that are included in the Sketchup model as ceiling surfaces	0.12	10.5
Blue	Wood frames that are missing from the Sketchup model	0.14	12.3
Grey	Remaining polycarbonate area	0.88	77.2

Figure 27: Representative window detail.

In TRNSYS, surfaces, such as walls and floors, are defined as components that are composed of layers. The layers used in the Biodome TRNSYS model and their properties are listed in Table 9. The layer composition of each component is listed in Table 10.

Table 9: Layers used in the TRNSYS model.

Layer	Conductivity (kJ/h·m·K)	Specific Heat Capacity (kJ/kg·K)	Density (kg/m^3)	Resistance (h·m^2·K/kJ)
SPRUCE_PIN	0.47	2	600	
PERPENDICU				0.036
HORIZONATAL				0.047
PLYWOOD	0.54	1.2	800	
MINERAL_WO	0.13	0.9	80	
POLYSTYREN	0.09	1.25	15	
GRANULAR_ROCK	12.6	1	2200	
TANK_PLASTIC				0.1
TANK_TOP				0.00001
SOIL_SURFACE				0.001

Table 10: Layer composition of each component used in the TRNSYS model.

Component	Layers
EXT_BED_SURFACE	HORIZONTAL
EXT_ROOF	SPRUCE_PIN
GRANULAR	GRANULAR_ROCK
GROUND_INSULATED	GRANULAR_ROCK, POLYSTYREN
KNEE_WALL	SPRUCE_PIN, PERPENDICU, PLYWOOD, MINERAL_WO, PLYWOOD, PERPENDICU, SPRUCE_PIN
SOIL_SURFACE	SOIL_SURFACE
TANK_TOP	TANK_TOP
TANK_WALL	TANK_PLASTIC
WOOD_WALL	SPRUCE_PIN

The properties of each component in a TRNSYS model are dependent on both the properties of the component's layers, such as the total thickness and the total u-value, as well as a set of defined values that are related to the component's surface properties, such as solar absorptance, the longwave emissions coefficient, and the convective heat transfer coefficient. The properties of each of the components used in the TRNSYS model are listed in Table 11. In TRNSYS the 'front' and 'back' of a component refer to the internal and external surfaces of the component, respectively (TRNSYS, 2012).

Table 11: Properties of each component used in the Biodome TRNSYS model.

Component	Total Thickness (m)	Total u-value ($W/m^2 \cdot K$)	Solar Absorptance of Wall		Longwave Emission Coefficient		Convective Heat Transfer Coefficient ($kJ/h \cdot m^2 \cdot K$)	
			Front	Back	Front	Back	Front	Back
EXT_BED_SURFACE	massless	2.948	0.6	0.6	0.9	0.9	11	64
EXT_ROOF	0.051	1.784	0.6	0.6	0.9	0.9	11	64
GRANULAR	0.102	5.022	0.6	0.6	0.9	0.9	11	0.001
GROUND_INSULATED	0.153	0.447	0.6	0.6	0.9	0.9	11	0.001
KNEE_WALL	0.318	0.177	0.6	0.6	0.9	0.9	11	11
SOIL_SURFACE	massless	5.76	0.6	0.6	0.9	0.9	11	11
TANK_TOP	massless	5.881	0.6	0.6	0.9	0.9	11	11
TANK_WALL	massless	1.887	0.6	0.6	0.9	0.9	11	11
WOOD_WALL	0.076	1.33	0.6	0.6	0.9	0.9	11	11

The default values for both the solar absorptance and the longwave emission coefficient were used, as more reliable data was not available. The convective heat transfer coefficient for each surface was set according to the guidelines provided in the TRNSYS manual, which states that standard values for inside and outside surfaces are

11 kJ/h·m^2·K and 64 kJ/h·m^2·K, respectively. Furthermore, for a boundary wall a value less than 0.001 indicates direct contact, while for other wall types a high convective heat transfer coefficient must be entered to ensure good contact (TRNSYS, 2012).

An air infiltration rate of one air change per hour was assumed, based on the estimated infiltration rates for greenhouses of different types and constructions provided by ASABE (2008), as shown in Table 12.

Table 12: Estimated infiltration rates for greenhouses by type and construction (Adapted from ASABE, 2008).

Construction	**Type**	**Infiltration Rate (N)[1]**	
		S $^{-1}$	**h $^{-1}$**
New Construction	Double plastic film	$2.1 \times 10^{-4} – 4.1 \times 10^{-4}$	0.75 – 1.5
	Glass or fiberglass	$1.4 \times 10^{-4} – 2.8 \times 10^{-4}$	0.50 – 1.0
Old Construction	Glass, good maintenance	$2.8 \times 10^{-4} – 5.6 \times 10^{-4}$	1.0 – 2.0
	Glass, poor maintenance	$5.6 \times 10^{-4} – 11.1 \times 10^{-4}$	2.0 – 4.0

[1] Internal air volume exchanges per unit time (s $^{-1}$ or h $^{-1}$). High winds or direct exposure to win will increase infiltration rates, conversely, low winds or protection from wind will reduce infiltration rates.

As is noted in Table 12, the air infiltration rate is affected by wind exposure and wind speed. In order to develop a more accurate estimate of the air infiltration, an equation relating the air infiltration to the wind speed may be used. Such an equation would require a measurement of the air tightness of the Biodome, which was not possible during the course of this thesis study. The Biodome is somewhat sheltered from the wind by surrounding buildings and trees, so the approximation of using a fixed infiltration rate was deemed acceptable for this study. Furthermore, it is the intent of those operating the Biodome to use forced ventilation and, as was noted earlier, Fuchs et al. (1997) found

that external wind speed has no significant effects on forced ventilation.

The Biodome is equipped with forced ventilation in the form of one solar powered exhaust ventilation fan with a maximum rated capacity of 500 cfm (0.24 m^3/s), depending on available solar radiation and intake ventilation area (GAF, 2015). The internal air volume of the Biodome is approximately 100 m^3, therefore the fan should provide a maximum of 8.6 air changes per hour. Given the fact that the ventilation intake area is limited, each of the openings is covered in a bug screen, and the solar panel will not always produce its maximum rated output, the ventilation rate was modelled as 4 air changes per hour, in addition to the 1 air change per hour due to infiltration. The fan's on/off control was modelled so that the fan is on whenever there is incident solar radiation in the plane of the solar panel, which faces south, with an approximate tilt of 50^o, and off when there is none.

The coupling air flow rate between the Dome zone and each of the Internal Air zones (A1-A4) and the Door Bottom zone was set to 5000 kg/h in order to ensure complete internal air mixing.

3.3.3 Calculators

There are three calculators used in the TRNSYS model, Wizard settings, Azimuth Angles, and Radiation, which are each described below.

The Wizard setting calculator was automatically generated when the 3D model was imported from Sketchup using the Multi-Zone Building Model Wizard. This calculator can be used to adjust the orientation of the Biodome by rotating it about the z-axis according to a defined number of degrees. There are no inputs to this calculator. The only

output from this calculator is to provide the Azimuth Angles calculator with the pre-defined number of degrees by which to rotate the Type 56 building.

The Azimuth Angles calculator is used to automatically calculate the azimuth angles of each of the surfaces in the model.

The Radiation calculator is used to calculate the amount of solar radiation incident on each of the surfaces in the model. The Radiation calculator is also used to turn on and off the ventilation according to whether where is any incident solar radiation in the plane of the exhaust vent's integrated solar panel.

3.3.4 Printers

There are three printers used in the TRNSYS model, Irradiation, Temperature, and System Printer. The Irradiation printer is automatically generated by the Multi-Zone Building Model Wizard. It is used to display a graph of the irradiation level on a given surface while the model is running. This data is not written to a file for future use. The Temperature printer is also automatically generated by the Multi-Zone Building Model Wizard and is similar to the Irradiation printer in that it is also used to display a graph of the temperature of a given zone while the model is running. This data is also not written to a file for future use. The system printer used in this model is Type25a. The system printer is used to log model results to a text file for a given set of data points for each time step in the model. In this model, the system printer is recording the air temperature of the dome, the soil temperature of the internal and external plant beds, and the temperature of the water tanks, each in one-hour time steps. This data can be retrieved after the model run is complete and can be used to do further data analysis.

3.4 Instrumentation and Control System

The main criteria in the design of the instrumentation and control system is that it be easily replicable and customizable for future projects, so all selected components must be readily accessible and affordable. The system must also be as energy efficient as possible, given the limited access to electricity and reliance on battery power.

A microcontroller, the Arduino UNO, is used as the data collection device. A microcontroller was chosen over a microcomputer because of its relative simplicity. A microcontroller is a single-chip microcomputer with on-board program ROM and programmable in/out pins, while a microcomputer uses a microprocessor, internal memory, and storage space to execute applications. The effect of this difference in architecture is that a microcontroller is only able to execute one program, which is programmed into the in/out pins, and it does not have the ability to perform data processing. A microcomputer is essentially a small personal computer and has all of the same capabilities and requirements, including the need to install an operating system, which may increase the difficulty of diagnosing problems, should they arise, and may also increase the required power consumption. Since there is no requirement in this project for data processing to be co-located with the sensors, as all data processing can be done remotely, a microcontroller is sufficient for this application.

With the rise in popularity and the drop in price of microcomputers and microcontrollers, there are now thousands of options available, both from both online retailers as well as electronics hobby shops, making the selection of an appropriate solution more difficult. Ultimately the Arduino UNO was selected because of its relative

ubiquity, low energy use, and low cost. According to its developers, “Arduino is an open-source electronics platform based on easy-to-use hardware and software... intended for anyone making interactive projects” (Arduino, 2015).

The main components connected to the Arduino UNO to form the instrumentation and control system include a power source, a real-time clock, a data storage module, thermocouples and thermocouple chips, voltage shifters, humidity sensors, and relays.

Each of these components is described in the following sections. A schematic of the Arduino UNO pin assignments is shown in Figure 28.

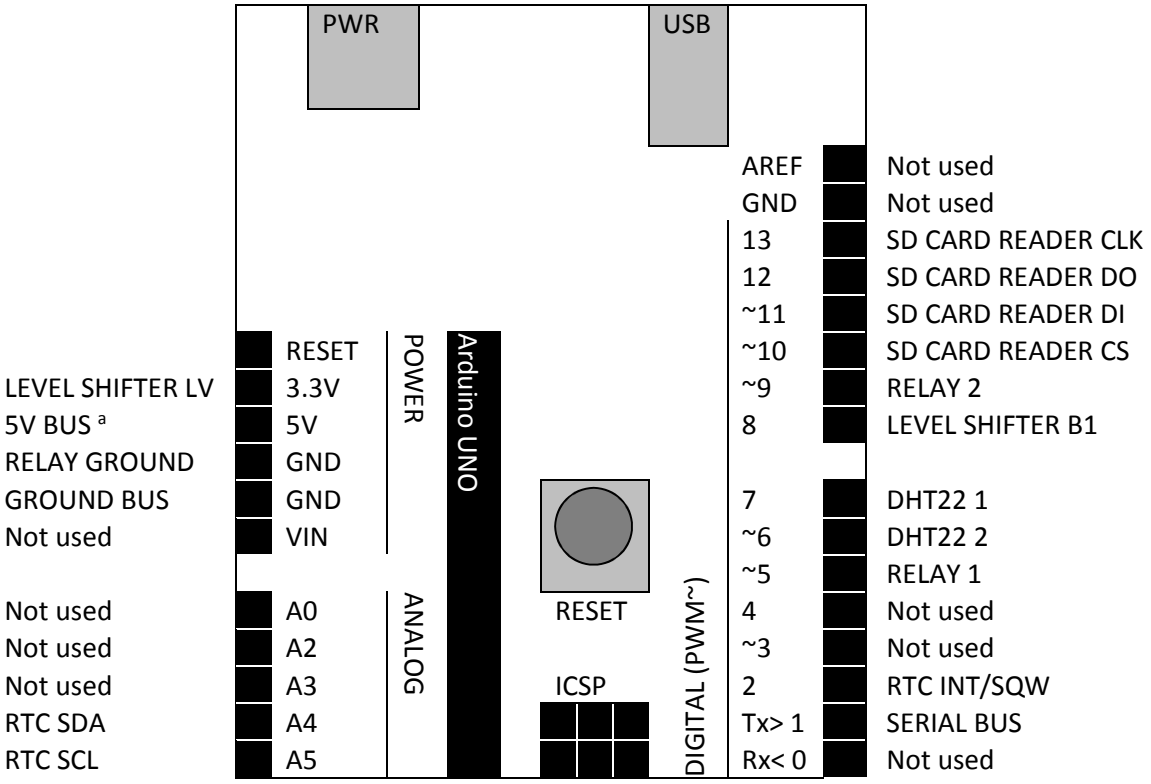

[a] When the Arduino UNO is powered by 12 V battery, via USB, the 5V pin is not used and the 5 V bus is instead powered by the 12 V battery through a step-down converter.

Figure 28: Schematic of Arduino UNO pin assignments.

3.4.1 Power

While actively reading data, the Arduino UNO was measured to have a current draw of approximately 50 mA and this stage lasts approximately three seconds. For the remainder of the 5 minute cycle between readings, the Arduino UNO was measured to have a current draw of approximately 29 mA, so the average current is approximately 29.2 mA, which at a voltage of 5 V means the Arduino requires 0.15 W of power, or 3.6 Wh of energy per day. Battery capacity is normally given in units of Ah, so the Arduino UNO would require a 5 V battery with a minimum capacity of about 700 mAh to run for 24 hours. During the initial testing phases, four 1.2 V rechargeable AA batteries with a capacity of 2500 mAh were used as the power source for the Arduino UNO and were connected via the barrel socket power input (PWR in Figure 28). These batteries were typically able to last just over 3 days before being recharged.

During the attempted EAHE fan tests the Arduino UNO was powered by the same 12 V batteries that were used to run the fans. A step-down converter was used to convert the 12 V source to a steady 3.3 V source that was connected to the Arduino UNO via the USB port (USB in Figure 28). Ultimately, the Arduino UNO will be connected to the 12 V batteries being charged by the solar panels, but as of November 2015 this system was not yet functional, so temporary solutions were implemented for the purposes of this study.

3.4.2 Real-Time Clock

The Arduino UNO does not have an integrated real-time clock (RTC), so it is only able to use an internal counter to calculate elapsed time. This method of calculating time is inaccurate and limited by the maximum number on the counter. Additionally, it cannot

be easily related to the real time, and is reset every time the Arduino UNO is reset (Buyapi, 2015).

The addition of an RTC allows the Arduino UNO to more accurately perform tasks that are time-dependent or cyclical, such as performing readings every 5 minutes, and facilitates the management of system energy consumption through the use of hibernation and wake-up schedules between actions. The RTC module used in this project uses the DS3231 high-precision RTC chip, manufactured by Maxim Integrated. The pin assignments and connections for the RTC module are shown in Figure 29.

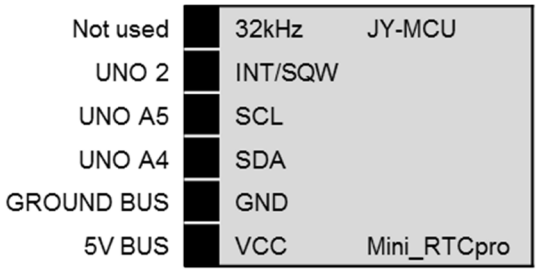

Figure 29: Real-time clock module pin diagram.

3.4.3 Data Storage Module

Data collected by the Arduino UNO is stored on a microSD card by the SD card reader module. A picture of the SD card reader module as well as the pin assignments and connections for the SD card reader module are shown in Figure 30.

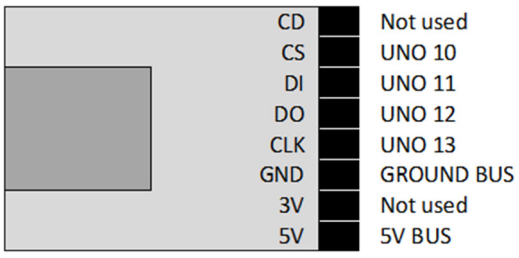

Figure 30: MicroSD card breakout board pin diagram.

The main advantage of using a microSD card is that it can be easily transferred between the system and another computer for data processing. Conversely, the main disadvantage of using a microSD card is that it can become corrupted from hard shutdowns, but these events should be rare. In the event that the microSD card becomes corrupted, it can be easily replaced.

3.4.4 Thermocouples

Thermocouples are used to sense temperature indirectly by measuring the electric current that is produced by two wires of different metals joined together. In order to convert the measurement of this electric current into a temperature, the reference temperature (T_A) or cold-compensation reference, must be known.

The thermocouples used in this project are made from K-type thermocouple wire that is polyvinyl insulated, 24 AWG stranded, with a special limit of error (SLE) designation. The SLE designation indicates a reduced error limit, which in this case is the greater of 1.1^{o}C or 0.4 percent. Each thermocouple end was covered in heat shrink to help protect it from the humidity in the greenhouse.

To read and interpret the voltage from the thermocouples, thermocouple amplifier breakout boards from Adafruit are used. Each breakout board includes a MAX31850K integrated circuit (IC), a 3.3 V regulator, and 10 uF bypass capacitors (Adafruit, 2015). These boards can be used with any microcontroller that has 1-Wire support. The thermocouples are attached to the breakout boards by screw terminals, which are provided separately and must be soldered in place. The pin assignments and connections for the breakout board are shown in Figure 31.

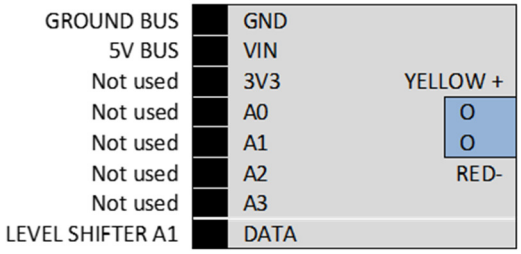

Figure 31: Thermocouple amplifier breakout board pin diagram.

As the Arduino UNO is a 5 V microcontroller and the thermocouple breakout boards used in this project require 3.3 V power on the data line, a level shifter is required to connect the breakout boards to the Arduino UNO. For this project a bi-directional logic level converter (BSS138) from Adafruit was used. The pin assignments and connections for the logic level converter are shown in Figure 32. It should be noted that a 4.7 K resistor is used to connect the LV and A1 pins on the level converter.

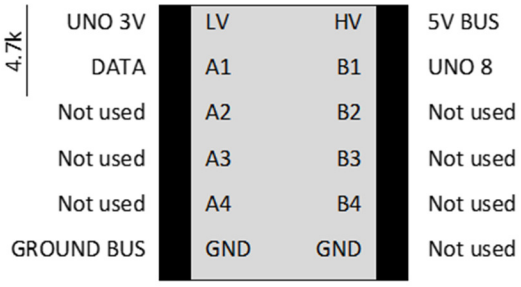

Figure 32: Logic level converter and pin diagram.

The IC on the thermocouple amplifier breakout board, which is manufactured by Maxim Integrated, is a “thermocouple-to-digital converter with a built-in 14-bit analog-to-digital converter, cold-junction compensation sensing and correction, a digital controller, a 1-Wire data interface, and associated control logic” (Maxim, 2013). Each IC has a unique hard-coded 64-bit serial code, which allows one microcontroller to monitor

the temperature from many thermocouples, all on the same bus (Maxim, 2013), connected by the data pin on each breakout board. Therefore, the data pins on all of the thermocouple breakout boards can be connected to each other in series, as shown in Figure 33.

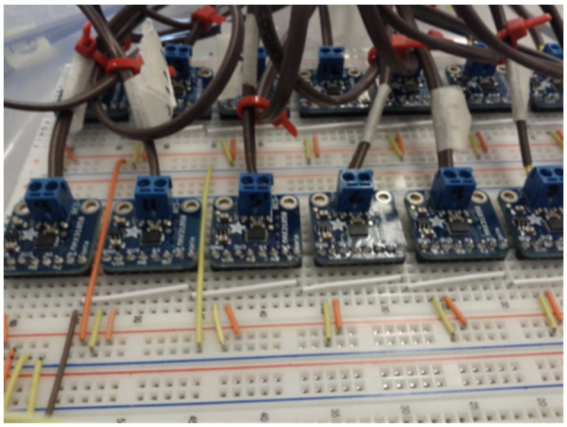

Figure 33: Assembled thermocouple breakout boards connected in series.

The cold-compensation equation, which is used by the IC to account for the difference between the thermocouple cold-junction side (device ambient temperature) and a 0°C virtual reference, is given in Equation 5.

$$V_{OUT} = (41.276) \times (T_R - T_A) \quad (5)$$

where: V_{OUT} is the thermocouple output voltage (µV)

41.276 is the gain term, or Seebeck Coefficient (µV/°C)

T_R is the temperature of the remote thermocouple junction, or hot-junction (°C)

T_A is the temperature of the device, or the cold-junction (°C)

Rearranging Equation 5 to solve for T_R, results in Equation 6.

$$T_R = \frac{V_{OUT}}{(41.276)} + T_A \quad (6)$$

3.4.5 Humidity Sensors

The temperature and humidity sensors used in this project are DHT22 sensors from Adafruit. The pin assignments for the humidity sensor are shown in Figure 34.

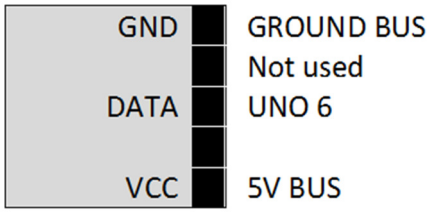

Figure 34: DHT22 Temperature and humidity sensor pin diagram.

The DHT22 uses a polymer capacitive humidity sensor and a thermistor to measure the surrounding air humidity and temperature, respectively, and produces a digital signal that can be read by any microcontroller. A 4.7K to 10K resistor is used as a pull-up from the data pin to VCC. The measuring range of this sensor is 0 to 100 percent relative humidity with 2 to 5 percent accuracy, and -40 to 125^{o}C temperature readings with ±0.5^{o}C accuracy. The ASABE (2008) recommends that humidity sensors be aspirated in order to reduce the temperature gradients in the vicinity of the sensors. No aspiration is provided for these sensors, which may increase the potential for errors.

3.4.6 Relays

The fans for the EAHE are run on 12 V power so relays are required to enable the fans to be controlled by the Arduino UNO, which is a 5 V microcontroller. For this project a Keyes 2-channel, 12 V, optically isolated, high-voltage relay module was used. The pin assignments and connections for the relays are shown in Figure 35.

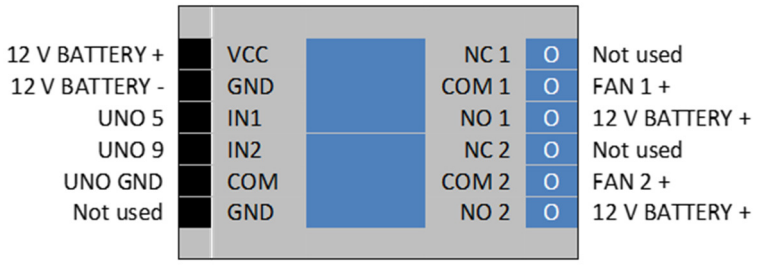

Figure 35: Relay module pin diagram.

The Arduino UNO offers the advantage of the availability of a free, user-friendly, open-source Integrated Development Environment, Arduino Software, which integrates an Arduino programming language editor and compiler. Open-source software is developed by many people, both individually and working in collaboration, and its distribution terms must comply with a set of defined criteria, as set out by the Open Source Definition (Open Source Initiative, 2015). There is also a vast amount of documentation, sample code, and support available online, which make programming an Arduino much easier.

The Arduino code used in this project is provided in Appendix C. This code may be used on any microcontroller with an Arduino chip, but must first be modified to include the applicable thermocouple breakout board addresses.

3.5 Instrumentation Plan

Thermocouples were placed in 22 locations throughout the Biodome, as listed in Table 13. The thermocouples placed in the EAHE pipes were carefully measured, tied together and pulled through the pipes so that they are located at one-third and two-thirds of the distance from the air intake box to the air outlet boxes, as well as one at the pipe opening in each outlet box and one at the pipe opening in the air intake box. The locations of the

thermocouples in the EAHE pipes were selected in order to measure the difference in temperature between pipes as well as the temperature gradient across the length of each pipe. Once installation of the solar panel battery charging system is complete and it becomes possible to power the fans in the EAHE system and perform experiments on the operation of the EAHE system, the distribution of thermocouples throughout the EAHE pipes will be important to characterize the heat transfer gradient across the length of the pipes.

Table 13: Thermocouple locations.

Thermocouple Locations			
1/3 of pipe 1	1/3 of pipe 4	Air intake box	North soil – 0.2 m depth
2/3 of pipe 1	2/3 of pipe 4	Air outlet box 1	South soil – 0.2 m depth
1/3 of pipe 2	1/3 of pipe 5	Air outlet box 2	South soil surface
2/3 of pipe 2	2/3 of pipe 5	South ceiling	Water tank
1/3 of pipe 3	1/3 of pipe 6	North ceiling	
2/3 of pipe 3	2/3 of pipe 6	Dome top	

Three thermocouples are used to measure the ambient air temperature inside the Biodome: two thermocouples are attached to ceiling trusses at opposite ends of the dome (northern-most wall and southern-most wall) at the half-way point between the dome floor and the dome apex; and one thermocouple was suspended 10 cm from the dome apex. These three thermocouples allow for partial measurement of air temperature gradients. Two thermocouples were placed in the centre of the soil in the planting boxes on either side of the air intake box, at a depth of 0.2 m. One thermocouple was placed in the centre of the soil in the southern-most planting box just below the soil surface, at a depth of 5 cm. The locations of the thermocouples in the soil were selected in order to

measure the vertical temperature gradient in the planting boxes. One thermocouple was suspended in the centre of one of the two water tanks as it is assumed that the temperature of the water will be uniform as it will be a well-mixed tank.

3.6 Model Calibration Approach

Many other greenhouse TRNSYS models have been used, but none have been models of geodesic dome greenhouses, so it is especially important to calibrate and validate the results of this model. Calibration is the process of developing estimates of unknown or variable model parameters by comparing model results for a given set of conditions and parameters with data collected under the same conditions. Uncertainly analysis is used to define potential errors in the observed data, which may affect the model calibration. The methods used to perform calibration and uncertainty analysis on the model are discussed below.

Calibration of the TRNSYS model was done manually and consisted of changing model parameter values while tracking the effect of these changes on the agreement between modelled and measured results. The agreement between the modelled and measured results was analysed using the sample correlation coefficient (r) and the Pearson coefficient of determination (r^2), as described below. The correlation coefficient, which is defined in Equation 7 can range from −1 to 1 and is a measure of the degree of closeness of the linear relationship between observed and simulated data.

$$\mathrm{r} = \frac{\sum \mathrm{x}_1 \mathrm{x}_2}{\sqrt{\sum \mathrm{x}_1^2 \sum \mathrm{x}_2^2}} \qquad (7)\ (\text{Snedecor and Cochran, 1982})$$

where: x_1 = Deviation of observed data from the sample means

x_2 = Deviation of the simulated data from the sample means

For example if r is equal to 0, no linear relationship exists, but if r equals either 1 or −1, a perfect positive or negative linear relationship exists, respectively.

Similarly, r^2 describes the proportion of the variance in the measured data that can be accounted for in the model. The values of r^2 can range from 0 to 1, with higher values indicating less error variance.

In addition to these two mathematical metrics, two graphical methods of model evaluation were employed during calibration. The first was a time series plot of modelled and measured air and soil temperatures in the Biodome throughout the calibration period, which was used to visually compare simulated and measured data and identify differences in magnitude and timing of peak and minimum temperatures. The second was a plot of modelled versus measured data points. The slope and y-intercept of the best-fit regression line of this plot can indicate how well modelled data match measured data. The slope indicates the relative relationship between modelled and measured values, while the y-intercept indicates the presence of bias, or the average tendency of the modelled data to be larger or smaller than the measured data. A slope of 1 and a y-intercept of 0 indicate perfect agreement between the modelled and measured data, assuming a linear relationship exists.

3.7 Summary

This section described the experimental and modelling approaches used in this thesis. The following chapter describes the actual experimental results and the corresponding modelled results.

Chapter 4

Results and Discussion

4.1 Introduction

This section begins with the model calibration results. Next, the experimental and modelled scenario results are presented, compared, and discussed. Finally, an uncertainly analysis of the experimental and modelled scenario results is presented.

4.2 Model Calibration

The data used to calibrate a model have a direct effect on the model validation and must therefore be chosen carefully. The period from hour 1944 to hour 2304 (March 23, at 12 am to April 6 at 12 am) was used for the model calibration as this is the first period for which there are continuous results and during which time most variables within the dome were kept constant. The model was run from hour 0, as opposed to starting at hour 1944, in order to allow each zone to reach realistic equilibrium conditions prior to the start of the calibration period, rather than starting from the pre-defined temperature, which was set to $0^{o}C$ for each zone in the model.

During the selected time period the water tanks were empty, the exhaust ventilation was off (with a couple of exceptions on days when volunteers at the Biodome inadvertently turned on the overhead ventilation system) and all of the ventilation windows were closed, resulting in low passive ventilation and low air infiltration.

As was described in Section 3.5, thermocouples were used to measure the air

temperature inside the dome at three different locations. A graph of the temperature readings at these three locations is shown in Figure 36, with a plot of outdoor air temperature included for reference. As shown in Figure 36, there is very little difference between the temperature readings at each of these three locations, indicating that there is little to no thermal stratification within the Biodome.

Also included in Figure 36 are the temperature readings taken in the EAHE air intake box and two outlet boxes (north and south). The damping effect of the thermal mass of the rock bed beneath the EAHE air intake box is evident from the difference in air temperature between this location and temperature of the air within the Biodome. The temperature fluctuations in the north and south outlet boxes were similarly buffered by the rock bed thermal mass.

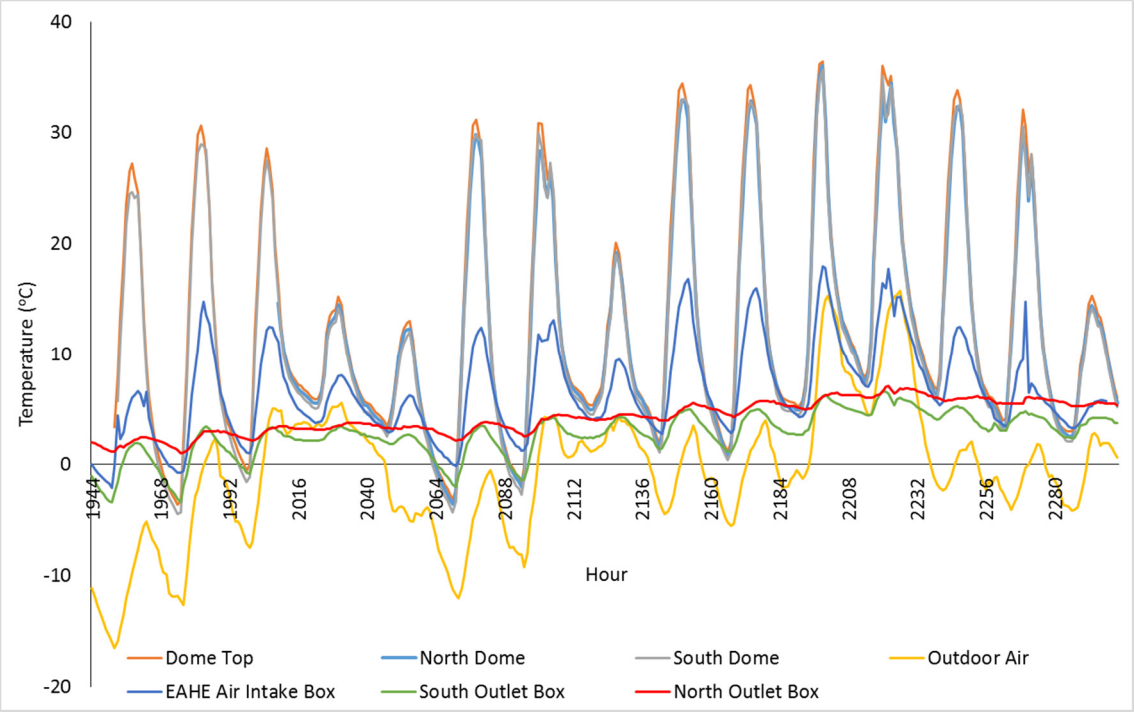

Figure 36: Measured Biodome and outdoor air temperatures for hours 1944 to 2304.

It was noted that the temperature variation in the south outlet box was much greater than that of the north outlet box. Upon further investigation a large gap was discovered in the exterior wall of the south outlet box, next to the door frame, which allowed a high air infiltration rate into this area, causing unusually high daily temperature swings. This gap was later repaired with spray-in foam insulation, which reduced the temperature difference between the two outlet boxes.

For the calibration between the modelled results and the measured results of the air temperature in the Biodome, an average of the temperature readings at the dome top, north, and south, will be used in order to account for the slight differences in air temperature due to stratification.

As shown in Figure 37, the temperature readings taken throughout the EAHE pipes and in the north and south soil are much more variable than the Biodome air temperature readings. The most variable EAHE pipe temperature readings were taken in pipe 3. These large variations can be attributed to the fact that pipe 3 shifted during installation and is located much closer to the surface of the rock bed than had been planned. As such, it is subject to larger temperature variations through the rock bed surface.

For the calibration between the modelled results and the measured results, an average of the temperature readings in the north soil, south soil, 2/3 of pipe 2, and 2/3 of pipe 5 will be used in order to incorporate the effect of the temperature gradient through the soil.

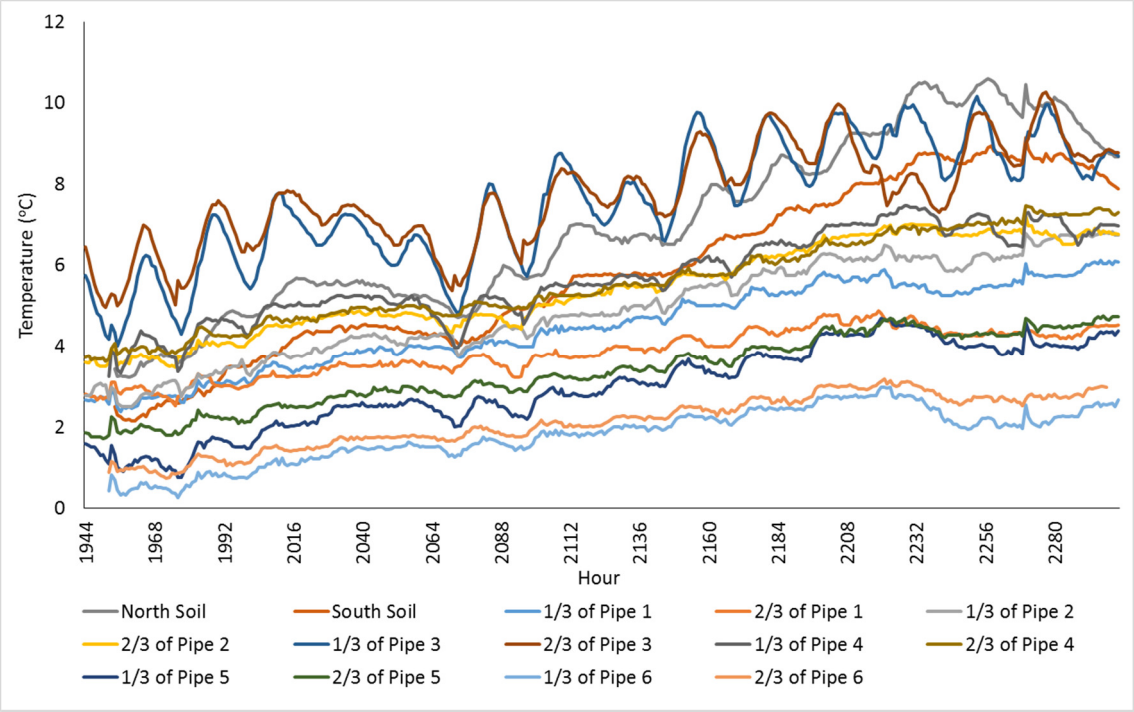

Figure 37: Measured Biodome underground air and soil temperatures for hours 1944 to 2304.

The initial model run, Model 1, produced results that were a good approximation of the Biodome air temperatures, with r and r^2 values of 0.953 and 0.908, respectively, as shown in Table 14. The modelled soil temperatures were not as accurate, with r and r^2 values of 0.914 and 0.835, respectively.

Table 14: Correlation between measured and modelled air and soil temperature.

Coefficient	Measured vs Model 1 Air Temperature	Measured vs Model 1 Soil Temperature
r	0.953	0.914
r^2	0.908	0.835

The time series plot of the Model 1 and measured air and soil temperatures in the Biodome, presented in Figure 38, confirms that the Model 1 air temperatures represent

a good approximation of the Biodome air temperatures over the calibration period, but the Model 1 soil temperatures do not. The average modelled soil temperatures are much higher than the average measured temperatures and include greater hourly fluctuations than are present in the measured data. The scatter plot of Model 1 modelled versus measured Biodome air and soil temperatures over the calibration period in Figure 39 further confirms that the modelled air temperatures represent a good approximation of the Biodome air temperatures over the calibration period and that the modelled soil temperatures do not.

It is likely that the differences between the modelled and measured soil temperatures are a result of the use of an average value for the measured soil temperature, which does not account for the temperature stratification in the soil. Another contributing factor is that the thermocouples are actually measuring the temperature of the air within the underground EAHE tubes, which may not be exactly the same as the temperature of the surrounding soil due to air infiltration through the ends of the EAHE tubes. It is also possible that the model does not accurately reflect all of the modes of heat transfer from the soil. For example, heat is lost from the soil when the plant beds are irrigated with cool water, which serves to both lower the soil temperature and to increase its thermal mass. Heat is also lost from the surface of the soil through evaporation, the effects of which are not included in the model.

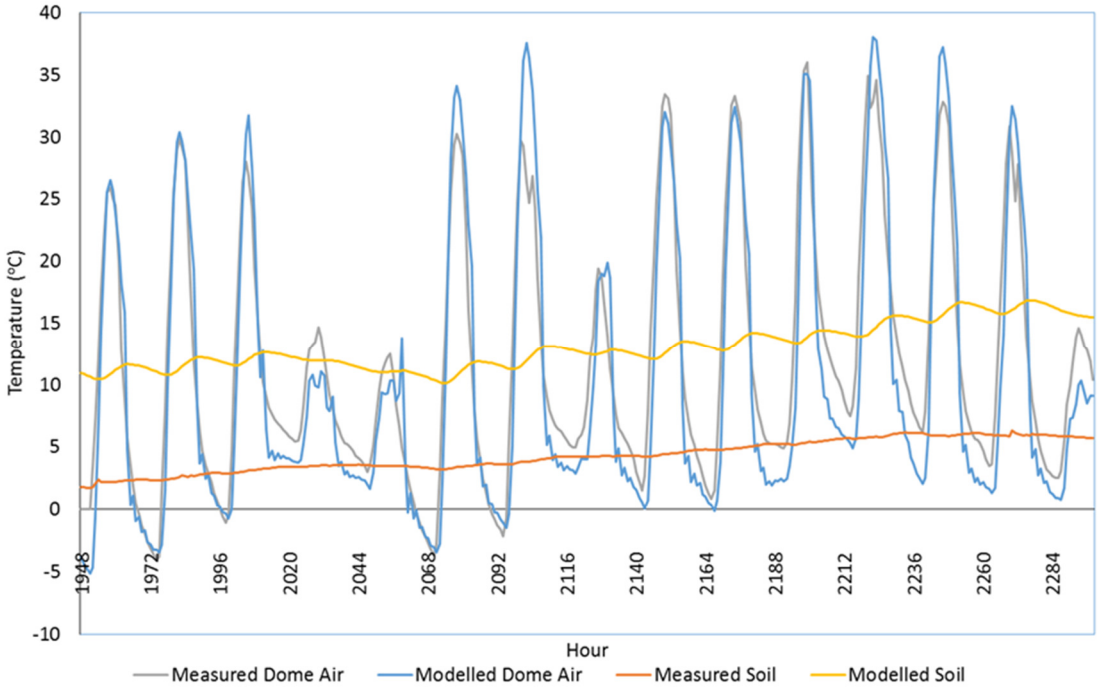

Figure 38: Time series plot of Model 1 and measured air and soil temperatures in the Biodome over the calibration period.

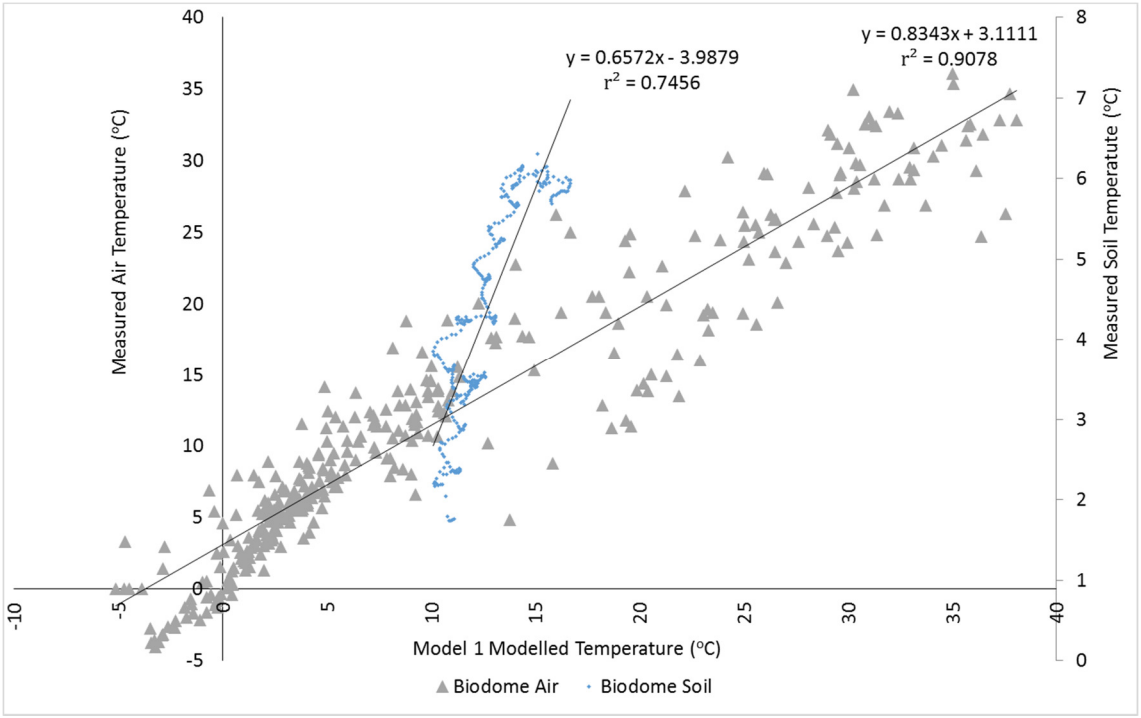

Figure 39: Scatter plot of Model 1 results versus measured Biodome air and soil temperatures over the calibration period.

Measurable or identifiable geometries, materials, and schedules were used in the model, but the physical characteristics of some materials were not known and were approximated. These approximated characteristics were used as adjustable parameters to improve model fit during the model calibration.

The only surface in the Biodome model for which physical characteristics were varied was that of the soil surface, as this is the main surface whose properties are most uncertain due to the variable nature of soil, which depend on its composition, moisture content, etc. The properties of the soil surface that were varied in order to determine their effect on model fit were solar absorptance and the convective heat transfer coefficient. Both of these properties and their effect on the model results are described in the following sections.

4.2.1 Solar Absorptance Calibration

For Model 2, the default solar absorptance values for the front and back surfaces of the soil were changed to 0.9, which would be appropriate for a near-black body. The r and r^2 for the measured versus modelled air and soil temperatures for Model 1 and Model 2 are shown in Table 15. Although the effects of these changes on the modelled air temperatures were very small, they resulted in less accurate modelled soil temperature results than those of Model 1.

Table 15: Effect on modelled results of changing soil surface solar absorptance.

Model	Solar Absorptance of Soil Surface		Measured versus Modelled Air Temperature		Measured versus Modelled Soil Temperature	
	Front	Back	r	r^2	r	r^2
Model 1	0.6	0.6	0.953	0.908	0.906	0.820
Model 2	0.9	0.9	0.953	0.908	0.895	0.801

As shown in Figure 40, the modelled air temperatures changed very little between Model 1 and Model 2, but the modelled soil temperature increased significantly, which represents a less accurate outcome than in Model 1.

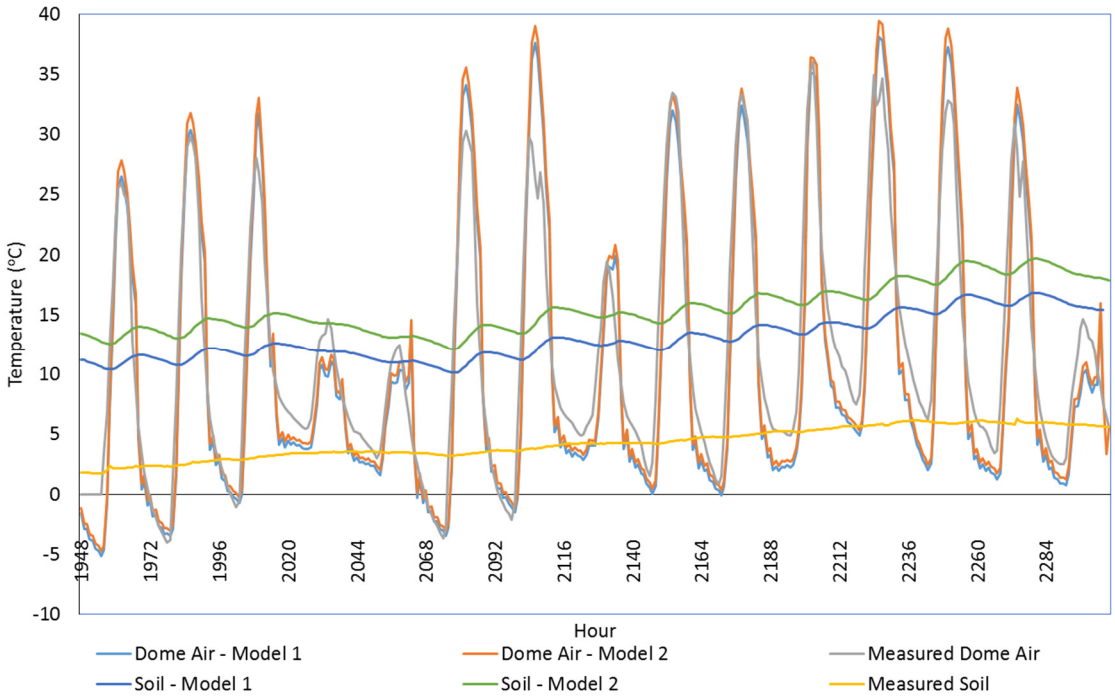

Figure 40: Graph of effect on modelled results of changing soil surface solar absorptance.

The scatter plot of Model 2 modelled versus measured Biodome air and soil temperatures over the calibration period in Figure 41 further confirms that the modelled air temperatures represent a good approximation of the Biodome air temperatures over the calibration period and that the modelled soil temperatures do not.

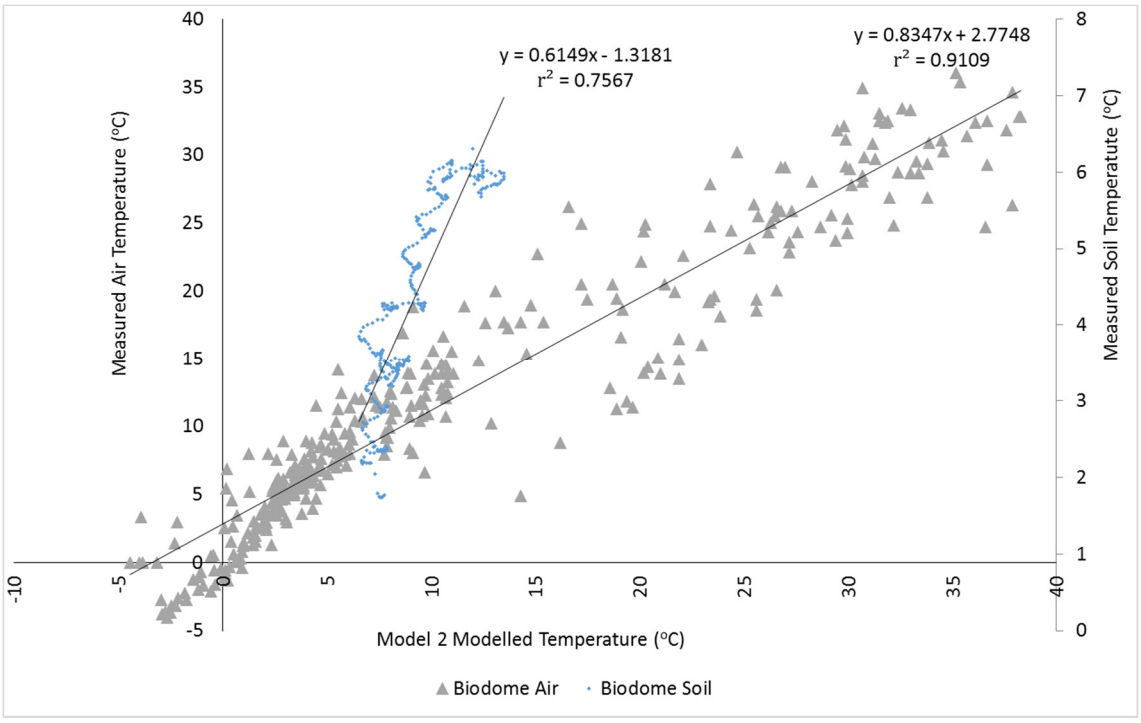

Figure 41: Scatter plot of effect on modelled results of changing soil surface solar absorptance.

4.2.2 Convective Heat Transfer Coefficient Calibration

The effect of changing the convective heat transfer coefficient of the back surface of the soil was studied by varying only this parameter, as shown in Table 16. The results of Model 1 are included for reference. The value of the solar absorptance of the soil surface was left at 0.6.

Table 16: Effect on modelled results of changing soil surface convective heat transfer coefficient.

Model	Convective Heat Transfer Coefficient of Soil Surface (kJ/h m^2 K)		Measured versus Modelled Air Temperature Results		Measured versus Modelled Soil Temperature Results	
	Front	Back	r^2	r	r^2	r
Model 1	11	11	90.8%	95.3%	82.0%	90.6%
Model 3	11	0.001	90.7%	95.2%	81.0%	90.0%
Model 4	11	64	90.9%	95.4%	84.0%	91.6%
Model 5	11	600	91.1%	95.4%	85.4%	92.4%
Model 6	11	1000	91.1%	95.4%	85.5%	92.5%
Model 7	11	3000	91.1%	95.4%	85.6%	92.5%
Model 8	11	Internal Calculation	91.1%	95.4%	85.6%	92.5%

For Model 3, the convective heat transfer coefficient of the back surface of the soil was reduced to 0.001 kJ/h m^2 K, which resulted in a slight decrease in r and r^2 values for both the air and soil comparisons between modelled and measured results, so this model was ruled out.

For Model 4 though Model 7, the convective heat transfer coefficient of the back surface of the soil was progressively increased from 64 to 3000 kJ/h m^2 K, which resulted in slightly higher r and r^2 values for both the air and soil comparisons between modelled and measured results.

For Model 8 an internal calculation was used, rather than a fixed value. This version of the model took approximately four times as long to run and the results were comparable to those where the heat transfer coefficient was set to 3000, so the increased computational time did not justify any possible increase in accuracy, for this variable.

As shown in Figure 42, the change in convective heat transfer coefficient of the back surface of the soil had very little effect on the modelled air temperature, but had a significant effect on the modelled soil temperatures, which became progressively lower and closer to the measured soil temperatures as the convective heat transfer coefficient was increased.

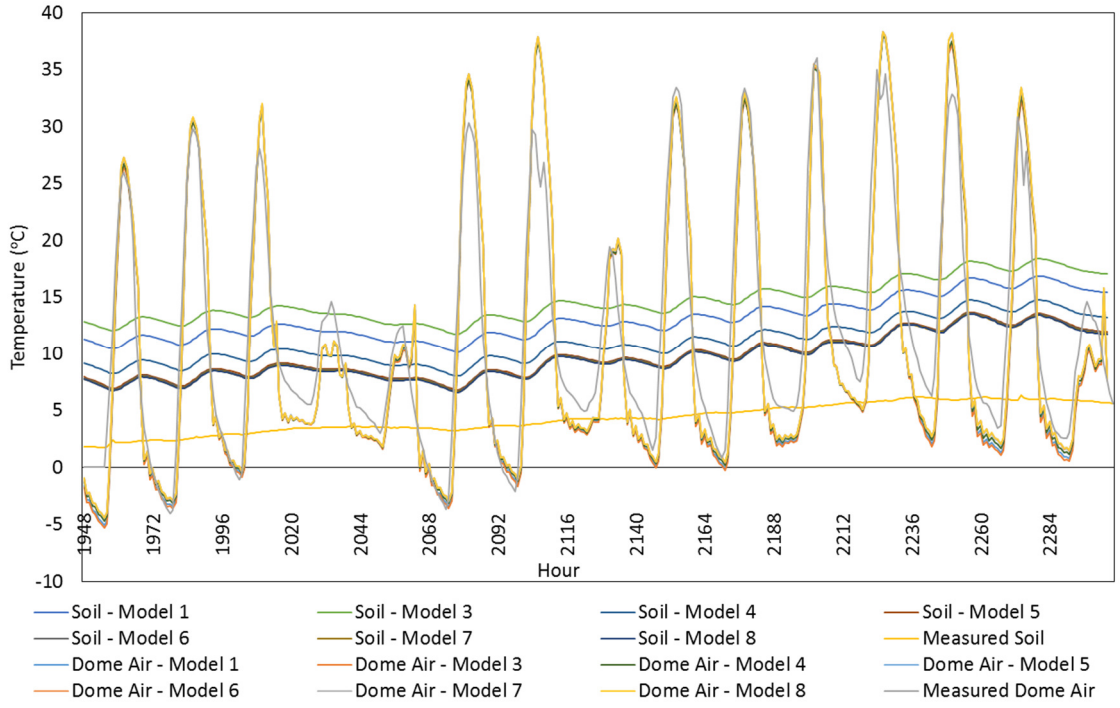

Figure 42: Graph of effect on modelled results of changes in modelled convective heat transfer coefficient of the soil surface.

Similarly, as shown in Table 17, the linear trend line equations of measured versus modelled air and soil temperatures improved with increasing convective heat transfer coefficients. Ultimately, Model 5, with a soil surface convective heat transfer coefficient of 600, was selected as the base model to be used in further analysis, as the increases in model accuracy for larger coefficients were only marginal, and it is unclear what other effects, if any, a much larger coefficient may have on other modelled values.

Table 17: Linear trend line equations of measured versus modelled air and soil temperatures for different convective heat transfer coefficients of the soil surface.

Model	Linear Trend Line Equation of Measured versus Modelled Air Temperatures	Linear Trend Line Equation of Measured versus Modelled Soil Temperatures
Model 1	y = 0.81x + 2.79	y = 0.59x - 4.56
Model 3	y = 0.83x + 3.22	y = 0.67x - 5.20
Model 4	y = 0.84x + 2.93	y = 0.63x - 2.37
Model 5	y = 0.83x + 2.80	y = 0.62x - 1.46
Model 6	y = 0.83x + 2.79	y = 0.62x - 1.40
Model 7	y = 0.83x + 2.78	y = 0.62x - 1.34
Model 8	y = 0.83x + 2.77	y = 0.61x - 1.32

4.3 Scenario Results

The calibrated model was run under each of the scenarios defined in Chapter 3 using actual 2015 weather data in order to compare these results to the experimental results measured in the Biodome over the same time period. As was the case during the model calibration, a model start time of 0 was used as opposed to starting the model at the hour at which actual measurements began for a particular scenario in order to allow each zone to reach equilibrium conditions prior to the start of the actual scenario period. The model scenarios were each run again for a full year using the CWEC weather data in order to compare the performance of each scenario for a typical weather year. The results for each of the modelled scenarios are described in the following sections.

4.3.1 Scenario A

Model Scenario A represents the case where the Biodome is run as a closed system, with no forced ventilation, no extra thermal mass. Measured results for the period from hour 1951 to 2302 are used as the actual results for this time period. This scenario presents the same conditions as those used for model calibration, so it also serves the function of model validation using the calibrated model.

As shown in the time series plot of Scenario A versus measured air and soil temperatures, in Figure 43, the modelled Scenario A results for Biodome air temperature match the measured air temperatures well, but the modelled soil temperatures are consistently higher and show more daily variation than the measured temperatures. The three visible dips in measured air temperature at hours 2103, 2222, and 2271 were all caused by the forced overhead ventilation being turned on inadvertently by volunteers working in the Biodome.

As shown in the scatter plot in Figure 44, the r^2 value of the modelled versus measured air and soil temperatures are 0.91 and 0.88, respectively, which further indicates good model fit of the air temperature results, but less good fit of the soil temperature results.

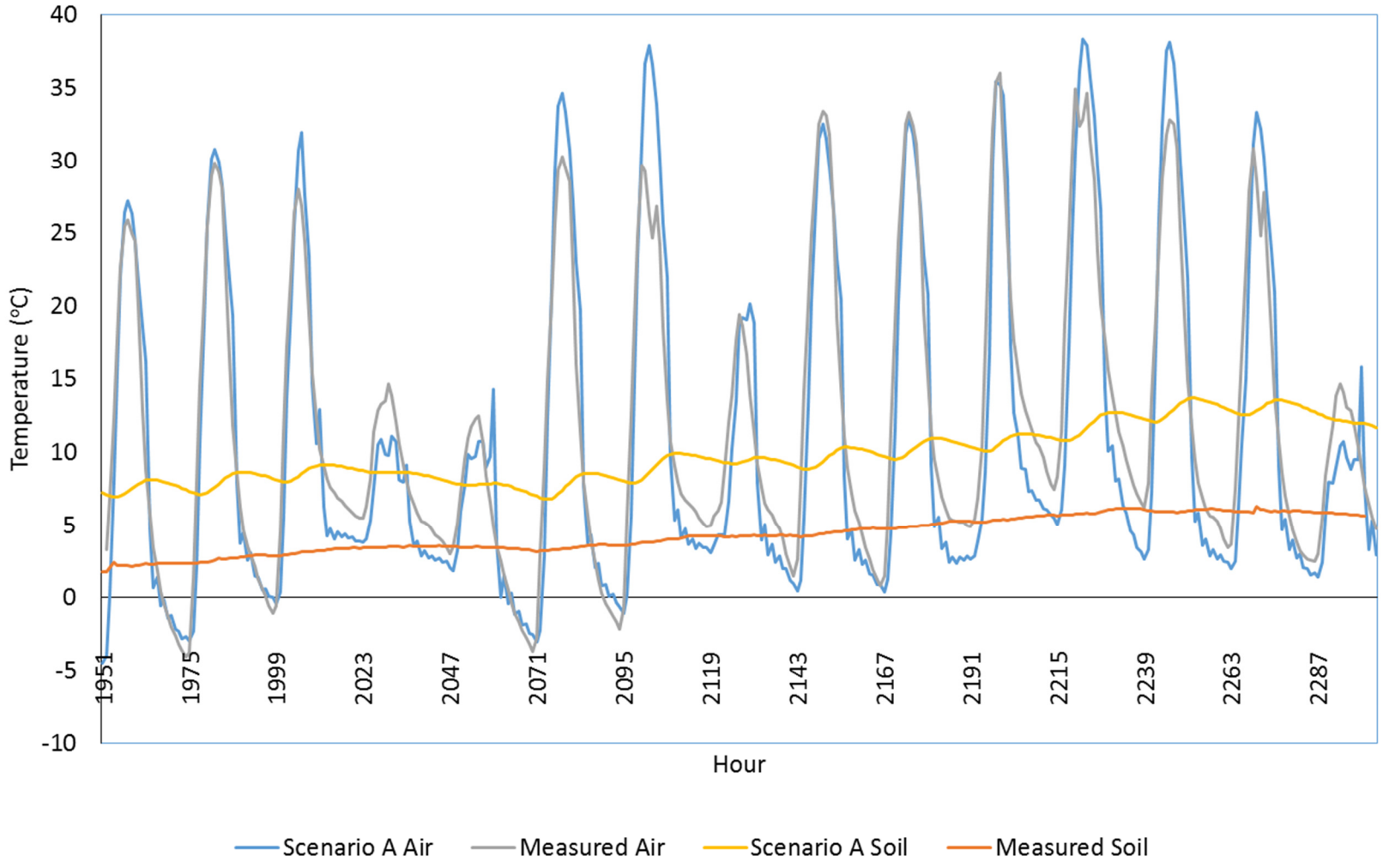

Figure 43: Time series plot of Scenario A modelled and measured air and soil temperatures in the Biodome.

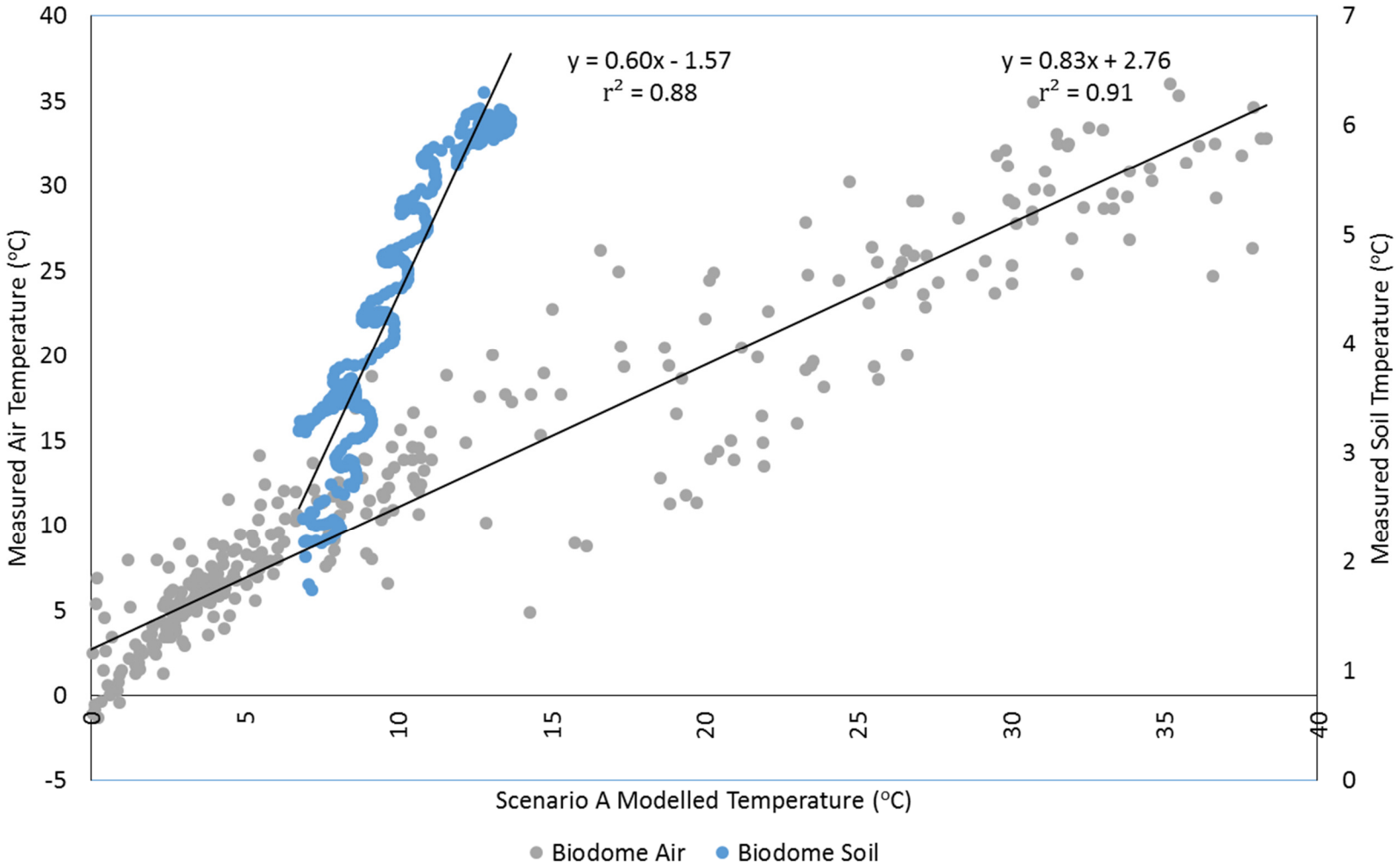

Figure 44: Scatter plot of Scenario A results versus measured Biodome air and soil temperatures for the same period.

4.3.2 Scenario B

Model Scenario B represents the case where the Biodome is run as a closed system, with extra thermal mass, in the form of a water tank, but no forced ventilation. Measured results for the period from hour 1626 to 1705 are used as the actual results for this time period. The period of measured results for this scenario is much shorter than for that of the other scenarios, as the water tank was emptied after the third day so that it could be moved in order to accommodate construction activities within the Biodome. The addition of water to the tank was modelled by increasing the thermal capacity of the water tank zone in the TRNSYS model to 10,203.9 kJ/K, which represents the thermal capacity of an equivalent volume of water.

As shown in the time series plot of Scenario B versus measured air and soil temperatures, in Figure 45, the modelled Scenario B results for Biodome air temperature match the measured air temperatures well and the modelled soil temperatures are consistently higher than the measured temperatures. The Scenario A results are included for reference and to demonstrate the negligible effect on the modelled air and soil temperature results of changing the water tank zone thermal properties. The Scenario B water tank temperatures are included for reference, but there are no measured values against which to compare these temperatures, as there was no thermocouple in the water tank during this time.

As shown in the scatter plot in Figure 46, the r^2 value of the modelled versus measured air and soil temperatures are 0.92 and 0.76, respectively, which further indicates good agreement for the air temperature results, but not for the soil.

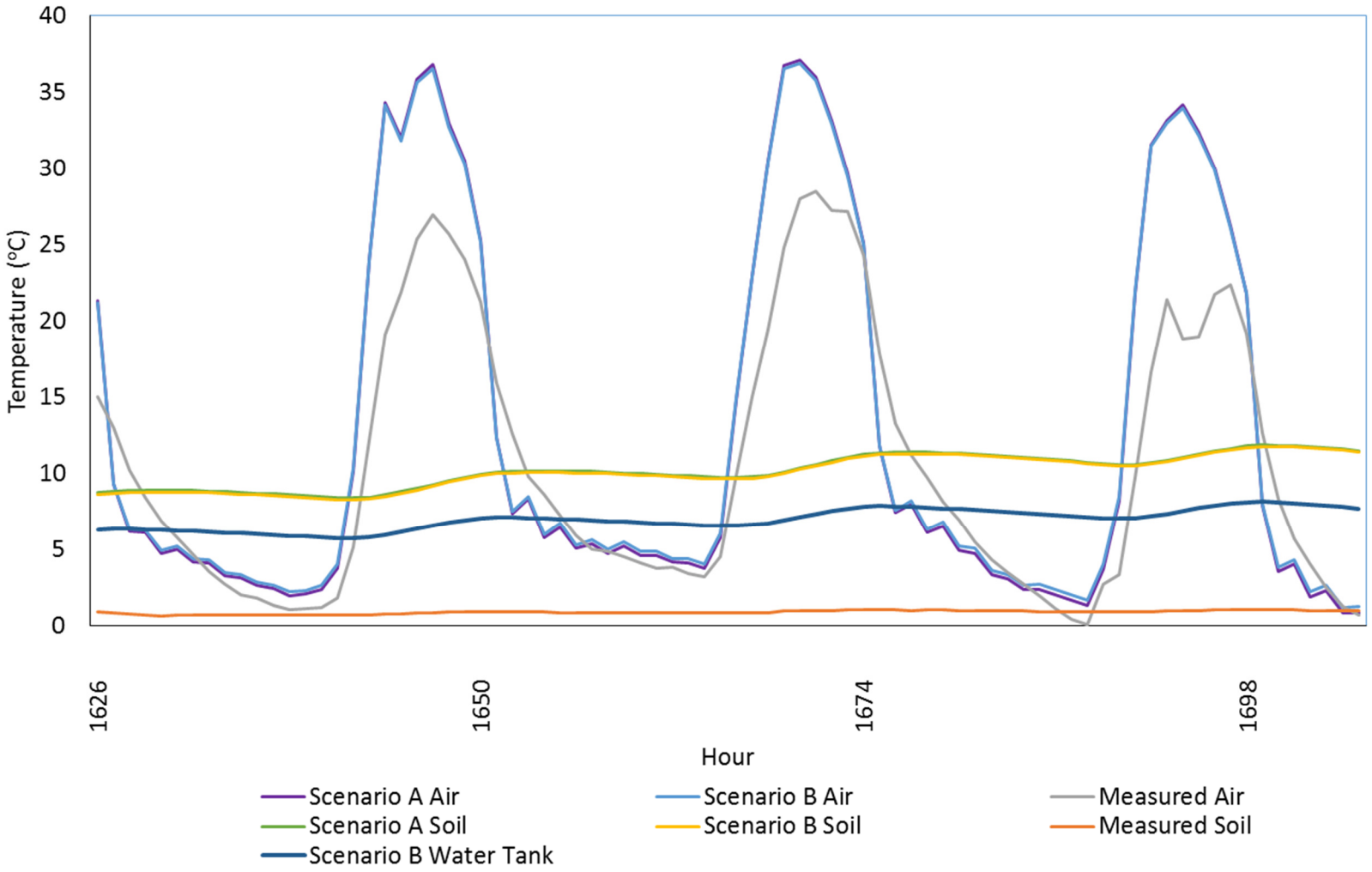

Figure 45: Time series plot of Scenario B modelled and measured air and soil temperatures in the Biodome.

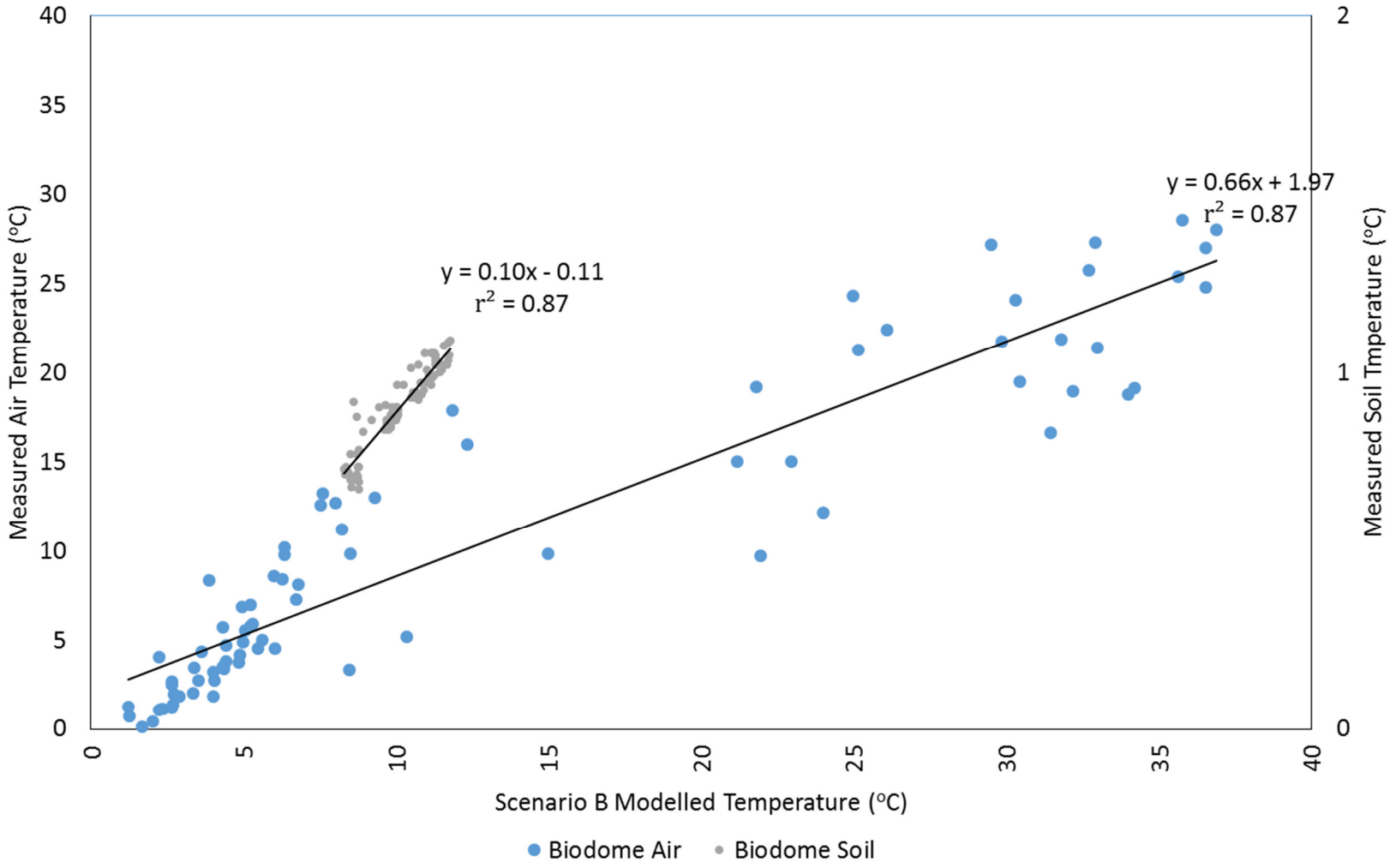

Figure 46: Scatter plot of Scenario B results versus measured Biodome air and soil temperatures for the same period.

4.3.3 Scenario C

Model Scenario C represents the case where the Biodome includes a ventilation rate of four air changes per hour, whenever there is solar radiation incident on the plane of the exhaust fan solar panel, and there is no extra thermal mass, in the form of a water tank. Measured results for the period from hour 2505 to 3388 are used as the actual results for this time period.

As shown in the time series plot of Scenario C versus measured air and soil temperatures in Figure 47, the modelled Scenario C results for Biodome air temperature match the measured air temperatures well, but the modelled soil temperatures are consistently higher and show more daily variation than the measured temperatures, as was the case in each of the previous two scenarios. The Scenario A results are included for reference and to demonstrate the effect of ventilation on maximum and minimum daily air temperatures, which was to lower the maximum temperature slightly and the minimum only marginally. The forced ventilation also resulted in lowered modelled soil temperature, but they were not low enough to match the measured soil temperatures.

The eight small spikes in soil temperature were caused by various attempts to run the EAHE fans over the course of several days. These attempts only lasted a few hours each, as there was not sufficient battery power available to run the fans any longer. These short tests did not appear to significantly affect the long term soil or air temperatures.

As shown in the scatter plot in Figure 48, the r^2 value of the modelled versus measured air and soil temperatures are 0.86 and 0.85, respectively, which indicates only fair agreement for both the air and soil temperature results.

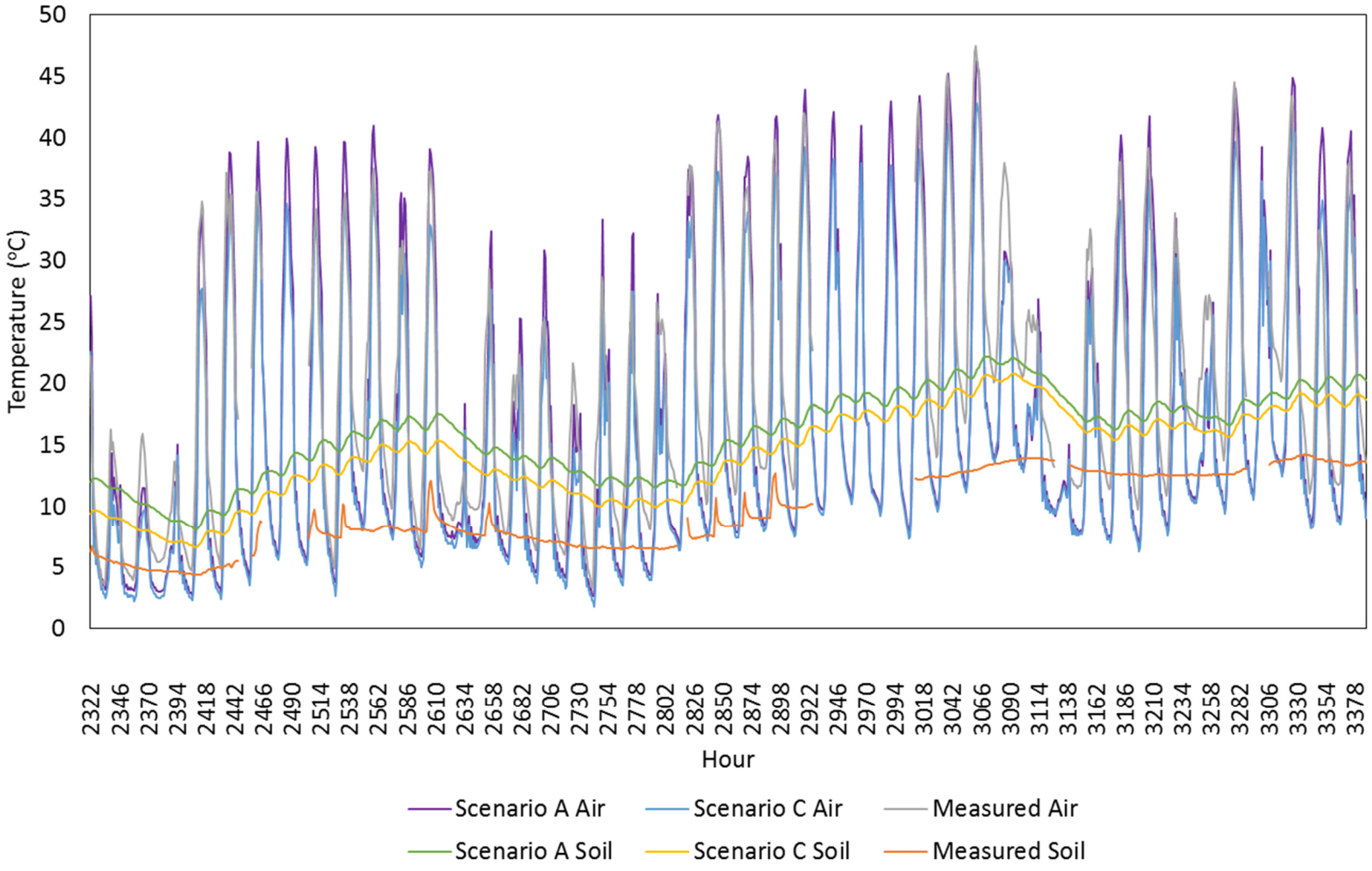

Figure 47: Time series plot of Scenario C modelled and measured air and soil temperatures in the Biodome.

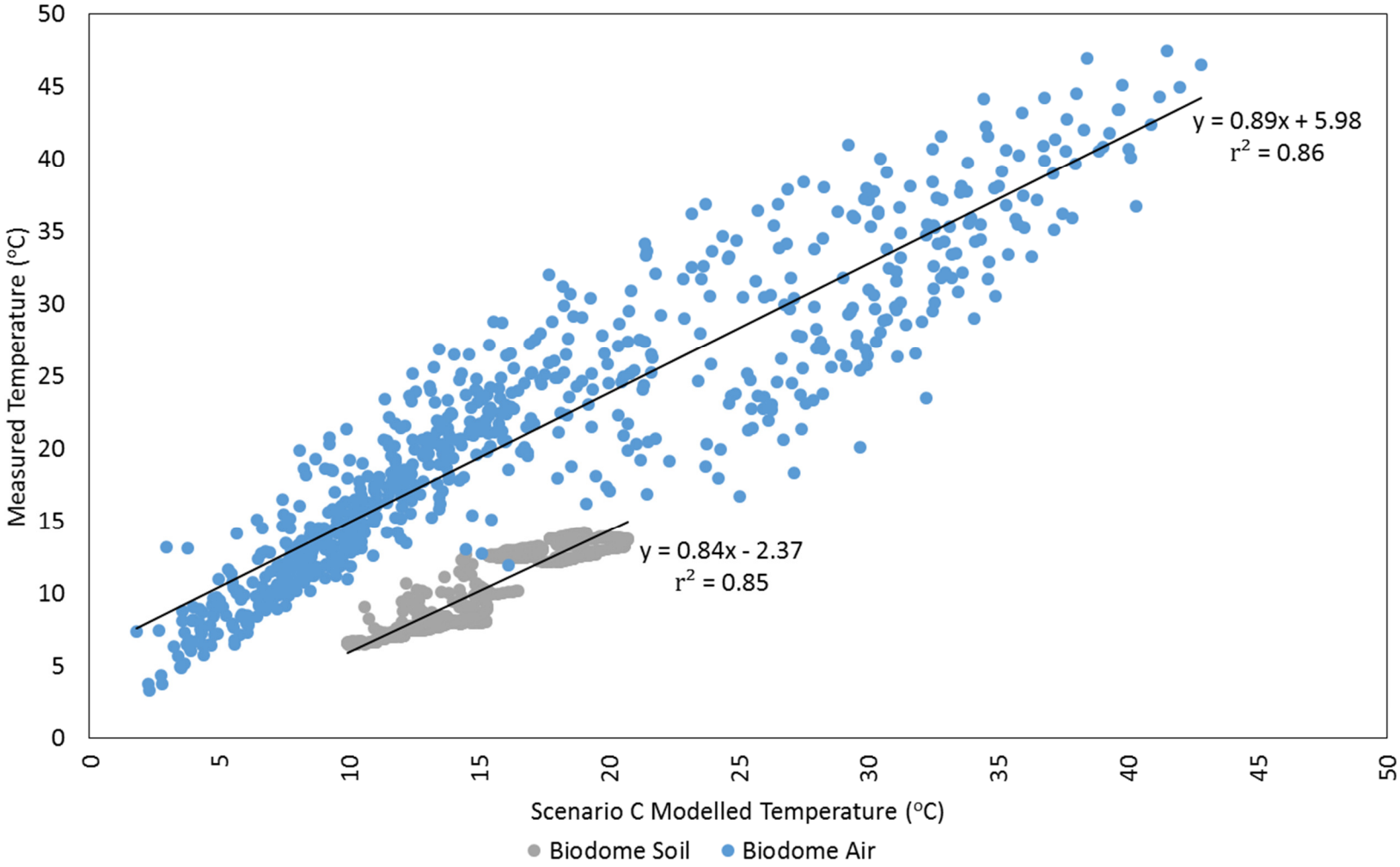

Figure 48: Scatter plot of Scenario C results versus measured Biodome air and soil temperatures for the same period.

4.3.4 Scenario D

Model Scenario D represents the case where the Biodome includes a ventilation rate of four air changes per hour, whenever there is solar radiation incident on the plane of the exhaust fan solar panel; there is extra thermal mass, in the form of the water tank containing 2592 L of water; and there is no shading resulting from the installation of the solar panels. Measured results for the period from hour 3883 to 4049 are used as the actual results for this time period.

As shown in the time series plot of Scenario D result versus measured air, water, and soil temperatures, in Figure 49, the modelled Scenario D results for Biodome air temperature are consistently lower than the measured results, although their hourly variation patterns are very similar. Similarly, the Scenario D soil temperatures were once again slightly higher than the measured soil temperatures. Conversely, the Scenario D water temperatures were much lower than the measured water temperatures, with differences of between 13 and 15^{o}C.

The Scenario C results are included for reference and to demonstrate the effect on the modelled air and soil temperature of changing the water tank zone thermal properties. Compared to Scenario C, the air temperatures variations are slightly dampened, but there is no significant difference in soil temperatures.

As shown in the scatter plot in Figure 50, the r^2 value of the modelled versus measured air, water, and soil temperatures are 0.85, 0.80, and 0.91, respectively, which indicates good agreement for soil temperatures, but not air or water temperatures.

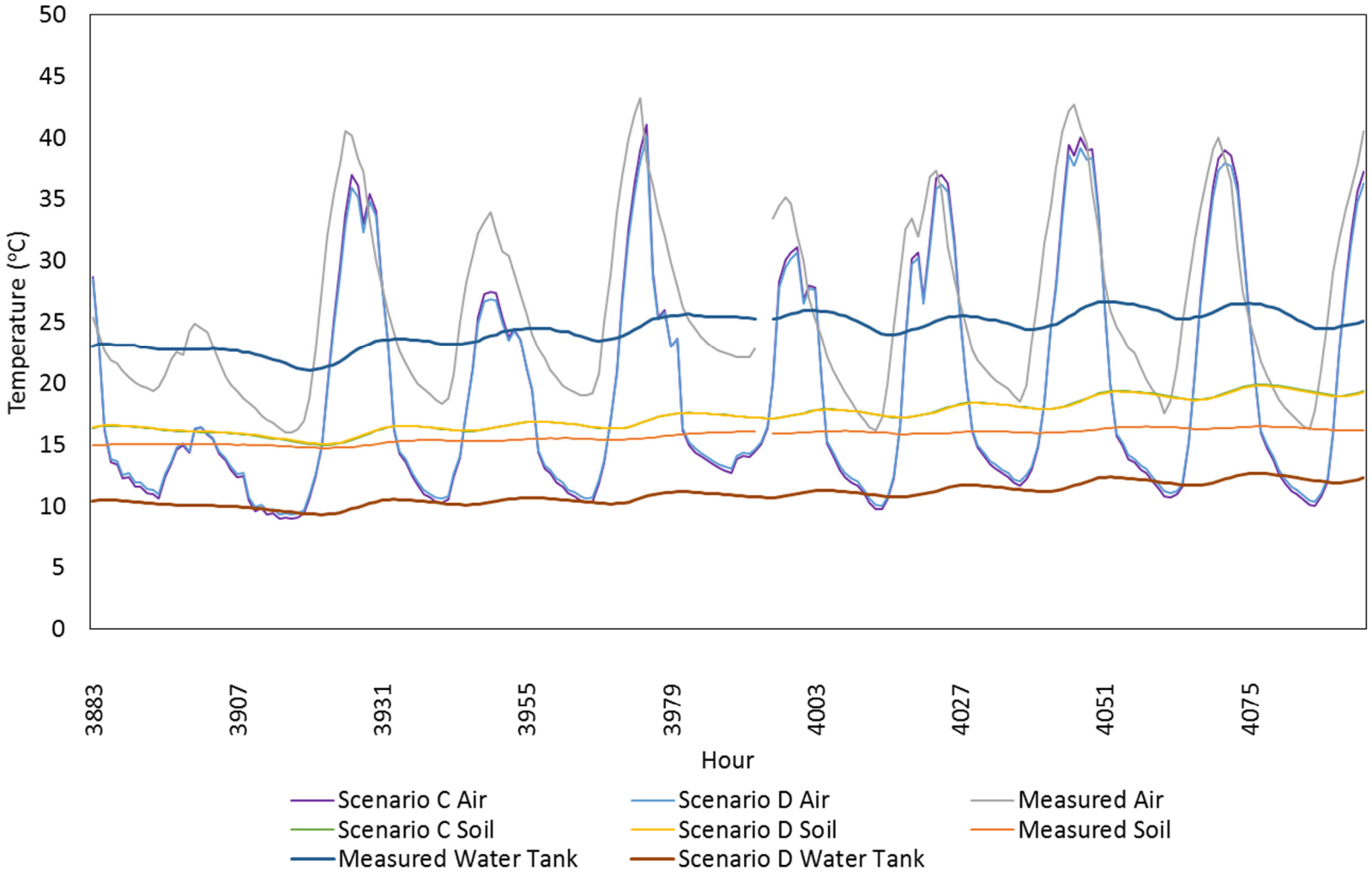

Figure 49: Time series plot of Scenario D modelled and measured air and soil temperatures in the Biodome.

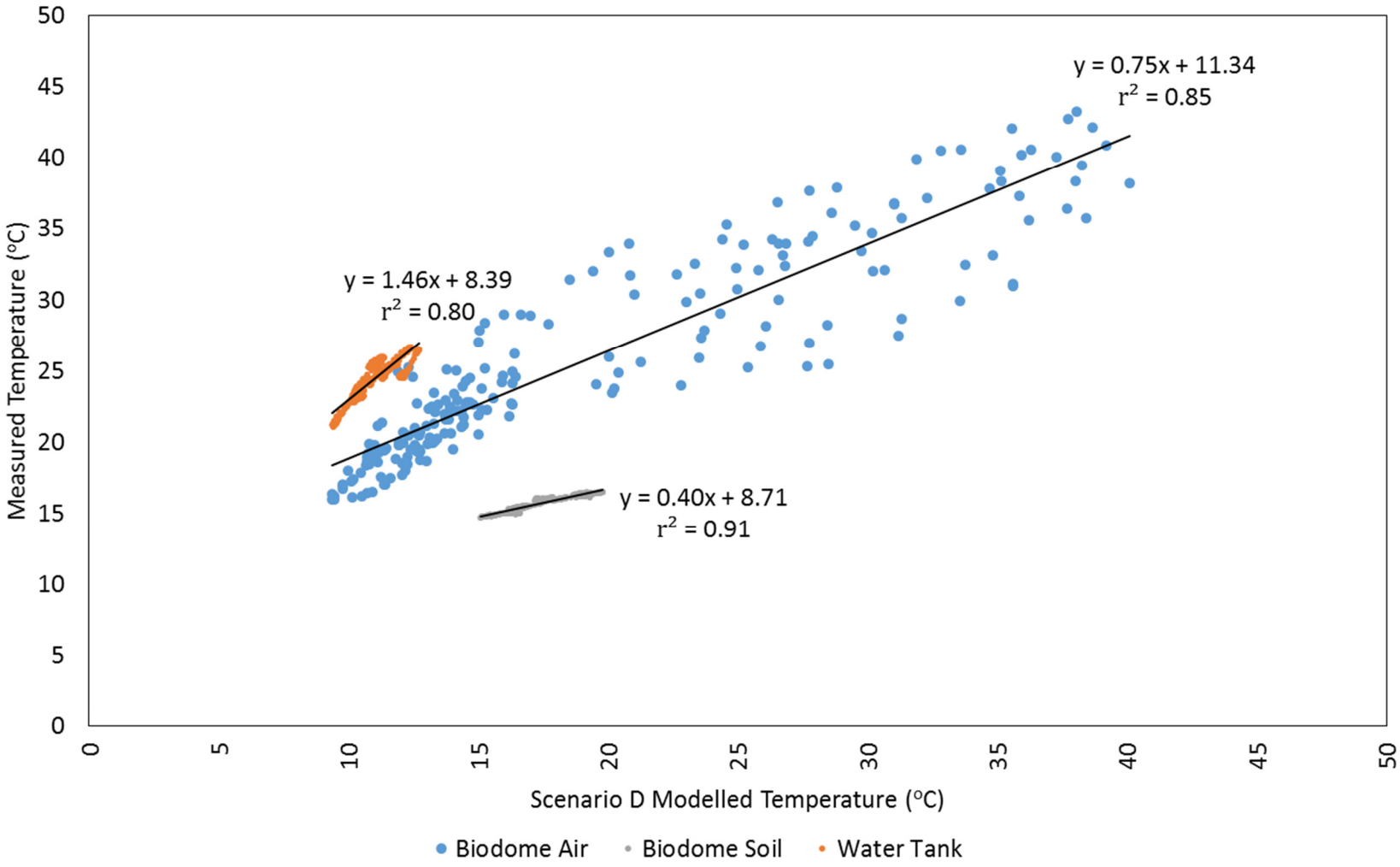

Figure 50: Scatter plot of Scenario D results versus measured Biodome air and soil temperatures for the same period.

4.3.5 Scenario E

Model Scenario E represents the case where the Biodome includes a ventilation rate of four air changes per hour, whenever there is solar radiation incident on the plane of the exhaust fan solar panel; there is extra thermal mass, in the form of the water tanks containing 2592 L of water; and there is shading resulting from the installation of solar panels. Measured results for the period from hour 4261 to 4353 are used as the actual results for this time period.

The time series plot of Scenario E and Scenario D results versus measured air, water, and soil temperatures, in Figure 51, shows that both Scenario E and Scenario D produce almost identical model temperatures. This result indicates that there is no effect on the model of shading two of the Biodome window panels. As there are only about three days of data under these conditions, it is unclear what the long term effect of the solar panel shading will be on the Biodome air, water, and soil temperatures.

As shown in the scatter plot Figure 52 in, the r^2 value of the modelled versus measured air, water, and soil temperatures are 0.84, 0.91, and 0.95, respectively.

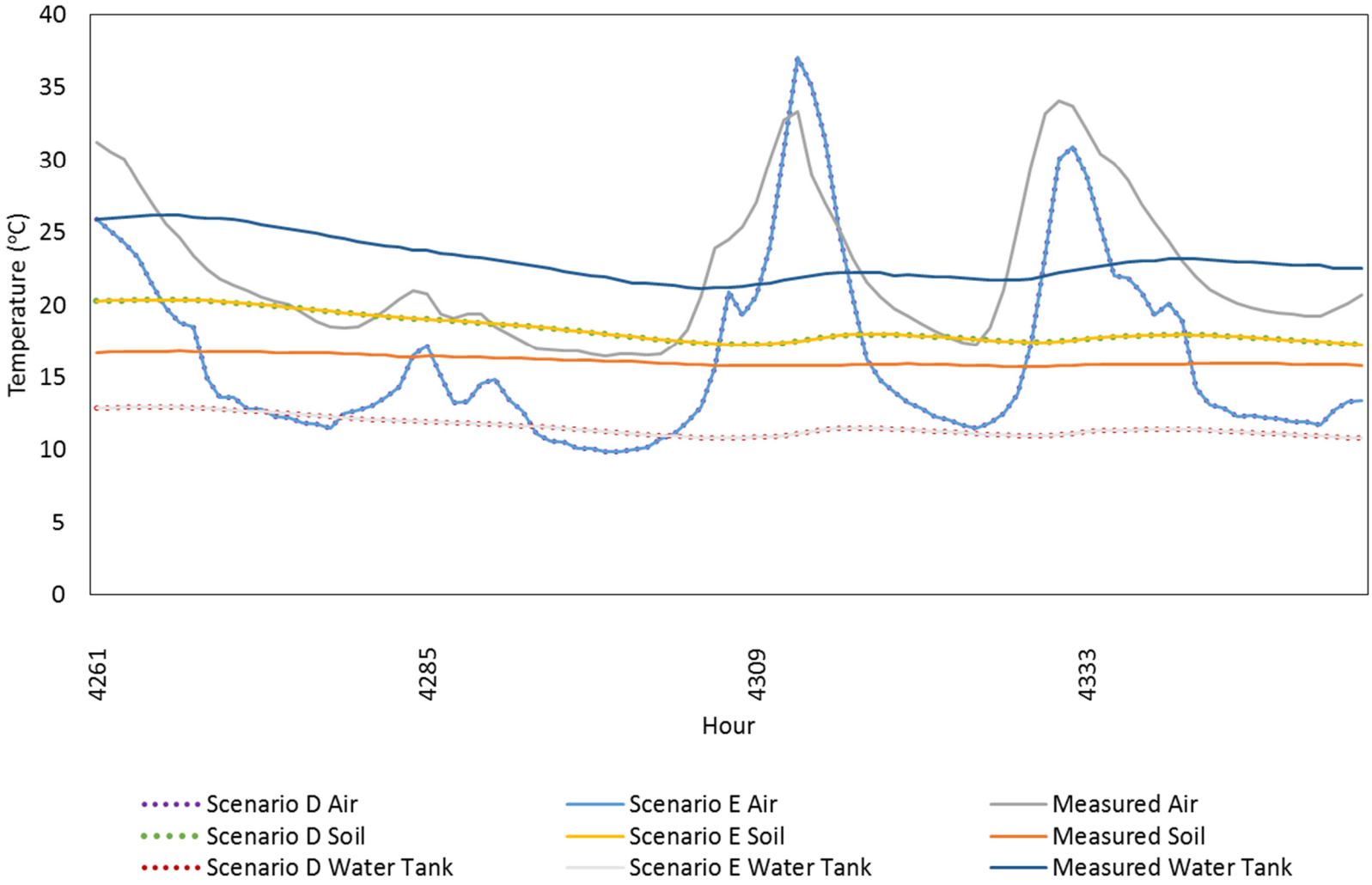

Figure 51: Time series plot of Scenario E modelled and measured air and soil temperatures in the Biodome.

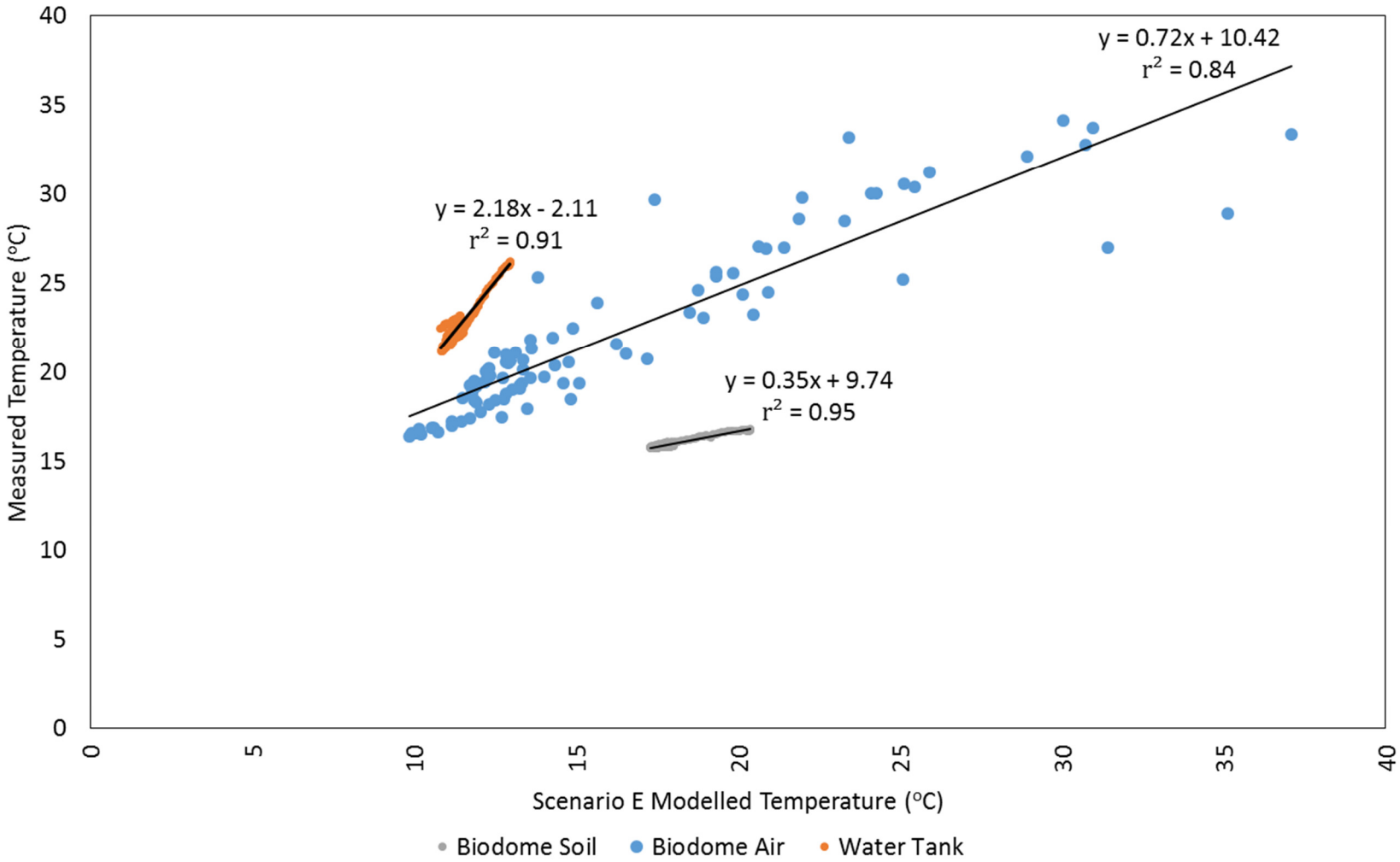

Figure 52: Scatter plot of Scenario E results versus measured Biodome air and soil temperatures for the same period.

4.4 Scenario Comparison

As shown in Table 18, Scenario D and E represent the most favourable set of operating conditions in order to maintain air temperatures below maximum threshold temperatures, during a typical weather year, however maximum temperatures are still expected to exceed 35°C for 158 hours, which means that further efforts are required to cool the Biodome air during particularly hot periods of the year.

Table 18: Hours per year above maximum temperature thresholds, by scenario

Maximum Air Temperature Threshold (°C)	Hours Per Year Above Maximum Air Temperature Threshold				
	Scenario A	Scenario B	Scenario C	Scenario D	Scenario E
25	1304	1324	1056	1007	1007
30	812	824	584	539	539
35	465	467	220	158	158
40	122	129	12	5	5

Scenarios D and E represent the cases where: the Biodome includes a ventilation rate of four air changes per hour, whenever there is solar radiation incident on the plane of the exhaust fan solar panel; there is extra thermal mass, in the form of the water tank containing 2592 L of water; and there is shading (Scenario D) and there is no shading (Scenario E) resulting from the installation of the solar panels.

As shown in Table 19, Scenario B represents the most favourable set of operating conditions in order to maintain air temperatures above minimum threshold temperatures, during a typical weather year. Even so, minimum temperatures still fall below 5°C for 3081 hours, which means that further efforts are required to heat the Biodome air during particularly cold periods of the year.

Table 19: hours per year below minimum temperature thresholds, by scenario

Minimum Air Temperature Threshold (°C)	Hours Per Year Below Minimum Air Temperature Threshold				
	Scenario A	Scenario B	Scenario C	Scenario D	Scenario E
5	3128	3081	3382	3398	3398
0	1597	1573	1861	1877	1877
-5	453	449	633	647	647
-10	4	2	33	38	38

4.5 Uncertainty Analysis

In addition to performing model calibration, it is important to also consider the possible sources of error in the measured data, through uncertainty analysis.

According to Moriasi et al. (2007):

> "Uncertainty analysis is defined as the process of quantifying the level of confidence in a given model simulation output based on the:
>
> 1. Quality and amount of measured data available;
> 2. Absence of measured data due to the lack of monitoring in certain locations;
> 3. Lack of knowledge about some physical processes and operational procedures;
> 4. Approximate nature of the mathematical equations used to simulate processes; and
> 5. Quality of the model sensitivity analysis and calibration."

Each of these aspects of uncertainty analysis is addressed in the following sections.

Quality and amount of measured data available

As was stated in Section 3.4.4, the thermocouples used in this project are made from K-type thermocouple wire that is polyvinyl insulated, 24 AWG stranded, with a special limit of error (SLE) designation, indicating a reduced error limit, which in this case is the greater of 1.1^{o}C or 0.4 percent.

The thermocouples were independently calibrated but the results of this calibration could not be used due to the nature of the ICs that were used to read and interpret the voltage from the thermocouples, as described in Section 3.4.4. A proper calibration procedure would have required the use of the completed instrumentation system, which was not ready until late February 2015 when it became imperative to install it in the Biodome and begin data collection.

As shown in Table 20, the temperature data resolution of the ICs is 0.25^{o}C and the temperature gain and offset error is ±1 to ±2^{o}C, guaranteed by design, depending on the cold-compensation temperature range and the temperature measurement range. As all of the measurements in this thesis are within the range of -100 to +100^{o}C, the temperature gain and offset error of the ICs is ±1^{o}C, guaranteed by design. The cold-junction temperature data resolution is 0.0625^{o}C, with an error range of ±2^{o}C.

Combining the error contributions from both the thermocouple wire and the ICs, the total error of the temperature measurements in this thesis is ±4.1^{o}C, not including any errors resulting from thermocouple placement or averaging of results.

Table 20: Thermal characteristics of the MAX31850K (Adapted from: Maxim, 2013).

Parameter	Conditions	MIN	MAX	Units
Temperature gain and offset error (41.276 µV/°C nominal sensitivity) [a]	T_R = -100 to +100°C, T_A = 0 to +70°C [b]	-1	+1	°C
	T_R = -200 to +700°C, T_A = -20 to +85°C [b]	-2	+2	
Thermocouple temperature data resolution		0.25		°C
Internal cold-junction temperature error	T_A = -40 to +100°C [c]	-2	+2	°C
Cold-junction temperature data resolution	T_A = -40 to +125°C,	0.0625		°C

[a] Not including cold-junction temperature error or thermocouple nonlinearity.
[b] Guaranteed by design. These limits represent six-sigma distribution for T_A = +25°C to +85°C. Outside this temperature range, these limits are three-sigma distribution.
[c] Guaranteed by design. These limits represent a three sigma-distribution.

The length of the thermocouple wire itself does not affect the accuracy of the measurement as a thermocouple does not experience a power loss along its length due to the very low current and voltages involved (RDC, 2013). The one risk of using long lengths of thermocouple wire is that electrical noise can be picked up by the wire and can affect the measurements. In this experiment, the thermocouples were not in the vicinity of any equipment that could cause electrical noise, therefore the length of the thermocouples should not affect the accuracy of the measurements.

Ideally, the model calibration would have been performed using a full year of data in order to account for seasonal changes, but delays in the construction of the Biodome and in the installation of the data collection system meant that data collection did not begin until late February of 2015, with results required for analysis by mid-summer of 2015 in order to complete this thesis report.

In addition to the reduced time period for the calibration data, various aspects of the Biodome operation were not kept consistent throughout the measurement periods, due to the nature of the operation. As was noted earlier, on a few occasions, volunteers inadvertently turned on the overhead ventilation, left the front door open, or opened side vents, which affected the temperature readings during these periods.

Absence of measured data due to the lack of monitoring in certain locations

As the initial intent of this project had been to study the effects of the EAHE on the temperature in the underground vents and in the plant root zone, a majority of the thermocouples are located in the EAHE pipes. Given the change in scope of this project to an assessment of the overall conditions within the Biodome throughout the year, it would have been useful to have more thermocouples spread out at different levels in the soil in order to getter a better representation of the soil temperature gradient.

It would have been useful also to have humidity readings of both the air and the soil, but the humidity sensors were all damaged early on in the process and were not replaced.

Lack of knowledge about some physical processes and operational procedures

The various mechanisms of heat transfer through the soil beds were not fully understood, as they were affected by the types of plants being grown, the amount of irrigation provided, the soil properties, etc.

Nature of the mathematical equations used to simulate processes

As was demonstrated in the literature review, plants have a significant effect on the heat gain and humidity within a greenhouse (AHSRAE, 2011), yet these effects were not

accounted for in the TRNSYS model because it was unclear what kinds of plants would actually be planted and the starting point for the experiment was bare soil. A more detailed model of the soil temperature gradients as well as the humidity cycle within the Biodome may have been appropriate and may have resulted in more accurate results.

A more accurate model of air infiltration may also have been possible if a blower door test had been done to determine the overall air tightness of the structure.

Finally, although the temperature-versus-voltage relationship of a thermocouple is not constant, the slope of the K-type thermocouple approaches a constant over the temperature range from 0 to 1000^{o}C, so a linear equation, such as the one used in this thesis provides a good approximation (Omega, 2015).

Quality of the model sensitivity analysis and calibration

As was described earlier, calibration of the TRNSYS model was done manually and consisted of changing the values of the soil surface solar absorptance and convective heat transfer coefficient while tracking the effect of these changes on the agreement between modelled and measured results. It is possible that a sensitivity analysis of other model parameters would also have been appropriate, but the focus was placed on these two parameters because they were the most uncertain.

4.6 Summary

Five different combinations of ventilation, water tank thermal mass, and solar panel shading were used to create five Biodome operating scenarios in order to test the effects of these variables on both the modelled and the experimentally measured results. A comparison of the results of these modelled scenarios, created using actual 2015 weather

data, to experimentally measured results taken over the same time period indicates that the model is able to accurately represent the effects of ventilation, but it may not be able to accurately reflect the effects of increased water tank thermal mass or solar panel shading, as insufficient measured data was available for these comparisons. Future work will be required to properly characterize these effects and to adjust and recalibrate the model.

Chapter 6

Contributions

A considerable amount of time and effort from several volunteers, including the author of this thesis paper, has resulted in the construction of a successful geodesic dome greenhouse demonstration project, the Biodome. Although not all of the original objectives of this thesis project were met, namely the investigation of the use and effectiveness of an EAHE system, many other useful discoveries have been made and have positively contributed to the on-going success of the Biodome project.

The main role the author of this thesis played in the Biodome project was to serve as Energy Lead. In this role, the author's main contributions to the project included:

- Researching and recommending the type of climate control technology to use in the Biodome (i.e. EAHE);
- Evaluating and providing advice on many other climate control technologies and techniques suggested by members of the BPCG association and members of the local community (i.e. radiant in-floor heating, roof-mounted solar thermal collectors, floating row covers, thermal screens, electric space heaters, etc.);
- Using the results of the literature review to design the EAHE, including the piping layout design, the materials specification, the fan sizing, and the fan control system design; and
- Providing answers and advice to questions and issues related to energy use and

energy requirements, over the course of the project, including battery sizing for the solar power system, specification of pump size and piping design, and installation for the aquaponics system.

In addition to the above contributions to the project, the author also provided support to the Biodome project in the following non-energy areas:

- Providing advice on the procurement of a geodesic dome greenhouse, as several options were available and had to be compared and evaluated;
- Participating in community consultation sessions;
- Providing advice on selecting a specific location for the Biodome within the available area at Brewer Park by comparing available options; and
- Providing physical labour and project management at various stages in the construction process, including during the installation of the EAHE and during the construction of the aquaponics system.

From a research perspective, the three main areas of contribution resulting from this thesis are the design of an appropriate data collection and control system, the collection and analysis of experimental data, and the design of a TRNSYS model that represents the base case scenario for the Biodome operation. The data collection system that was designed for this research will continue to log data in the Biodome and will be used to continue to improve the operations of the Biodome. The specifications for this systems are explicitly described so that they can be adapted for use in other projects. In fact, this design is currently being adapted for use in another greenhouse operation in Ottawa. Once the solar panels are connected to the battery bank, this system will also be

used to control the pump in the aquaponics system and the fans in the EAHE system.

As was demonstrated in Chapter 6, the TRNSYS model is able to provide a good representation of the Biodome air temperature, in the base case scenario. This model can be used a reference point against which to compare the Biodome air temperature after future design and operation modifications are made to the Biodome. The main shortcoming of the Biodome TRNSYS model is that it is not able to provide a good representation of the Biodome soil or water tank temperatures. Both of these areas of the model require further work to better reflect the conditions in the Biodome.

Chapter 7

Conclusions and Future Work

Some conclusions that can be drawn from the results of the full year models that were created using the CWEC typical weather year data, are that further efforts will be required to cool the Biodome air during hot periods of the year and energy will be required to heat the Biodome air during cold periods of the year. In summary, with the current Biodome design, appropriate growing conditions (as defined in Chapter 2) cannot be maintained in the Biodome year-round without the use of auxiliary power, in the form of a supplementary heating source, such as propane, natural gas, or biomass.

Even though year-round operation is not possible with the current Biodome design, this project is nonetheless valuable for demonstrating the performance of this non-conventional greenhouse structure and for showcasing different growing methods and supporting member-driven educational projects, all of which were stated goals of the project. Furthermore, future work on the use of the EAHE may also extend the growing season within the Biodome and improve the benefits of this project.

Some improvements that should be made to the existing Biodome structure in order to optimize its thermal performance include:

Add more ventilation windows. The relatively small windows currently installed in the Biodome do not provide sufficient air intake area for the forced ventilation system. Overheating of the Biodome air could be reduced through proper summer ventilation, which would be facilitated by the installation of larger ventilation windows.

Cover the water tanks at night. This practice will help to reduce evaporation from the water's surface and will help to lower the indoor air humidity.

Seal air leaks. Some air leaks were identified during the course of this study and were subsequently repaired. A more thorough inspection of the Biodome should be performed in order to identify and repair any other major air leaks in order to reduce the heat loss during the colder months.

Use shade cloth. In the summer, the use of shade cloths over the south side of the Biodome should be investigated to help reduce the risk of overheating and scorching of the plants.

Once the solar panels are properly connected and are charging the batteries in the Biodome, more work should be done to characterize the effects of the EAHE on both soil and air temperature. Future work in this area could include fan parametric tests whereby the EAHE fans can be run for different lengths of time to evaluate their effect on air and soil temperatures and to determine the optimal operating conditions. Different combinations of fans can also be used to investigate the effect of changes to EAHE air flow. Replacement humidity sensors should also be added to the data collection system, as this information would further help to characterize the effects of the EAHE and would facilitated the calibration of any future models

Other improvements that could be made to the Biodome TRNSYS model in the future include the addition of an evapotranspiration model to represent the crops, a humidity and evaporation model to account for the aquaponics system, and a shading profile to account for shading from the surrounding trees. The soil and water tank

portions of the model should also be investigated further, as neither one is able to provide an accurate representation of actual results.

References

Adafruit. (2015). http://www.adafruit.com/

Agriculture Canada. *Energy Conserving Urban Greenhouse for Canada: Construction and Management*. 1987.

Alexandra R. Rempel, Alan W. Rempel, Katharine V. Cashman, Ken N. Gates, Catherine J. Page, Barbara Shaw. *Interpretation of passive solar field data with EnergyPlus models: Un-conventional wisdom from four sunspaces in Eugene, Oregon*. Building and Environment [Journal], Volume 60, February 2013, Pages 158-172, Retrieved from http://www.sciencedirect.com/science/article/pii/S0360132312003022

American Society of Agricultural and Biological Engineers. 2008. *Heating, Ventilating and Cooling Greenhouses.* ANSI/ASAE EP 406.4 Jan 2003 (R2008). St. Joseph, MI.

American Society of Heating, Refrigerating and Air-Conditioning Engineers, Inc. 2011 *ASHRAE Handbook - Heating, Ventilating, and Air-Conditioning Applications* (SI Edition). 2011.

Arduino. (2015). *What is Arduino?* Retrieved from https://www.arduino.cc/

Banff Greenhouse Gardening Society. (2013). Retrieved from http://banffgreenhouse.com/

Bansal, Vikas, Misra, Rohit, Das Agarwal, Ghansyam, Mathur, Jyotirmay. *Transient effect of soil thermal conductivity and duration of operation on performance of Earth Air Tunnel Heat Exchanger*. Applied Energy [Journal] 103, 2013, Pages 1–11.

Bill C-36: *Ontario Local Food Act*. (2013) Royal Assent received, November 6, 2013. 40th Legislature, 2nd session. Ontario: Legislative Assembly of Ontario. Retrieved June 11, 2015.

Brewer Park Community Garden. (2013). Retrieved from http://brewerparkcommunitygarden.weebly.com/

Buckminster Fuller Institute. (2015). *About Fuller*. Retrieved from https://bfi.org/about-fuller/big-ideas/geodesic-domes

Buyapi. (2015). *Arduino Compatible Precision Real Time Clock Module w/ Temperature Sensor (DS3231).* Retrieved from http://www.buyapi.ca/product/arduino-compatible-precision-real-time-clock-module-w-temperature-sensor-ds3231/

Campen, J.B., Bot, G.P.A., de Zwart, H.F.. *Dehumidification of Greenhouses at Northern Latitudes*. Biosystems Engineering (2003) 86 (4), 487–493 doi:10.1016/j.biosystemseng.2003.08.008

Chandler, Nathan. 2015. *How Geodesic Domes Work*. Retrieved from http://science.howstuffworks.com/engineering/structural/geodesic-dome.htm

City of Ottawa, 2009. *Community Garden Action Plan Evaluation*. Retrieved from https://app06.ottawa.ca/calendar/ottawa/citycouncil/occ/2009/04-08/cpsc/01%20-%20ACS2009-COS-RCS-0005%20Gardens.htm

City of Vancouver. (2012). *Community gardens growing at record pace across the city*. Retrieved from http://vancouver.ca/news-calendar/community-gardens-growing-at-record-pace-across-the-city.aspx

Diver, Steve. *Aquaponics—Integration of Hydroponics with Aquaculture*. 2006. Retrieved from http://www.backyardaquaponics.com/Travis/aquaponic.pdf

D. N. Moriasi, J. G. Arnold, M. W. Van Liew, R. L. Bingner, R. D. Harmel, T. L. Veith. 2007. *Model evaluation guidelines for systematic quantification of accuracy in watershed simulations.* American Society of Agricultural and Biological Engineers ISSN 0001−235, Vol. 50(3): 885−900.

Eden Project. 2015. *Architecture at Eden*. Retrieved from http://www.edenproject.com/eden-story/behind-the-scenes/architecture-at-eden

Environment Canada. 2015. *1971 to 2000 Canadian Climate Normals station data*. Retrieved from http://climate.weather.gc.ca/climate_normals/results_1981_2010_e.html?stnID=4333&lang=e&StationName=ottawa&SearchType=Contains&stnNameSubmit=go&dCode=1. Date modified: 2015-02-11

Exner-Pirot, Heather*. 2012. Guidelines for Establishing a Northern Greenhouse Project*. International Centre for Northern Governance and Development. 2012.

Fuchs, M., E. Dayan, D. Shmuel and I. Zipori, 1997. *Effects of ventilation on the energy balance of a greenhouse with bare soil.* Agricultural and Forest Meteorol., 86 (3-4): 273-282.

Fuller R.J., Meyer C.P. and Sale P.J.M. *Validation of a dynamic model for predicting energy use in greenhouse* [Journal] // Journal of Agricultural Engineering. 1987. 38. pp. 1-14.

Fuller, R.J.. *Solar heating systems for recirculating aquaculture*. Aquacultural Engineering 36 (2007) 250–260.

GAF. *Green Machine Solar-Powered EcoSmart Roof Vent*. 2005 Retrieved from http://www.gaf.ca/Roofing/Residential/Products/Roof_Vents/MasterFlow_Solar_Powered_Exhaust

Geo-dome. *Geodesic dome frequency explained*. Retrieved from http://geo-dome.co.uk/article.asp?uname=domefreq

Ghosal, M.K., Tiwari, G.N., 2006. *Modeling and parametric studies for thermal performance of an earth to air heat exchanger integrated with a greenhouse*. Energy Conversion and Management 47 (13–14), 1779–1798.

Goch, Taff. *Geodesic Dome Construction Tutorial*. Retrieved from https://3dwarehouse.sketchup.com/model.html?id=81a19157ae1a77fa8f41a8466c140b06

Google Maps. (2015). *Brewer Park Community Garden*. [Street map]. Google. Retrieved from https://www.google.ca/maps/place/Brewer+Park+Community+Garden/@45.3890787,-75.6920159

Google Maps. (2015b). *Brewer Park Community Garden*. [Earth]. Google. Retrieved from https://www.google.ca/maps/@45.3944733,-75.7110596,13994m/data=!3m1!1e3

Gupta, Amita, Tiwari, G.N. *Computer model and its validation for prediction of storage effect of water mass in a greenhouse: a transient analysis.* Energy Conversion and Management, Volume 43, Issue 18, December 2002, Pages 2625-2640, ISSN 0196-8904, http://dx.doi.org/10.1016/S0196-8904(01)00196-0. (http://www.sciencedirect.com/science/article/pii/S0196890401001960)

Hoes H. and Desmedt J. *The GESKAS project, closed greenhouse as energy source and optimal growing environment*. [Journal] // ActaHort.. [s.l.] : ISHS, 2008. - 801.

Hollmuller, Pierre and Lachal, Bernard. *TRNSYS compatible moist air hypocaust model*. [Report] Final report / University De Geneve. - [s.l.]: Centre universitaire d'tude des problemes de l'energie, 1998. - Project number 19507.

Ipsos-Reid. *Canadians See Many Benefits of Locally Grown Food.* December 1, 2006, Ipsos-Reid press release. Retrieved from http://www.ipsos-na.com/news/pressrelease.cfm?id=3298.

Johannes F.J. Max, Gerhard Reisinger, Thomas Hofmann, Josef Hinken, Hans-Jürgen Tantau, Andreas Ulbrich, Susanne Lambrecht, Burkhard von Elsner, Ulrich Schurr. *Glass–film-combination: Opto-physical properties and energy saving potential of a novel greenhouse glazing system*. Energy and Buildings, Volume 50, July 2012, Pages 298-307, ISSN 0378-7788, Retrieved from http://dx.doi.org/10.1016/j.enbuild.2012.03.051.

Just Food. *Community Gardening Network*. 2015. Retrieved from http://www.justfood.ca/community-gardening-network/

Lamnatou, Chr., Chemisan, D. *Solar radiation manipulations and their role in greenhouse claddings: Fresen lenses, NIR- and UV-blocking materials*. 49:135-146. Renewable and Sustainable Energy Reviews 18 (2013) 271–287.

LBNL, 2013, WINDOW 6.3, Lawrence Berkeley National Laboratory: https://windows.lbl.gov/software/window/6/

Maxim Integrated. (2013). *MAX31850/MAX31851 Cold-Junction Compensated, 1-Wire Thermocouple-to-Digital Converters*. Retrieved from http://www.adafruit.com/datasheets/MAX31850-MAX31851.pdf

McCullagh, James C. *The Solar Greenhouse Book*. Rodale Press, Inc. 1978.

Missouri Botanical Garden. (2015). *Climatron: Geodesic Dome Conservatory*. Retrieved from http://www.missouribotanicalgarden.org/gardens-gardening/our-garden/gardens-conservatories/conservatories/climatron.aspx

Moretti, Elisa, Zinzi, Michele, Belloni, Elisa. *Polycarbonate panels for buildings: Experimental investigation of thermal and optical performance*. Energy and Buildings 70 (2014) 23-35.

N. Katsoulas, T. Bartzanas, T. Boulard, M. Mermier, C. Kittas. *Effect of Vent Openings and Insect Screens on Greenhouse Ventilation*. Biosystems Engineering (2006) 93 (4), 427–436 doi:10.1016/j.biosystemseng.2005.01.001 SE—Structures and Environment

Numerical Logics. 1999. *Canadian Weather for Energy Calculations, Users Manual and CD-ROM*. Downsview, Ontario: Environment Canada.

Omega. (2015). *Reference Temperatures*. Retrieved from http://www.omega.com/temperature/z/pdf/z021-032.pdf

Open Source Initiative. (2015). *The Open Source Definition (Annotated).* Retrieved from http://opensource.org/osd-annotated

Pérez Parra, J., Baeza, E., López, J.C., Pérez, C., Montero, J.I. and Antón, A. (2003). *Effect of vent types and insect screens on ventilation of "parral" greenhouses.* Acta Hortic. 614, 393-400. Retrieved from http://dx.doi.org/10.17660/ActaHortic.2003.614.59"

Polygal. 2011. *Polygal Polycarbonate Multiwall Sheets Technical Specifications.* Retrieved from http://polygal-northamerica.com/pdf/Polygal-Technical-Guide.pdf

Prime Minister of Canada Stephen Harper. *PM announces measures to promote Northern agriculture*. Retrieved from http://pm.gc.ca/eng/news/2014/08/22/pm-announces-measures-promote-northern-agriculture

Provenzano Jr, Anthony J., Joseph G. Winfield. *Performance of a Recirculating Fish Production System Stocked with Tilapia Hybrids.* Aquacultural Engineering 6.1 (1987): 15-26. Web. 14 July 2015.

RDC Control. *Introduction to Thermocouples*. 2013. Retrieved from http://rdccontrol.com/thermocouples/thermocouples-101/introduction-to-thermocouples/is-there-a-maximum-length-for-thermocouples-and-thermocouple-wiring/

Reichel, Justina. *Vancouver Community Gardens a Growing Trend*. 2012. Retrieved from http://www.theepochtimes.com/n2/canada/vancouver-community-gardens-a-growing-trend-251691.html.

Rubel, F., and M. Kottek. 2010. *Observed and projected climate shifts 1901-2100 depicted by world maps of the Köppen-Geiger climate classification*. Meteorol. Z., 19, 135-141. DOI: 10.1127/0941-2948/2010/0430.

Santamouris, M., Balaras, C.A., Dascalaki, E., Vallindras, M., 1994. *Passive solar agricultural greenhouses: a worldwide classification and evaluation of technologies and systems used for heating purposes.* Solar Energy 53 (5), 411–426.

Sethi V.P. and S.K. Sharma. (2007). *Thermal modeling of a greenhouse integrated to an aquifer coupled cavity flow heat exchanger system* [Journal] Solar Energy 81. pp. 723-741.

Sethi, V.P. *On the selection of shape and orientation of a greenhouse: Thermal modeling and experimental validation*. [Journal] Solar Energy 83 (2009) 21–38.

Sethi, V.P., Sharma, S.K.. *Survey and evaluation of cooling technologies for worldwide agricultural greenhouse applications*. [Journal] Solar Energy 81 (2007) 1447-1459

Sethi, V.P., Sharma, S.K.. *Survey and evaluation of heating technologies for worldwide agricultural greenhouse applications*. [Journal] Solar Energy 82 (2008) 832–859

Snedecor, G.W. and Cochran, W.G. (1982) *Statistical Methods*. 7th Edition, Iowa State University Press, Towa, 511.

Solar Energy Laboratory, University of Wisconsin–Madison. (2012). *TRNSYS: A Transient Systems Simulation Tool*. Accessible online at http://sel.me. wisc.edu/trnsys/.

Statistics Canada. Table 001-0047: *Estimates of specialized greenhouse operations, greenhouse area, and months of operation, annual*. CANSIM (database). (accessed: 2015-07-05)

Vadiee, Amir. (2013). *Energy management in large scale solar buildings: The closed greenhouse concept*. (Doctoral Thesis) KTH School of Industrial Engineering and Management, Department of Energy Technology Division of Heat and Power Technology, Stockholm, Sweden.

Willits D.H., Chandra P. and Peet M.M. *Modelling solar energy storage system for greenhouse* [Journal] // Journal of Agricultural Engineering. 1985. 32. pp. 73-79. Retrieved from http://www.sciencedirect.com/science/article/pii/0021863485901209

Wong, B., McClung, L., Snijders, A., McClenahan, D., Thornton, J., 2011. *The Application of Aquifer Thermal Energy Storage in the Canadian Greenhouse Industry.* [Journal] Acta Hortic. 893, 437-444. Retrieved from http://dx.doi.org/10.17660/ActaHortic.2011.893.42

Zhu, S., Deltour, J., Wang, S.. *Modeling the thermal characteristics of greenhouse pond systems*. [Journal] Aquacultural Engineering 18 (1998) 201–217.

Appendix A: TRNSYS Input File

```
        TRNSYS - the TRaNsient SYstem Simulation program

  The Solar Energy Lab at the University of Wisconsin - Madison, USA
Le Centre Scientifique et Technique du Batiment, Sophia Antipolis, France
        Transsolar Energietechnik GmbH, Stuttgart, Germany
      Thermal Energy System Specialists, LLC, Madison Wisconsin, USA

                  Release 17.01.0028

*** Notice at time       :       0.000000
   Generated by Unit     : Not applicable or not available
   Generated by Type     : Not applicable or not available
   Message               : The TRNSYS Executable (TRNExe.exe) and main DLL (TRNDll.dll) are
located in "C:\Trnsys17\Exe"

 *** Pre-Processing the TRNSYS EQUATIONs and CONSTANTs to check for fatal errors.

 *** Pre-Processing of EQUATIONs and CONSTANTs completed with no fatal errors found.

 *** Evaluating the EQUATIONs and CONSTANTs to determine their initial values.

 *** Finished evaluating the EQUATIONs and CONSTANTs and ready to begin processing
the remainder of the TRNSYS input file.

 VERSION       17
**************************************************************************
*******
*** TRNSYS input file (deck) generated by TrnsysStudio
*** on Sunday, October 25, 2015 at 21:36
***                    from                    TrnsysStudio                    project:
C:\Users\pclau_000\Dropbox\Thesis\TRNSYS\June_12\July_28_A.tpf
***
*** If you edit this file, use the File/Import TRNSYS Input File function in
*** TrnsysStudio to update the project.
***
*** If you have problems, questions or suggestions please contact your local
*** TRNSYS distributor or mailto:software@cstb.fr
***
**************************************************************************
*******
**************************************************************************
```

```
*******
*** Units
*************************************************************************
*******
*************************************************************************
*******
*** Control cards
*************************************************************************
*******
* START, STOP and STEP

 CONSTANTS   3
   START=0
   STOP=8760
   STEP=1
! Start time      End time         Time step

 SIMULATION                  0.0000000000000000E+00          8.7600000000000000E+03
1.0000000000000000E+00
! Integration     Convergence

 TOLERANCES        1.0000000000000002E-03    1.0000000000000002E-03
! Max iterations          Max warnings Trace limit

 LIMITS       30       30       31
! TRNSYS numerical integration solver method

 DFQ   1
! TRNSYS output file width, number of characters

 WIDTH    72
! NOLIST statement

 LIST
! MAP statement
! Solver statement      Minimum relaxation factor     Maximum relaxation factor

 SOLVER  0
   1.000000000000000
   1.000000000000000
! Nan DEBUG statement

 NAN_CHECK   0
! Overwrite DEBUG statement
```

```
 OVERWRITE_CHECK   0
! disable time report

 TIME_REPORT   0
! EQUATION SOLVER statement
 EQUATION SOLVING METHOD        0
* User defined CONSTANTS
* EQUATIONS "Wizard settings"
*

 EQUATIONS   5
!Rotation angle for building used for adapting azimuth angles
    TURN = 0
! Close blinds - radiation on facade in [W/m2 * 3.6]=[kJ/hr]
    SHADE_CLOSE = 140 * 3.6
! Open blinds - radiation on facade in [W/m2 * 3.6]=[kJ/hr]
    SHADE_OPEN = 120 * 3.6
! Maximum opaque fraction of internal shading device
    MAX_ISHADE = 0/100
! Maximum opaque fraction of external shading device
    MAX_ESHADE = 0/100
*$UNIT_NAME Wizard settings
*$LAYER Main
*$POSITION 73 180
*---------------------------------------------------------------------------
* EQUATIONS "AzimuthAngles"
*

 EQUATIONS  92
! azimuth angle of orientation
    AA_H_0_0 = 0 + TURN
! azimuth angle of orientation
    AA_S_0_50 = 0 + TURN
! azimuth angle of orientation
    AA_S_0_25 = 0 + TURN
! azimuth angle of orientation
    AA_S_0_10 = 0 + TURN
! azimuth angle of orientation
    AA_S_0_65 = 0 + TURN
! azimuth angle of orientation
    AA_S_5_90 = 5 + TURN
! azimuth angle of orientation
    AA_S_10_70 = 10 + TURN
```

```
! azimuth angle of orientation
   AA_S_10_90 = 10 + TURN
! azimuth angle of orientation
   AA_S_15_45 = 15 + TURN
! azimuth angle of orientation
   AA_S_20_30 = 20 + TURN
! azimuth angle of orientation
   AA_S_25_55 = 25 + TURN
! azimuth angle of orientation
   AA_S_25_65 = 25 + TURN
! azimuth angle of orientation
   AA_S_35_75 = 35 + TURN
! azimuth angle of orientation
   AA_S_35_90 = 35 + TURN
! azimuth angle of orientation
   AA_W_45_55 = 45 + TURN
! azimuth angle of orientation
   AA_W_50_30 = 50 + TURN
! azimuth angle of orientation
   AA_W_50_65 = 50 + TURN
! azimuth angle of orientation
   AA_W_55_45 = 55 + TURN
! azimuth angle of orientation
   AA_W_60_75 = 60 + TURN
! azimuth angle of orientation
   AA_W_60_90 = 60 + TURN
! azimuth angle of orientation
   AA_W_70_50 = 70 + TURN
! azimuth angle of orientation
   AA_W_70_10 = 70 + TURN
! azimuth angle of orientation
   AA_W_70_25 = 70 + TURN
! azimuth angle of orientation
   AA_W_70_65 = 70 + TURN
! azimuth angle of orientation
   AA_W_85_90 = 85 + TURN
! azimuth angle of orientation
   AA_W_85_75 = 85 + TURN
! azimuth angle of orientation
   AA_W_90_45 = 90 + TURN
! azimuth angle of orientation
   AA_W_95_30 = 95 + TURN
! azimuth angle of orientation
   AA_W_95_70 = 95 + TURN
```

```
! azimuth angle of orientation
    AA_W_100_55 = 100 + TURN
! azimuth angle of orientation
    AA_W_110_75 = 110 + TURN
! azimuth angle of orientation
    AA_W_110_90 = 110 + TURN
! azimuth angle of orientation
    AA_W_115_55 = 115 + TURN
! azimuth angle of orientation
    AA_W_120_30 = 120 + TURN
! azimuth angle of orientation
    AA_W_120_70 = 120 + TURN
! azimuth angle of orientation
    AA_W_125_45 = 125 + TURN
! azimuth angle of orientation
    AA_W_130_75 = 130 + TURN
! azimuth angle of orientation
    AA_N_135_90 = 135 + TURN
! azimuth angle of orientation
    AA_N_145_50 = 145 + TURN
! azimuth angle of orientation
    AA_N_145_25 = 145 + TURN
! azimuth angle of orientation
    AA_N_145_10 = 145 + TURN
! azimuth angle of orientation
    AA_N_145_65 = 145 + TURN
! azimuth angle of orientation
    AA_N_155_75 = 155 + TURN
! azimuth angle of orientation
    AA_N_155_90 = 155 + TURN
! azimuth angle of orientation
    AA_N_160_45 = 160 + TURN
! azimuth angle of orientation
    AA_N_160_90 = 160 + TURN
! azimuth angle of orientation
    AA_N_165_30 = 165 + TURN
! azimuth angle of orientation
    AA_N_165_70 = 165 + TURN
! azimuth angle of orientation
    AA_N_170_55 = 170 + TURN
! azimuth angle of orientation
    AA_N_175_90 = 175 + TURN
! azimuth angle of orientation
    AA_N_180_75 = 180 + TURN
```

```
! azimuth angle of orientation
    AA_N_180_90 = 180 + TURN
! azimuth angle of orientation
    AA_N_190_55 = 190 + TURN
! azimuth angle of orientation
    AA_N_195_30 = 195 + TURN
! azimuth angle of orientation
    AA_N_195_70 = 195 + TURN
! azimuth angle of orientation
    AA_N_200_45 = 200 + TURN
! azimuth angle of orientation
    AA_N_205_75 = 205 + TURN
! azimuth angle of orientation
    AA_N_205_90 = 205 + TURN
! azimuth angle of orientation
    AA_N_215_50 = 215 + TURN
! azimuth angle of orientation
    AA_N_215_25 = 215 + TURN
! azimuth angle of orientation
    AA_N_215_10 = 215 + TURN
! azimuth angle of orientation
    AA_N_215_65 = 215 + TURN
! azimuth angle of orientation
    AA_E_230_75 = 230 + TURN
! azimuth angle of orientation
    AA_E_230_90 = 230 + TURN
! azimuth angle of orientation
    AA_E_235_45 = 235 + TURN
! azimuth angle of orientation
    AA_E_240_30 = 240 + TURN
! azimuth angle of orientation
    AA_E_250_65 = 250 + TURN
! azimuth angle of orientation
    AA_E_250_90 = 250 + TURN
! azimuth angle of orientation
    AA_E_265_30 = 265 + TURN
! azimuth angle of orientation
    AA_E_270_45 = 270 + TURN
! azimuth angle of orientation
    AA_E_275_75 = 275 + TURN
! azimuth angle of orientation
    AA_E_275_90 = 275 + TURN
! azimuth angle of orientation
    AA_E_290_10 = 290 + TURN
```

```
! azimuth angle of orientation
    AA_E_290_25 = 290 + TURN
! azimuth angle of orientation
    AA_E_290_50 = 290 + TURN
! azimuth angle of orientation
    AA_E_290_65 = 290 + TURN
! azimuth angle of orientation
    AA_E_300_75 = 300 + TURN
! azimuth angle of orientation
    AA_E_300_90 = 300 + TURN
! azimuth angle of orientation
    AA_E_305_45 = 305 + TURN
! azimuth angle of orientation
    AA_E_310_30 = 310 + TURN
! azimuth angle of orientation
    AA_E_310_65 = 310 + TURN
! azimuth angle of orientation
    AA_S_315_55 = 315 + TURN
! azimuth angle of orientation
    AA_S_325_75 = 325 + TURN
! azimuth angle of orientation
    AA_S_325_90 = 325 + TURN
! azimuth angle of orientation
    AA_S_330_90 = 330 + TURN
! azimuth angle of orientation
    AA_S_335_55 = 335 + TURN
! azimuth angle of orientation
    AA_S_335_65 = 335 + TURN
! azimuth angle of orientation
    AA_S_340_30 = 340 + TURN
! azimuth angle of orientation
    AA_S_345_45 = 345 + TURN
! azimuth angle of orientation
    AA_S_350_70 = 350 + TURN
! azimuth angle of orientation
    AA_S_350_90 = 350 + TURN
! solar azimuth corrected by building rotation - Input for Type 56 sun position for SHM
and ISM
    AAZM_TYPE56 = AAZM - (TURN)
*$UNIT_NAME AzimuthAngles
*$LAYER Main
*$POSITION 73 63
*-------------------------------------------------------------------------------
* EQUATIONS "Radiation"
```

*

EQUATIONS 276
AZEN = [15,16]
AAZM = [15,17]
IT_H_0_0 = [15,24]
IB_H_0_0 = [15,49]
AI_H_0_0 = [15,149]
IT_S_0_50 = [15,25]
IB_S_0_50 = [15,50]
AI_S_0_50 = [15,150]
IT_S_0_25 = [15,26]
IB_S_0_25 = [15,51]
AI_S_0_25 = [15,151]
IT_S_0_10 = [15,27]
IB_S_0_10 = [15,52]
AI_S_0_10 = [15,152]
IT_S_0_65 = [15,28]
IB_S_0_65 = [15,53]
AI_S_0_65 = [15,153]
IT_S_5_90 = [15,29]
IB_S_5_90 = [15,54]
AI_S_5_90 = [15,154]
IT_S_10_70 = [15,30]
IB_S_10_70 = [15,55]
AI_S_10_70 = [15,155]
IT_S_10_90 = [15,31]
IB_S_10_90 = [15,56]
AI_S_10_90 = [15,156]
IT_S_15_45 = [15,32]
IB_S_15_45 = [15,57]
AI_S_15_45 = [15,157]
IT_S_20_30 = [15,33]
IB_S_20_30 = [15,58]
AI_S_20_30 = [15,158]
IT_S_25_55 = [15,34]
IB_S_25_55 = [15,59]
AI_S_25_55 = [15,159]
IT_S_25_65 = [15,35]
IB_S_25_65 = [15,60]
AI_S_25_65 = [15,160]
IT_S_35_75 = [15,36]
IB_S_35_75 = [15,61]
AI_S_35_75 = [15,161]

IT_S_35_90 = [15,37]
IB_S_35_90 = [15,62]
AI_S_35_90 = [15,162]
IT_W_45_55 = [15,38]
IB_W_45_55 = [15,63]
AI_W_45_55 = [15,163]
IT_W_50_30 = [15,39]
IB_W_50_30 = [15,64]
AI_W_50_30 = [15,164]
IT_W_50_65 = [15,40]
IB_W_50_65 = [15,65]
AI_W_50_65 = [15,165]
IT_W_55_45 = [15,41]
IB_W_55_45 = [15,66]
AI_W_55_45 = [15,166]
IT_W_60_75 = [15,42]
IB_W_60_75 = [15,67]
AI_W_60_75 = [15,167]
IT_W_60_90 = [15,43]
IB_W_60_90 = [15,68]
AI_W_60_90 = [15,168]
IT_W_70_50 = [15,44]
IB_W_70_50 = [15,69]
AI_W_70_50 = [15,169]
IT_W_70_10 = [15,45]
IB_W_70_10 = [15,70]
AI_W_70_10 = [15,170]
IT_W_70_25 = [15,46]
IB_W_70_25 = [15,71]
AI_W_70_25 = [15,171]
IT_W_70_65 = [15,47]
IB_W_70_65 = [15,72]
AI_W_70_65 = [15,172]
IT_W_85_90 = [15,48]
IB_W_85_90 = [15,73]
AI_W_85_90 = [15,173]
IT_W_85_75 = [15,49]
IB_W_85_75 = [15,74]
AI_W_85_75 = [15,174]
IT_W_90_45 = [15,50]
IB_W_90_45 = [15,75]
AI_W_90_45 = [15,175]
IT_W_95_30 = [15,51]
IB_W_95_30 = [15,76]

AI_W_95_30 = [15,176]
IT_W_95_70 = [15,52]
IB_W_95_70 = [15,77]
AI_W_95_70 = [15,177]
IT_W_100_55 = [15,53]
IB_W_100_55 = [15,78]
AI_W_100_55 = [15,178]
IT_W_110_75 = [15,54]
IB_W_110_75 = [15,79]
AI_W_110_75 = [15,179]
IT_W_110_90 = [15,55]
IB_W_110_90 = [15,80]
AI_W_110_90 = [15,180]
IT_W_115_55 = [15,56]
IB_W_115_55 = [15,81]
AI_W_115_55 = [15,181]
IT_W_120_30 = [15,57]
IB_W_120_30 = [15,82]
AI_W_120_30 = [15,182]
IT_W_120_70 = [15,58]
IB_W_120_70 = [15,83]
AI_W_120_70 = [15,183]
IT_W_125_45 = [15,59]
IB_W_125_45 = [15,84]
AI_W_125_45 = [15,184]
IT_W_130_75 = [15,60]
IB_W_130_75 = [15,85]
AI_W_130_75 = [15,185]
IT_N_135_90 = [15,61]
IB_N_135_90 = [15,86]
AI_N_135_90 = [15,186]
IT_N_145_50 = [15,62]
IB_N_145_50 = [15,87]
AI_N_145_50 = [15,187]
IT_N_145_25 = [15,63]
IB_N_145_25 = [15,88]
AI_N_145_25 = [15,188]
IT_N_145_10 = [15,64]
IB_N_145_10 = [15,89]
AI_N_145_10 = [15,189]
IT_N_145_65 = [15,65]
IB_N_145_65 = [15,90]
AI_N_145_65 = [15,190]
IT_N_155_75 = [15,66]

IB_N_155_75 = [15,91]
AI_N_155_75 = [15,191]
IT_N_155_90 = [15,67]
IB_N_155_90 = [15,92]
AI_N_155_90 = [15,192]
IT_N_160_45 = [15,68]
IB_N_160_45 = [15,93]
AI_N_160_45 = [15,193]
IT_N_160_90 = [15,69]
IB_N_160_90 = [15,94]
AI_N_160_90 = [15,194]
IT_N_165_30 = [15,70]
IB_N_165_30 = [15,95]
AI_N_165_30 = [15,195]
IT_N_165_70 = [15,72]
IB_N_165_70 = [15,97]
AI_N_165_70 = [15,197]
IT_N_170_55 = [15,73]
IB_N_170_55 = [15,98]
AI_N_170_55 = [15,198]
IT_N_175_90 = [15,74]
IB_N_175_90 = [15,99]
AI_N_175_90 = [15,199]
IT_N_180_75 = [15,75]
IB_N_180_75 = [15,100]
AI_N_180_75 = [15,200]
IT_N_180_90 = [15,76]
IB_N_180_90 = [15,101]
AI_N_180_90 = [15,201]
IT_N_190_55 = [15,77]
IB_N_190_55 = [15,102]
AI_N_190_55 = [15,202]
IT_N_195_30 = [15,78]
IB_N_195_30 = [15,103]
AI_N_195_30 = [15,203]
IT_N_195_70 = [15,79]
IB_N_195_70 = [15,104]
AI_N_195_70 = [15,204]
IT_N_200_45 = [15,80]
IB_N_200_45 = [15,105]
AI_N_200_45 = [15,205]
IT_N_205_75 = [15,81]
IB_N_205_75 = [15,106]
AI_N_205_75 = [15,206]

IT_N_205_90 = [15,82]
IB_N_205_90 = [15,107]
AI_N_205_90 = [15,207]
IT_N_215_50 = [15,83]
IB_N_215_50 = [15,108]
AI_N_215_50 = [15,208]
IT_N_215_25 = [15,84]
IB_N_215_25 = [15,109]
AI_N_215_25 = [15,209]
IT_N_215_10 = [15,85]
IB_N_215_10 = [15,110]
AI_N_215_10 = [15,210]
IT_N_215_65 = [15,86]
IB_N_215_65 = [15,111]
AI_N_215_65 = [15,211]
IT_E_230_75 = [15,87]
IB_E_230_75 = [15,112]
AI_E_230_75 = [15,212]
IT_E_230_90 = [15,88]
IB_E_230_90 = [15,113]
AI_E_230_90 = [15,213]
IT_E_235_45 = [15,89]
IB_E_235_45 = [15,114]
AI_E_235_45 = [15,214]
IT_E_240_30 = [15,90]
IB_E_240_30 = [15,115]
AI_E_240_30 = [15,215]
IT_E_250_65 = [15,91]
IB_E_250_65 = [15,116]
AI_E_250_65 = [15,216]
IT_E_250_90 = [15,92]
IB_E_250_90 = [15,117]
AI_E_250_90 = [15,217]
IT_E_265_30 = [15,93]
IB_E_265_30 = [15,118]
AI_E_265_30 = [15,218]
IT_E_270_45 = [15,94]
IB_E_270_45 = [15,119]
AI_E_270_45 = [15,219]
IT_E_275_75 = [15,95]
IB_E_275_75 = [15,120]
AI_E_275_75 = [15,220]
IT_E_275_90 = [15,96]
IB_E_275_90 = [15,121]

AI_E_275_90 = [15,221]
IT_E_290_10 = [15,97]
IB_E_290_10 = [15,122]
AI_E_290_10 = [15,222]
IT_E_290_25 = [15,98]
IB_E_290_25 = [15,123]
AI_E_290_25 = [15,223]
IT_E_290_50 = [15,99]
IB_E_290_50 = [15,124]
AI_E_290_50 = [15,224]
IT_E_290_65 = [15,100]
IB_E_290_65 = [15,125]
AI_E_290_65 = [15,225]
IT_E_300_75 = [15,101]
IB_E_300_75 = [15,126]
AI_E_300_75 = [15,226]
IT_E_300_90 = [15,102]
IB_E_300_90 = [15,127]
AI_E_300_90 = [15,227]
IT_E_305_45 = [15,103]
IB_E_305_45 = [15,128]
AI_E_305_45 = [15,228]
IT_E_310_30 = [15,104]
IB_E_310_30 = [15,129]
AI_E_310_30 = [15,229]
IT_E_310_65 = [15,105]
IB_E_310_65 = [15,130]
AI_E_310_65 = [15,230]
IT_S_315_55 = [15,106]
IB_S_315_55 = [15,131]
AI_S_315_55 = [15,231]
IT_S_325_75 = [15,107]
IB_S_325_75 = [15,132]
AI_S_325_75 = [15,232]
IT_S_325_90 = [15,108]
IB_S_325_90 = [15,133]
AI_S_325_90 = [15,233]
IT_S_330_90 = [15,109]
IB_S_330_90 = [15,134]
AI_S_330_90 = [15,234]
IT_S_335_55 = [15,110]
IB_S_335_55 = [15,135]
AI_S_335_55 = [15,235]
IT_S_335_65 = [15,111]

```
    IB_S_335_65 = [15,136]
    AI_S_335_65 = [15,236]
    IT_S_340_30 = [15,112]
    IB_S_340_30 = [15,137]
    AI_S_340_30 = [15,237]
    IT_S_345_45 = [15,113]
    IB_S_345_45 = [15,138]
    AI_S_345_45 = [15,238]
    IT_S_350_70 = [15,114]
    IB_S_350_70 = [15,139]
    AI_S_350_70 = [15,239]
    IT_S_350_90 = [15,115]
    IB_S_350_90 = [15,140]
    AI_S_350_90 = [15,240]
    SOLAR_PANEL = [15,25]/max(1, [15,25])
*$UNIT_NAME Radiation
*$LAYER Main
*$POSITION 196 180
*-------------------------------------------------------------------------------
* Model "Weather data" (Type 15)
*

 UNIT  15    TYPE  15    data
*$UNIT_NAME Weather data
*$MODEL .\Weather Data Reading and Processing\Standard Format\Canadian Weather
for Energy Calculations Files (CWEC)\Type15-5.tmf
*$POSITION 195 298
*$LAYER Main # #
     PARAMETERS 279
! 1 File Type
! 2 Logical unit
! 3 Tilted Surface Radiation Mode
! 4 Ground reflectance - no snow
! 5 Ground reflectance - snow cover
! 6 Number of surfaces
! 7 Tracking mode-1
! 8 Slope of surface-1
! 9 Azimuth of surface-1
! 10 Tracking mode-2
! 11 Slope of surface-2
! 12 Azimuth of surface-2
! 13 Tracking mode-3
! 14 Slope of surface-3
! 15 Azimuth of surface-3
```

! 16 Tracking mode-4
! 17 Slope of surface-4
! 18 Azimuth of surface-4
! 19 Tracking mode-5
! 20 Slope of surface-5
! 21 Azimuth of surface-5
! 22 Tracking mode-6
! 23 Slope of surface-6
! 24 Azimuth of surface-6
! 25 Tracking mode-7
! 26 Slope of surface-7
! 27 Azimuth of surface-7
! 28 Tracking mode-8
! 29 Slope of surface-8
! 30 Azimuth of surface-8
! 31 Tracking mode-9
! 32 Slope of surface-9
! 33 Azimuth of surface-9
! 34 Tracking mode-10
! 35 Slope of surface-10
! 36 Azimuth of surface-10
! 37 Tracking mode-11
! 38 Slope of surface-11
! 39 Azimuth of surface-11
! 40 Tracking mode-12
! 41 Slope of surface-12
! 42 Azimuth of surface-12
! 43 Tracking mode-13
! 44 Slope of surface-13
! 45 Azimuth of surface-13
! 46 Tracking mode-14
! 47 Slope of surface-14
! 48 Azimuth of surface-14
! 49 Tracking mode-15
! 50 Slope of surface-15
! 51 Azimuth of surface-15
! 52 Tracking mode-16
! 53 Slope of surface-16
! 54 Azimuth of surface-16
! 55 Tracking mode-17
! 56 Slope of surface-17
! 57 Azimuth of surface-17
! 58 Tracking mode-18
! 59 Slope of surface-18

! 60 Azimuth of surface-18
! 61 Tracking mode-19
! 62 Slope of surface-19
! 63 Azimuth of surface-19
! 64 Tracking mode-20
! 65 Slope of surface-20
! 66 Azimuth of surface-20
! 67 Tracking mode-21
! 68 Slope of surface-21
! 69 Azimuth of surface-21
! 70 Tracking mode-22
! 71 Slope of surface-22
! 72 Azimuth of surface-22
! 73 Tracking mode-23
! 74 Slope of surface-23
! 75 Azimuth of surface-23
! 76 Tracking mode-24
! 77 Slope of surface-24
! 78 Azimuth of surface-24
! 79 Tracking mode-25
! 80 Slope of surface-25
! 81 Azimuth of surface-25
! 82 Tracking mode-26
! 83 Slope of surface-26
! 84 Azimuth of surface-26
! 85 Tracking mode-27
! 86 Slope of surface-27
! 87 Azimuth of surface-27
! 88 Tracking mode-28
! 89 Slope of surface-28
! 90 Azimuth of surface-28
! 91 Tracking mode-29
! 92 Slope of surface-29
! 93 Azimuth of surface-29
! 94 Tracking mode-30
! 95 Slope of surface-30
! 96 Azimuth of surface-30
! 97 Tracking mode-31
! 98 Slope of surface-31
! 99 Azimuth of surface-31
! 100 Tracking mode-32
! 101 Slope of surface-32
! 102 Azimuth of surface-32
! 103 Tracking mode-33

! 104 Slope of surface-33
! 105 Azimuth of surface-33
! 106 Tracking mode-34
! 107 Slope of surface-34
! 108 Azimuth of surface-34
! 109 Tracking mode-35
! 110 Slope of surface-35
! 111 Azimuth of surface-35
! 112 Tracking mode-36
! 113 Slope of surface-36
! 114 Azimuth of surface-36
! 115 Tracking mode-37
! 116 Slope of surface-37
! 117 Azimuth of surface-37
! 118 Tracking mode-38
! 119 Slope of surface-38
! 120 Azimuth of surface-38
! 121 Tracking mode-39
! 122 Slope of surface-39
! 123 Azimuth of surface-39
! 124 Tracking mode-40
! 125 Slope of surface-40
! 126 Azimuth of surface-40
! 127 Tracking mode-41
! 128 Slope of surface-41
! 129 Azimuth of surface-41
! 130 Tracking mode-42
! 131 Slope of surface-42
! 132 Azimuth of surface-42
! 133 Tracking mode-43
! 134 Slope of surface-43
! 135 Azimuth of surface-43
! 136 Tracking mode-44
! 137 Slope of surface-44
! 138 Azimuth of surface-44
! 139 Tracking mode-45
! 140 Slope of surface-45
! 141 Azimuth of surface-45
! 142 Tracking mode-46
! 143 Slope of surface-46
! 144 Azimuth of surface-46
! 145 Tracking mode-47
! 146 Slope of surface-47
! 147 Azimuth of surface-47

! 148 Tracking mode-48
! 149 Slope of surface-48
! 150 Azimuth of surface-48
! 151 Tracking mode-49
! 152 Slope of surface-49
! 153 Azimuth of surface-49
! 154 Tracking mode-50
! 155 Slope of surface-50
! 156 Azimuth of surface-50
! 157 Tracking mode-51
! 158 Slope of surface-51
! 159 Azimuth of surface-51
! 160 Tracking mode-52
! 161 Slope of surface-52
! 162 Azimuth of surface-52
! 163 Tracking mode-53
! 164 Slope of surface-53
! 165 Azimuth of surface-53
! 166 Tracking mode-54
! 167 Slope of surface-54
! 168 Azimuth of surface-54
! 169 Tracking mode-55
! 170 Slope of surface-55
! 171 Azimuth of surface-55
! 172 Tracking mode-56
! 173 Slope of surface-56
! 174 Azimuth of surface-56
! 175 Tracking mode-57
! 176 Slope of surface-57
! 177 Azimuth of surface-57
! 178 Tracking mode-58
! 179 Slope of surface-58
! 180 Azimuth of surface-58
! 181 Tracking mode-59
! 182 Slope of surface-59
! 183 Azimuth of surface-59
! 184 Tracking mode-60
! 185 Slope of surface-60
! 186 Azimuth of surface-60
! 187 Tracking mode-61
! 188 Slope of surface-61
! 189 Azimuth of surface-61
! 190 Tracking mode-62
! 191 Slope of surface-62

! 192 Azimuth of surface-62
! 193 Tracking mode-63
! 194 Slope of surface-63
! 195 Azimuth of surface-63
! 196 Tracking mode-64
! 197 Slope of surface-64
! 198 Azimuth of surface-64
! 199 Tracking mode-65
! 200 Slope of surface-65
! 201 Azimuth of surface-65
! 202 Tracking mode-66
! 203 Slope of surface-66
! 204 Azimuth of surface-66
! 205 Tracking mode-67
! 206 Slope of surface-67
! 207 Azimuth of surface-67
! 208 Tracking mode-68
! 209 Slope of surface-68
! 210 Azimuth of surface-68
! 211 Tracking mode-69
! 212 Slope of surface-69
! 213 Azimuth of surface-69
! 214 Tracking mode-70
! 215 Slope of surface-70
! 216 Azimuth of surface-70
! 217 Tracking mode-71
! 218 Slope of surface-71
! 219 Azimuth of surface-71
! 220 Tracking mode-72
! 221 Slope of surface-72
! 222 Azimuth of surface-72
! 223 Tracking mode-73
! 224 Slope of surface-73
! 225 Azimuth of surface-73
! 226 Tracking mode-74
! 227 Slope of surface-74
! 228 Azimuth of surface-74
! 229 Tracking mode-75
! 230 Slope of surface-75
! 231 Azimuth of surface-75
! 232 Tracking mode-76
! 233 Slope of surface-76
! 234 Azimuth of surface-76
! 235 Tracking mode-77

! 236 Slope of surface-77
! 237 Azimuth of surface-77
! 238 Tracking mode-78
! 239 Slope of surface-78
! 240 Azimuth of surface-78
! 241 Tracking mode-79
! 242 Slope of surface-79
! 243 Azimuth of surface-79
! 244 Tracking mode-80
! 245 Slope of surface-80
! 246 Azimuth of surface-80
! 247 Tracking mode-81
! 248 Slope of surface-81
! 249 Azimuth of surface-81
! 250 Tracking mode-82
! 251 Slope of surface-82
! 252 Azimuth of surface-82
! 253 Tracking mode-83
! 254 Slope of surface-83
! 255 Azimuth of surface-83
! 256 Tracking mode-84
! 257 Slope of surface-84
! 258 Azimuth of surface-84
! 259 Tracking mode-85
! 260 Slope of surface-85
! 261 Azimuth of surface-85
! 262 Tracking mode-86
! 263 Slope of surface-86
! 264 Azimuth of surface-86
! 265 Tracking mode-87
! 266 Slope of surface-87
! 267 Azimuth of surface-87
! 268 Tracking mode-88
! 269 Slope of surface-88
! 270 Azimuth of surface-88
! 271 Tracking mode-89
! 272 Slope of surface-89
! 273 Azimuth of surface-89
! 274 Tracking mode-90
! 275 Slope of surface-90
! 276 Azimuth of surface-90
! 277 Tracking mode-91
! 278 Slope of surface-91
! 279 Azimuth of surface-91

5.0000000000000000E+00 2.0900000000000000E+02 5.0000000000000000E+00
2.0000000000000001E-01 7.0000000000000007E-01
9.1000000000000000E+01 1.0000000000000000E+00 0.0000000000000000E+00
0.0000000000000000E+00 1.0000000000000000E+00
5.0000000000000000E+01 0.0000000000000000E+00 1.0000000000000000E+00
2.5000000000000000E+01 0.0000000000000000E+00
1.0000000000000000E+00 1.0000000000000000E+01 0.0000000000000000E+00
1.0000000000000000E+00 6.5000000000000000E+01
0.0000000000000000E+00 1.0000000000000000E+00 9.0000000000000000E+01
5.0000000000000000E+00 1.0000000000000000E+00
7.0000000000000000E+01 1.0000000000000000E+01 1.0000000000000000E+00
9.0000000000000000E+01 1.0000000000000000E+01
1.0000000000000000E+00 4.5000000000000000E+01 1.5000000000000000E+01
1.0000000000000000E+00 3.0000000000000000E+01
2.0000000000000000E+01 1.0000000000000000E+00 5.5000000000000000E+01
2.5000000000000000E+01 1.0000000000000000E+00
6.5000000000000000E+01 2.5000000000000000E+01 1.0000000000000000E+00
7.5000000000000000E+01 3.5000000000000000E+01
1.0000000000000000E+00 9.0000000000000000E+01 3.5000000000000000E+01
1.0000000000000000E+00 5.5000000000000000E+01
4.5000000000000000E+01 1.0000000000000000E+00 3.0000000000000000E+01
5.0000000000000000E+01 1.0000000000000000E+00
6.5000000000000000E+01 5.0000000000000000E+01 1.0000000000000000E+00
4.5000000000000000E+01 5.5000000000000000E+01
1.0000000000000000E+00 7.5000000000000000E+01 6.0000000000000000E+01
1.0000000000000000E+00 9.0000000000000000E+01
6.0000000000000000E+01 1.0000000000000000E+00 5.0000000000000000E+01
7.0000000000000000E+01 1.0000000000000000E+00
1.0000000000000000E+01 7.0000000000000000E+01 1.0000000000000000E+00
2.5000000000000000E+01 7.0000000000000000E+01
1.0000000000000000E+00 6.5000000000000000E+01 7.0000000000000000E+01
1.0000000000000000E+00 9.0000000000000000E+01
8.5000000000000000E+01 1.0000000000000000E+00 7.5000000000000000E+01
8.5000000000000000E+01 1.0000000000000000E+00
4.5000000000000000E+01 9.0000000000000000E+01 1.0000000000000000E+00
3.0000000000000000E+01 9.5000000000000000E+01
1.0000000000000000E+00 7.0000000000000000E+01 9.5000000000000000E+01
1.0000000000000000E+00 5.5000000000000000E+01
1.0000000000000000E+02 1.0000000000000000E+00 7.5000000000000000E+01
1.1000000000000000E+02 1.0000000000000000E+00
9.0000000000000000E+01 1.1000000000000000E+02 1.0000000000000000E+00
5.5000000000000000E+01 1.1500000000000000E+02
1.0000000000000000E+00 3.0000000000000000E+01 1.2000000000000000E+02
1.0000000000000000E+00 7.0000000000000000E+01

1.2000000000000000E+02 1.0000000000000000E+00 4.5000000000000000E+01
1.2500000000000000E+02 1.0000000000000000E+00
7.5000000000000000E+01 1.3000000000000000E+02 1.0000000000000000E+00
9.0000000000000000E+01 1.3500000000000000E+02
1.0000000000000000E+00 5.0000000000000000E+01 1.4500000000000000E+02
1.0000000000000000E+00 2.5000000000000000E+01
1.4500000000000000E+02 1.0000000000000000E+00 1.0000000000000000E+01
1.4500000000000000E+02 1.0000000000000000E+00
6.5000000000000000E+01 1.4500000000000000E+02 1.0000000000000000E+00
7.5000000000000000E+01 1.5500000000000000E+02
1.0000000000000000E+00 9.0000000000000000E+01 1.5500000000000000E+02
1.0000000000000000E+00 4.5000000000000000E+01
1.6000000000000000E+02 1.0000000000000000E+00 9.0000000000000000E+01
1.6000000000000000E+02 1.0000000000000000E+00
3.0000000000000000E+01 1.6500000000000000E+02 1.0000000000000000E+00
7.0000000000000000E+01 1.6500000000000000E+02
1.0000000000000000E+00 5.5000000000000000E+01 1.7000000000000000E+02
1.0000000000000000E+00 9.0000000000000000E+01
1.7500000000000000E+02 1.0000000000000000E+00 7.5000000000000000E+01
1.8000000000000000E+02 1.0000000000000000E+00
9.0000000000000000E+01 1.8000000000000000E+02 1.0000000000000000E+00
5.5000000000000000E+01 1.9000000000000000E+02
1.0000000000000000E+00 3.0000000000000000E+01 1.9500000000000000E+02
1.0000000000000000E+00 7.0000000000000000E+01
1.9500000000000000E+02 1.0000000000000000E+00 4.5000000000000000E+01
2.0000000000000000E+02 1.0000000000000000E+00
7.5000000000000000E+01 2.0500000000000000E+02 1.0000000000000000E+00
9.0000000000000000E+01 2.0500000000000000E+02
1.0000000000000000E+00 5.0000000000000000E+01 2.1500000000000000E+02
1.0000000000000000E+00 2.5000000000000000E+01
2.1500000000000000E+02 1.0000000000000000E+00 1.0000000000000000E+01
2.1500000000000000E+02 1.0000000000000000E+00
6.5000000000000000E+01 2.1500000000000000E+02 1.0000000000000000E+00
7.5000000000000000E+01 2.3000000000000000E+02
1.0000000000000000E+00 9.0000000000000000E+01 2.3000000000000000E+02
1.0000000000000000E+00 4.5000000000000000E+01
2.3500000000000000E+02 1.0000000000000000E+00 3.0000000000000000E+01
2.4000000000000000E+02 1.0000000000000000E+00
6.5000000000000000E+01 2.5000000000000000E+02 1.0000000000000000E+00
9.0000000000000000E+01 2.5000000000000000E+02
1.0000000000000000E+00 3.0000000000000000E+01 2.6500000000000000E+02
1.0000000000000000E+00 4.5000000000000000E+01
2.7000000000000000E+02 1.0000000000000000E+00 7.5000000000000000E+01
2.7500000000000000E+02 1.0000000000000000E+00

```
    9.0000000000000000E+01    2.7500000000000000E+02    1.0000000000000000E+00
1.0000000000000000E+01    2.9000000000000000E+02
    1.0000000000000000E+00    2.5000000000000000E+01    2.9000000000000000E+02
1.0000000000000000E+00    5.0000000000000000E+01
    2.9000000000000000E+02    1.0000000000000000E+00    6.5000000000000000E+01
2.9000000000000000E+02    1.0000000000000000E+00
    7.5000000000000000E+01    3.0000000000000000E+02    1.0000000000000000E+00
9.0000000000000000E+01    3.0000000000000000E+02
    1.0000000000000000E+00    4.5000000000000000E+01    3.0500000000000000E+02
1.0000000000000000E+00    3.0000000000000000E+01
    3.1000000000000000E+02    1.0000000000000000E+00    6.5000000000000000E+01
3.1000000000000000E+02    1.0000000000000000E+00
    5.5000000000000000E+01    3.1500000000000000E+02    1.0000000000000000E+00
7.5000000000000000E+01    3.2500000000000000E+02
    1.0000000000000000E+00    9.0000000000000000E+01    3.2500000000000000E+02
1.0000000000000000E+00    9.0000000000000000E+01
    3.3000000000000000E+02    1.0000000000000000E+00    5.5000000000000000E+01
3.3500000000000000E+02    1.0000000000000000E+00
    6.5000000000000000E+01    3.3500000000000000E+02    1.0000000000000000E+00
3.0000000000000000E+01    3.4000000000000000E+02
    1.0000000000000000E+00    4.5000000000000000E+01    3.4500000000000000E+02
1.0000000000000000E+00    7.0000000000000000E+01
    3.5000000000000000E+02    1.0000000000000000E+00    9.0000000000000000E+01
3.5000000000000000E+02
*** External files
 ASSIGN  C:\Users\pclau_000\Dropbox\Thesis\TRNSYS\Ottawa  CWEC  Data  2014-
2015\CAN_ON_Ottawa.716280_CWEC.epw  209
*|? Which file contains the CWEC weather data? |1000
*-------------------------------------------------------------------------
* Model "Building" (Type 56)
*

 UNIT  56   TYPE  56
*$UNIT_NAME Building
*$MODEL .\Loads and Structures\Multi-Zone Building\Type56.tmf
*$POSITION 483 173
*$LAYER Main # # #
*$#
    PARAMETERS  3
! 1 Logical unit for building description file (.bui)
! 2 Star network calculation switch
! 3 Weighting factor for operative temperature
    2.1000000000000000E+02    1.0000000000000000E+00    5.0000000000000000E-01
    INPUTS  14
```

```
! Weather data:Dry bulb temperature -> 1- TAMB
! Weather data:Percent relative humidity -> 2- RELHUMAMB
! Weather data:Effective sky temperature -> 3- TSKY
! Weather data:Dry bulb temperature -> 4- TSGRD
! Weather data:Solar zenith angle -> 5- AZEN
! AzimuthAngles:AAZM_TYPE56 -> 6- AAZM
! [unconnected]  7- GRDREF
! [unconnected]  8- TGROUND
! [unconnected]  9- TBOUNDARY
! [unconnected]  10- BRIGHT
! [unconnected]  11- SHADE_CLOSE
! [unconnected]  12- SHADE_OPEN
! [unconnected]  13- MAX_ISHADE
! [unconnected]  14- MAX_ESHADE
     15,1              15,7              15,4              15,1              15,16
     AAZM_TYPE56       CONST             CONST             CONST             CONST
     CONST             CONST             CONST             CONST
*** INITIAL INPUT VALUES
     0.0000000000000000E+00    0.0000000000000000E+00    0.0000000000000000E+00
0.0000000000000000E+00    0.0000000000000000E+00
     0.0000000000000000E+00    0.0000000000000000E+00    0.0000000000000000E+00
0.0000000000000000E+00    0.0000000000000000E+00
     0.0000000000000000E+00    0.0000000000000000E+00    0.0000000000000000E+00
0.0000000000000000E+00
*** External files
  ASSIGN July_28_A.b17  210
*|? Building description file (*.bui) |1000
*--------------------------------------------------------------------------
* Model "Irradiation" (Type 65)
*

  UNIT   65     TYPE   65
*$UNIT_NAME Irradiation
*$MODEL .\Output\Online Plotter\Online Plotter Without File\Type65d.tmf
*$POSITION 317 223
*$LAYER Main # # #
     PARAMETERS  12
! 1 Nb. of left-axis variables
! 2 Nb. of right-axis variables
! 3 Left axis minimum
! 4 Left axis maximum
! 5 Right axis minimum
! 6 Right axis maximum
! 7 Number of plots per simulation
```

```
! 8 X-axis gridpoints
! 9 Shut off Online w/o removing
! 10 Logical unit for output file
! 11 Output file units
! 12 Output file delimiter
     1.0000000000000000E+00    1.0000000000000000E+00    0.0000000000000000E+00
3.6000000000000000E+03    0.0000000000000000E+00
     3.6000000000000000E+03    1.0000000000000000E+00    1.2000000000000000E+01
0.0000000000000000E+00   -1.0000000000000000E+00
     0.0000000000000000E+00    0.0000000000000000E+00
     INPUTS    2
! Radiation:IT_H_0_0 ->Left axis variable
! Radiation:IB_H_0_0 ->Right axis variable
     IT_H_0_0              IB_H_0_0
*** INITIAL INPUT VALUES
     IT_H_0_0                        IB_H_0_0
     LABELS    3
     Total   Incident Solar Radition [kJ/hr m²]
     Beam   Incident Solar Radition [kJ/hr m²]
     Irradition
*-------------------------------------------------------------------------------
* Model "Temperature" (Type 65)
*

  UNIT   66     TYPE   65
*$UNIT_NAME Temperature
*$MODEL .\Output\Online Plotter\Online Plotter Without File\Type65d.tmf
*$POSITION 449 298
*$LAYER Main # # #
     PARAMETERS  12
! 1 Nb. of left-axis variables
! 2 Nb. of right-axis variables
! 3 Left axis minimum
! 4 Left axis maximum
! 5 Right axis minimum
! 6 Right axis maximum
! 7 Number of plots per simulation
! 8 X-axis gridpoints
! 9 Shut off Online w/o removing
! 10 Logical unit for output file
! 11 Output file units
! 12 Output file delimiter
     1.0000000000000000E+00    2.0000000000000000E+00   -2.0000000000000000E+01
3.5000000000000000E+01   -2.0000000000000000E+01
```

```
     3.5000000000000000E+01    1.0000000000000000E+00    1.2000000000000000E+01
0.0000000000000000E+00   -1.0000000000000000E+00
     0.0000000000000000E+00    0.0000000000000000E+00
     INPUTS    3
! Weather data:Dry bulb temperature ->Left axis variable
! Building: 16- TAIR_DOME ->Right axis variable-1
! Building: 1- TAIR_WATER_TANK ->Right axis variable-2
     15,1                56,16                56,1
*** INITIAL INPUT VALUES
     Tamb                          DOME                          DOME
     LABELS    3
     Temperatures    [deg C]
     Temperatures    [deg C]
     Temperatures
*-------------------------------------------------------------------------------
* Model "System_Printer" (Type 25)
*

  UNIT    9    TYPE   25
*$UNIT_NAME System_Printer
*$MODEL \Trnsys17\Studio\lib\System_Output\Type25a.tmf
*$POSITION 328 106
*$LAYER OutputSystem #
     PARAMETERS  10
! 1 Printing interval
! 2 Start time
! 3 Stop time
! 4 Logical unit
! 5 Units printing mode
! 6 Relative or absolute start time
! 7 Overwrite or Append
! 8 Print header
! 9 Delimiter
! 10 Print labels
     1.0000000000000000E+00    0.0000000000000000E+00    8.7600000000000000E+03
2.1100000000000000E+02    2.0000000000000000E+00
     0.0000000000000000E+00   -1.0000000000000000E+00   -1.0000000000000000E+00
0.0000000000000000E+00    1.0000000000000000E+00
     INPUTS   31
! Building: 1- TAIR_WATER_TANK ->Input to be printed-1
! Building: 2- TAIR_B1 ->Input to be printed-2
! Building: 3- TAIR_B2 ->Input to be printed-3
! Building: 4- TAIR_B3 ->Input to be printed-4
! Building: 5- TAIR_B4 ->Input to be printed-5
```

```
! Building: 6- TAIR_B5 ->Input to be printed-6
! Building: 7- TAIR_B6 ->Input to be printed-7
! Building: 8- TAIR_B7 ->Input to be printed-8
! Building: 9- TAIR_B8 ->Input to be printed-9
! Building: 10- TAIR_B9 ->Input to be printed-10
! Building: 11- TAIR_B10 ->Input to be printed-11
! Building: 12- TAIR_B11 ->Input to be printed-12
! Building: 13- TAIR_B12 ->Input to be printed-13
! Building: 14- TAIR_B13 ->Input to be printed-14
! Building: 15- TAIR_B14 ->Input to be printed-15
! Building: 16- TAIR_DOME ->Input to be printed-16
! Building: 17- TAIR_DOOR_BOTTOM ->Input to be printed-17
! Building: 18- TAIR_C6 ->Input to be printed-18
! Building: 19- TAIR_C5 ->Input to be printed-19
! Building: 20- TAIR_C4 ->Input to be printed-20
! Building: 21- TAIR_C3 ->Input to be printed-21
! Building: 22- TAIR_C2 ->Input to be printed-22
! Building: 23- TAIR_C1 ->Input to be printed-23
! Building: 24- TAIR_C14 ->Input to be printed-24
! Building: 25- TAIR_C8 ->Input to be printed-25
! Building: 26- TAIR_C9 ->Input to be printed-26
! Building: 27- TAIR_C10 ->Input to be printed-27
! Building: 28- TAIR_C11 ->Input to be printed-28
! Building: 29- TAIR_C12 ->Input to be printed-29
! Building: 30- TAIR_C13 ->Input to be printed-30
! Radiation:IT_S_0_50 ->Input to be printed-31
    56,1          56,2          56,3          56,4          56,5
    56,6          56,7          56,8          56,9          56,10
    56,11         56,12         56,13         56,14         56,15
    56,16         56,17         56,18         56,19         56,20
    56,21         56,22         56,23         56,24         56,25
    56,26         56,27         56,28         56,29         56,30
    IT_S_0_50
*** INITIAL INPUT VALUES
    TAIR_WATER_TANK          T_B1          T_B2          T_B3
T_B4
    T_B5          T_B6          T_B7          T_B8
T_B9
    T_B10         T_B11         T_B12         T_B13
T_B14
    T_DOME        T_DOOR        T_C6          T_C5
T_C4
    T_C3          T_C2          T_C1          T_C14
T_C8
```

```
     T_C9                    T_C10                   T_C11                   T_C12
T_C13
     SOLAR_VENT_RAD
*** External files
 ASSIGN Type25a.txt  211
*|? Which file should contain the printed results? You can use the deck filename by entering "***", e.g. "***.out", or "***.dat"  |1000
*-------------------------------------------------------------------------------

 END

      TRANSIENT SIMULATION     STARTING AT TIME =  0.0000000000000000E+00
                        STOPPING AT TIME =  8.7600000000000000E+03
                             TIMESTEP =        1 /       1
          DIFFERENTIAL EQUATION ERROR TOLERANCE =  1.0000000000000002E-03
             ALGEBRAIC CONVERGENCE TOLERANCE =  1.0000000000000002E-03

    DIFFERENTIAL EQUATIONS SOLVED BY MODIFIED EULER

*** Notice at time       :       0.000000
   Generated by Unit     : Not applicable or not available
   Generated by Type     : Not applicable or not available
   TRNSYS Message      89 : TRNDll.dll is compiled in debug mode. External DLLs will be loaded from the .\UserLib\DebugDLLs\ directory.
   Reported information  : Not available

*** Notice at time       :       0.000000
   Generated by Unit     : Not applicable or not available
   Generated by Type     : Not applicable or not available
   Message               : The following Types were loaded from TRNDll.dll: Type25, Type15, Type65

 *** Notice at time       :       0.000000
   Generated by Unit     : Not applicable or not available
   Generated by Type     : Not applicable or not available
   Message             : "FileReader.dll" was found but did not contain any components from the input file.

*** Notice at time       :       0.000000
   Generated by Unit     : Not applicable or not available
   Generated by Type     : Not applicable or not available
   Message               : "type127.dll" was found but did not contain any components from the input file.
```

*** Notice at time : 0.000000
Generated by Unit : Not applicable or not available
Generated by Type : Not applicable or not available
Message : "Type157_debug.dll" was found but did not contain any components from the input file.

*** Notice at time : 0.000000
Generated by Unit : Not applicable or not available
Generated by Type : Not applicable or not available
Message : The following Types were loaded from "Type56.dll": Type56

*** Notice at time : 0.000000
Generated by Unit : Not applicable or not available
Generated by Type : Not applicable or not available
Message : "Type76Lib.dll" was found but did not contain any components from the input file.

*** Notice at time : 0.000000
Generated by Unit : Not applicable or not available
Generated by Type : Not applicable or not available
Message : "Type82Lib.dll" was found but did not contain any components from the input file.

*** Notice at time : 0.000000
Generated by Unit : Not applicable or not available
Generated by Type : Not applicable or not available
TRNSYS Message 199 : TRNSYS found at least one user DLL in the UserLib directory. (Note: Only DLL's including Types that are used in the simulation are loaded)
Reported information : 1 user DLL was loaded after searching in "C:\Trnsys17\UserLib\DebugDLLs"

*** Notice at time : 0.000000
Generated by Unit : 56
Generated by Type : 56
Message : View factor file *.vfm exists and will be used for zones with detailed radiation mode.

*** Notice at time : 0.000000
Generated by Unit : 56
Generated by Type : 56
Message : Shading mask file *.shm for external windows does not exist.

*** Notice at time : 0.000000
Generated by Unit : 56

Generated by Type : 56
Message : TRNFLOW (multi zone air flow model) messages are written in a separate file *.cer! Please, always check the *.cer file for information!!!

*** Notice at time : 0.000000
Generated by Unit : 56
Generated by Type : 56
Message : Active layers and internal window calculations integrated

*** Notice at time : 0.000000
Generated by Unit : 56
Generated by Type : 56
Message : No internal humidity calculations are performed and no condensation warnings are printed. if any of the outputs ntype 9,10,11,26,29,40,41,47,48 or 49 is specified The humidity calculations, using an internal timestep, will be switched on and condensation checks are performed

*** Notice at time : 0.000000
Generated by Unit : 56
Generated by Type : 56
Message : Star network calculation: every iteration step of TRNSYS

*** The TRNSYS components will be called in the following order:
Unit # 15 Type # 15
Unit # 56 Type # 56
Unit # 65 Type # 65
Unit # 66 Type # 65
Unit # 9 Type # 25

*** Warning at time : 8760.000000
Generated by Unit : 15
Generated by Type : 15
Message : The calculated total horizontal radiation exceeded the horizontal extraterrestrial radiation and was set to the extraterrestrial for 14 timesteps during the simulation.

****
****
The Following UNIT Numbers, TYPE Numbers, and Logical Units Were Used in the Supplied TRNSYS Input File:

9	15	4
15	25	6
56	56	9
65	65	209

66 210
211
212
213
214
215
216
217

****
****
Total TRNSYS Calculation Time: 2237.6201 Seconds

Appendix B: TRNSYS Deck File

```
VERSION 17
**********************************************************************
*******
*** TRNSYS input file (deck) generated by TrnsysStudio
*** on Wednesday, November 25, 2015 at 15:19
*** from TrnsysStudio project:
C:\Users\pclau_000\Dropbox\Thesis\TRNSYS\June_12\July_28_A.tpf
***
*** If you edit this file, use the File/Import TRNSYS Input File function in
*** TrnsysStudio to update the project.
***
*** If you have problems, questions or suggestions please contact your local
*** TRNSYS distributor or mailto:software@cstb.fr
***
**********************************************************************
*******



**********************************************************************
*******
*** Units
```

```
**********************************************************************
*******

**********************************************************************
*******
*** Control cards
**********************************************************************
*******
* START, STOP and STEP
CONSTANTS 3
START=0
STOP=8760
STEP=1
SIMULATION    START  STOP    STEP   ! Start time     End time        Time step
TOLERANCES 0.001 0.001                    ! Integration     Convergence
LIMITS 30 30 30                           ! Max iterations        Max warnings Trace
limit
DFQ 1                             ! TRNSYS numerical integration solver method
WIDTH 72                          ! TRNSYS output file width, number of characters
LIST                              ! NOLIST statement
                                  ! MAP statement
SOLVER 0 1 1                      ! Solver statement     Minimum   relaxation   factor
```

```
        Maximum relaxation factor
NAN_CHECK 0                     ! Nan DEBUG statement
OVERWRITE_CHECK 0               ! Overwrite DEBUG statement
TIME_REPORT 0                   ! disable time report
EQSOLVER 0                      ! EQUATION SOLVER statement
* User defined CONSTANTS



* EQUATIONS "Wizard settings"
*
EQUATIONS 5
TURN = 0   !Rotation angle for building used for adapting azimuth angles
SHADE_CLOSE = 140 * 3.6! Close blinds - radiation on facade in [W/m2 * 3.6]=[kJ/hr]
SHADE_OPEN = 120 * 3.6! Open blinds - radiation on facade in [W/m2 * 3.6]=[kJ/hr]
MAX_ISHADE = 0/100 ! Maximum opaque fraction of internal shading device
MAX_ESHADE = 0/100 ! Maximum opaque fraction of external shading device
*$UNIT_NAME Wizard settings
*$LAYER Main
*$POSITION 73 180


*-------------------------------------------------------------------------------
```

* EQUATIONS "AzimuthAngles"

*

EQUATIONS 92

AA_H_0_0 = 0 + TURN ! azimuth angle of orientation

AA_S_0_50 = 0 + TURN ! azimuth angle of orientation

AA_S_0_25 = 0 + TURN ! azimuth angle of orientation

AA_S_0_10 = 0 + TURN ! azimuth angle of orientation

AA_S_0_65 = 0 + TURN ! azimuth angle of orientation

AA_S_5_90 = 5 + TURN ! azimuth angle of orientation

AA_S_10_70 = 10 + TURN ! azimuth angle of orientation

AA_S_10_90 = 10 + TURN ! azimuth angle of orientation

AA_S_15_45 = 15 + TURN ! azimuth angle of orientation

AA_S_20_30 = 20 + TURN ! azimuth angle of orientation

AA_S_25_55 = 25 + TURN ! azimuth angle of orientation

AA_S_25_65 = 25 + TURN ! azimuth angle of orientation

AA_S_35_75 = 35 + TURN ! azimuth angle of orientation

AA_S_35_90 = 35 + TURN ! azimuth angle of orientation

AA_W_45_55 = 45 + TURN ! azimuth angle of orientation

AA_W_50_30 = 50 + TURN ! azimuth angle of orientation

AA_W_50_65 = 50 + TURN ! azimuth angle of orientation

AA_W_55_45 = 55 + TURN ! azimuth angle of orientation

AA_W_60_75 = 60 + TURN ! azimuth angle of orientation

AA_W_60_90 = 60 + TURN ! azimuth angle of orientation

AA_W_70_50 = 70 + TURN ! azimuth angle of orientation

AA_W_70_10 = 70 + TURN ! azimuth angle of orientation

AA_W_70_25 = 70 + TURN ! azimuth angle of orientation

AA_W_70_65 = 70 + TURN ! azimuth angle of orientation

AA_W_85_90 = 85 + TURN ! azimuth angle of orientation

AA_W_85_75 = 85 + TURN ! azimuth angle of orientation

AA_W_90_45 = 90 + TURN ! azimuth angle of orientation

AA_W_95_30 = 95 + TURN ! azimuth angle of orientation

AA_W_95_70 = 95 + TURN ! azimuth angle of orientation

AA_W_100_55 = 100 + TURN ! azimuth angle of orientation

AA_W_110_75 = 110 + TURN ! azimuth angle of orientation

AA_W_110_90 = 110 + TURN ! azimuth angle of orientation

AA_W_115_55 = 115 + TURN ! azimuth angle of orientation

AA_W_120_30 = 120 + TURN ! azimuth angle of orientation

AA_W_120_70 = 120 + TURN ! azimuth angle of orientation

AA_W_125_45 = 125 + TURN ! azimuth angle of orientation

AA_W_130_75 = 130 + TURN ! azimuth angle of orientation

AA_N_135_90 = 135 + TURN ! azimuth angle of orientation

AA_N_145_50 = 145 + TURN ! azimuth angle of orientation

AA_N_145_25 = 145 + TURN ! azimuth angle of orientation

AA_N_145_10 = 145 + TURN ! azimuth angle of orientation

AA_N_145_65 = 145 + TURN ! azimuth angle of orientation

AA_N_155_75 = 155 + TURN ! azimuth angle of orientation

AA_N_155_90 = 155 + TURN ! azimuth angle of orientation

AA_N_160_45 = 160 + TURN ! azimuth angle of orientation

AA_N_160_90 = 160 + TURN ! azimuth angle of orientation

AA_N_165_30 = 165 + TURN ! azimuth angle of orientation

AA_N_165_70 = 165 + TURN ! azimuth angle of orientation

AA_N_170_55 = 170 + TURN ! azimuth angle of orientation

AA_N_175_90 = 175 + TURN ! azimuth angle of orientation

AA_N_180_75 = 180 + TURN ! azimuth angle of orientation

AA_N_180_90 = 180 + TURN ! azimuth angle of orientation

AA_N_190_55 = 190 + TURN ! azimuth angle of orientation

AA_N_195_30 = 195 + TURN ! azimuth angle of orientation

AA_N_195_70 = 195 + TURN ! azimuth angle of orientation

AA_N_200_45 = 200 + TURN ! azimuth angle of orientation

AA_N_205_75 = 205 + TURN ! azimuth angle of orientation

AA_N_205_90 = 205 + TURN ! azimuth angle of orientation

AA_N_215_50 = 215 + TURN ! azimuth angle of orientation

AA_N_215_25 = 215 + TURN ! azimuth angle of orientation

AA_N_215_10 = 215 + TURN ! azimuth angle of orientation

AA_N_215_65 = 215 + TURN ! azimuth angle of orientation

AA_E_230_75 = 230 + TURN ! azimuth angle of orientation

AA_E_230_90 = 230 + TURN ! azimuth angle of orientation

AA_E_235_45 = 235 + TURN ! azimuth angle of orientation

AA_E_240_30 = 240 + TURN ! azimuth angle of orientation

AA_E_250_65 = 250 + TURN ! azimuth angle of orientation

AA_E_250_90 = 250 + TURN ! azimuth angle of orientation

AA_E_265_30 = 265 + TURN ! azimuth angle of orientation

AA_E_270_45 = 270 + TURN ! azimuth angle of orientation

AA_E_275_75 = 275 + TURN ! azimuth angle of orientation

AA_E_275_90 = 275 + TURN ! azimuth angle of orientation

AA_E_290_10 = 290 + TURN ! azimuth angle of orientation

AA_E_290_25 = 290 + TURN ! azimuth angle of orientation

AA_E_290_50 = 290 + TURN ! azimuth angle of orientation

AA_E_290_65 = 290 + TURN ! azimuth angle of orientation

AA_E_300_75 = 300 + TURN ! azimuth angle of orientation

AA_E_300_90 = 300 + TURN ! azimuth angle of orientation

AA_E_305_45 = 305 + TURN ! azimuth angle of orientation

AA_E_310_30 = 310 + TURN ! azimuth angle of orientation

AA_E_310_65 = 310 + TURN ! azimuth angle of orientation

AA_S_315_55 = 315 + TURN ! azimuth angle of orientation

AA_S_325_75 = 325 + TURN ! azimuth angle of orientation

AA_S_325_90 = 325 + TURN ! azimuth angle of orientation

AA_S_330_90 = 330 + TURN ! azimuth angle of orientation

AA_S_335_55 = 335 + TURN ! azimuth angle of orientation

AA_S_335_65 = 335 + TURN ! azimuth angle of orientation

AA_S_340_30 = 340 + TURN ! azimuth angle of orientation

AA_S_345_45 = 345 + TURN ! azimuth angle of orientation

AA_S_350_70 = 350 + TURN ! azimuth angle of orientation

AA_S_350_90 = 350 + TURN ! azimuth angle of orientation

AAZM_TYPE56 = AAZM - (TURN) ! solar azimuth corrected by building rotation - Input for Type 56 sun position for SHM and ISM

*$UNIT_NAME AzimuthAngles

*$LAYER Main

*$POSITION 73 63

*--

* EQUATIONS "Radiation"

*

EQUATIONS 276

AZEN = [15,16]

AAZM = [15,17]

IT_H_0_0 = [15,24]

IB_H_0_0 = [15,49]

AI_H_0_0 = [15,149]

IT_S_0_50 = [15,25]

IB_S_0_50 = [15,50]

AI_S_0_50 = [15,150]

IT_S_0_25 = [15,26]

IB_S_0_25 = [15,51]

AI_S_0_25 = [15,151]

IT_S_0_10 = [15,27]

IB_S_0_10 = [15,52]

AI_S_0_10 = [15,152]

IT_S_0_65 = [15,28]

IB_S_0_65 = [15,53]

AI_S_0_65 = [15,153]

IT_S_5_90 = [15,29]

IB_S_5_90 = [15,54]

AI_S_5_90 = [15,154]

IT_S_10_70 = [15,30]

IB_S_10_70 = [15,55]

AI_S_10_70 = [15,155]

IT_S_10_90 = [15,31]

IB_S_10_90 = [15,56]

AI_S_10_90 = [15,156]

IT_S_15_45 = [15,32]

IB_S_15_45 = [15,57]

AI_S_15_45 = [15,157]

IT_S_20_30 = [15,33]

IB_S_20_30 = [15,58]

AI_S_20_30 = [15,158]

IT_S_25_55 = [15,34]

IB_S_25_55 = [15,59]

AI_S_25_55 = [15,159]

IT_S_25_65 = [15,35]

IB_S_25_65 = [15,60]

AI_S_25_65 = [15,160]

IT_S_35_75 = [15,36]

IB_S_35_75 = [15,61]

AI_S_35_75 = [15,161]

IT_S_35_90 = [15,37]

IB_S_35_90 = [15,62]

AI_S_35_90 = [15,162]

IT_W_45_55 = [15,38]

IB_W_45_55 = [15,63]

AI_W_45_55 = [15,163]

IT_W_50_30 = [15,39]

IB_W_50_30 = [15,64]

AI_W_50_30 = [15,164]

IT_W_50_65 = [15,40]

IB_W_50_65 = [15,65]

AI_W_50_65 = [15,165]

IT_W_55_45 = [15,41]

IB_W_55_45 = [15,66]

AI_W_55_45 = [15,166]

IT_W_60_75 = [15,42]

IB_W_60_75 = [15,67]

AI_W_60_75 = [15,167]

IT_W_60_90 = [15,43]

IB_W_60_90 = [15,68]

AI_W_60_90 = [15,168]

IT_W_70_50 = [15,44]

IB_W_70_50 = [15,69]

AI_W_70_50 = [15,169]

IT_W_70_10 = [15,45]

IB_W_70_10 = [15,70]

AI_W_70_10 = [15,170]

IT_W_70_25 = [15,46]

IB_W_70_25 = [15,71]

AI_W_70_25 = [15,171]

IT_W_70_65 = [15,47]

IB_W_70_65 = [15,72]

AI_W_70_65 = [15,172]

IT_W_85_90 = [15,48]

IB_W_85_90 = [15,73]

AI_W_85_90 = [15,173]

IT_W_85_75 = [15,49]

IB_W_85_75 = [15,74]

AI_W_85_75 = [15,174]

IT_W_90_45 = [15,50]

IB_W_90_45 = [15,75]

AI_W_90_45 = [15,175]

IT_W_95_30 = [15,51]

IB_W_95_30 = [15,76]

AI_W_95_30 = [15,176]

IT_W_95_70 = [15,52]

IB_W_95_70 = [15,77]

AI_W_95_70 = [15,177]

IT_W_100_55 = [15,53]

IB_W_100_55 = [15,78]

AI_W_100_55 = [15,178]

IT_W_110_75 = [15,54]

IB_W_110_75 = [15,79]

AI_W_110_75 = [15,179]

IT_W_110_90 = [15,55]

IB_W_110_90 = [15,80]

AI_W_110_90 = [15,180]

IT_W_115_55 = [15,56]

IB_W_115_55 = [15,81]

AI_W_115_55 = [15,181]

IT_W_120_30 = [15,57]

IB_W_120_30 = [15,82]

AI_W_120_30 = [15,182]

IT_W_120_70 = [15,58]

IB_W_120_70 = [15,83]

AI_W_120_70 = [15,183]

IT_W_125_45 = [15,59]

IB_W_125_45 = [15,84]

AI_W_125_45 = [15,184]

IT_W_130_75 = [15,60]

IB_W_130_75 = [15,85]

AI_W_130_75 = [15,185]

IT_N_135_90 = [15,61]

IB_N_135_90 = [15,86]

AI_N_135_90 = [15,186]

IT_N_145_50 = [15,62]

IB_N_145_50 = [15,87]

AI_N_145_50 = [15,187]

IT_N_145_25 = [15,63]

IB_N_145_25 = [15,88]

AI_N_145_25 = [15,188]

IT_N_145_10 = [15,64]

IB_N_145_10 = [15,89]

AI_N_145_10 = [15,189]

IT_N_145_65 = [15,65]

IB_N_145_65 = [15,90]

AI_N_145_65 = [15,190]

IT_N_155_75 = [15,66]

IB_N_155_75 = [15,91]

AI_N_155_75 = [15,191]

IT_N_155_90 = [15,67]

IB_N_155_90 = [15,92]

AI_N_155_90 = [15,192]

IT_N_160_45 = [15,68]

IB_N_160_45 = [15,93]

AI_N_160_45 = [15,193]

IT_N_160_90 = [15,69]

IB_N_160_90 = [15,94]

AI_N_160_90 = [15,194]

IT_N_165_30 = [15,70]

IB_N_165_30 = [15,95]

AI_N_165_30 = [15,195]

IT_N_165_70 = [15,72]

IB_N_165_70 = [15,97]

AI_N_165_70 = [15,197]

IT_N_170_55 = [15,73]

IB_N_170_55 = [15,98]

AI_N_170_55 = [15,198]

IT_N_175_90 = [15,74]

IB_N_175_90 = [15,99]

AI_N_175_90 = [15,199]

IT_N_180_75 = [15,75]

IB_N_180_75 = [15,100]

AI_N_180_75 = [15,200]

IT_N_180_90 = [15,76]

IB_N_180_90 = [15,101]

AI_N_180_90 = [15,201]

IT_N_190_55 = [15,77]

IB_N_190_55 = [15,102]

AI_N_190_55 = [15,202]

IT_N_195_30 = [15,78]

IB_N_195_30 = [15,103]

AI_N_195_30 = [15,203]

IT_N_195_70 = [15,79]

IB_N_195_70 = [15,104]

AI_N_195_70 = [15,204]

IT_N_200_45 = [15,80]

IB_N_200_45 = [15,105]

AI_N_200_45 = [15,205]

IT_N_205_75 = [15,81]

IB_N_205_75 = [15,106]

AI_N_205_75 = [15,206]

IT_N_205_90 = [15,82]

IB_N_205_90 = [15,107]

AI_N_205_90 = [15,207]

IT_N_215_50 = [15,83]

IB_N_215_50 = [15,108]

AI_N_215_50 = [15,208]

IT_N_215_25 = [15,84]

IB_N_215_25 = [15,109]

AI_N_215_25 = [15,209]

IT_N_215_10 = [15,85]

IB_N_215_10 = [15,110]

AI_N_215_10 = [15,210]

IT_N_215_65 = [15,86]

IB_N_215_65 = [15,111]

AI_N_215_65 = [15,211]

IT_E_230_75 = [15,87]

IB_E_230_75 = [15,112]

AI_E_230_75 = [15,212]

IT_E_230_90 = [15,88]

IB_E_230_90 = [15,113]

AI_E_230_90 = [15,213]

IT_E_235_45 = [15,89]

IB_E_235_45 = [15,114]

AI_E_235_45 = [15,214]

IT_E_240_30 = [15,90]

IB_E_240_30 = [15,115]

AI_E_240_30 = [15,215]

IT_E_250_65 = [15,91]

IB_E_250_65 = [15,116]

AI_E_250_65 = [15,216]

IT_E_250_90 = [15,92]

IB_E_250_90 = [15,117]

AI_E_250_90 = [15,217]

IT_E_265_30 = [15,93]

IB_E_265_30 = [15,118]

AI_E_265_30 = [15,218]

IT_E_270_45 = [15,94]

IB_E_270_45 = [15,119]

AI_E_270_45 = [15,219]

IT_E_275_75 = [15,95]

IB_E_275_75 = [15,120]

AI_E_275_75 = [15,220]

IT_E_275_90 = [15,96]

IB_E_275_90 = [15,121]

AI_E_275_90 = [15,221]

IT_E_290_10 = [15,97]

IB_E_290_10 = [15,122]

AI_E_290_10 = [15,222]

IT_E_290_25 = [15,98]

IB_E_290_25 = [15,123]

AI_E_290_25 = [15,223]

IT_E_290_50 = [15,99]

IB_E_290_50 = [15,124]

AI_E_290_50 = [15,224]

IT_E_290_65 = [15,100]

IB_E_290_65 = [15,125]

AI_E_290_65 = [15,225]

IT_E_300_75 = [15,101]

IB_E_300_75 = [15,126]

AI_E_300_75 = [15,226]

IT_E_300_90 = [15,102]

IB_E_300_90 = [15,127]

AI_E_300_90 = [15,227]

IT_E_305_45 = [15,103]

IB_E_305_45 = [15,128]

AI_E_305_45 = [15,228]

IT_E_310_30 = [15,104]

IB_E_310_30 = [15,129]

AI_E_310_30 = [15,229]

IT_E_310_65 = [15,105]

IB_E_310_65 = [15,130]

AI_E_310_65 = [15,230]

IT_S_315_55 = [15,106]

IB_S_315_55 = [15,131]

AI_S_315_55 = [15,231]

IT_S_325_75 = [15,107]

IB_S_325_75 = [15,132]

AI_S_325_75 = [15,232]

IT_S_325_90 = [15,108]

IB_S_325_90 = [15,133]

AI_S_325_90 = [15,233]

IT_S_330_90 = [15,109]

IB_S_330_90 = [15,134]

AI_S_330_90 = [15,234]

IT_S_335_55 = [15,110]

IB_S_335_55 = [15,135]

AI_S_335_55 = [15,235]

IT_S_335_65 = [15,111]

IB_S_335_65 = [15,136]

AI_S_335_65 = [15,236]

IT_S_340_30 = [15,112]

IB_S_340_30 = [15,137]

AI_S_340_30 = [15,237]

IT_S_345_45 = [15,113]

IB_S_345_45 = [15,138]

AI_S_345_45 = [15,238]

IT_S_350_70 = [15,114]

IB_S_350_70 = [15,139]

AI_S_350_70 = [15,239]

IT_S_350_90 = [15,115]

IB_S_350_90 = [15,140]

AI_S_350_90 = [15,240]

SOLAR_PANEL = [15,25]/max(1, [15,25])

*$UNIT_NAME Radiation

*$LAYER Main

*$POSITION 196 180

*--

* Model "Weather data" (Type 15)

*

UNIT 15 TYPE 15 Weather data

*$UNIT_NAME Weather data

*$MODEL .\Weather Data Reading and Processing\Standard Format\Canadian Weather

for Energy Calculations Files (CWEC)\Type15-5.tmf

*$POSITION 195 298

*$LAYER Main # #

PARAMETERS 279

5 ! 1 File Type

209 ! 2 Logical unit

5 ! 3 Tilted Surface Radiation Mode

0.2 ! 4 Ground reflectance - no snow

0.7 ! 5 Ground reflectance - snow cover

91 ! 6 Number of surfaces

1 ! 7 Tracking mode-1

0 ! 8 Slope of surface-1

AA_H_0_0 ! 9 Azimuth of surface-1

1 ! 10 Tracking mode-2

50 ! 11 Slope of surface-2

AA_S_0_50 ! 12 Azimuth of surface-2

1 ! 13 Tracking mode-3

25 ! 14 Slope of surface-3

AA_S_0_25 ! 15 Azimuth of surface-3

1 ! 16 Tracking mode-4

10 ! 17 Slope of surface-4

AA_S_0_10 ! 18 Azimuth of surface-4

```
1               ! 19 Tracking mode-5
65              ! 20 Slope of surface-5
AA_S_0_65           ! 21 Azimuth of surface-5
1               ! 22 Tracking mode-6
90              ! 23 Slope of surface-6
AA_S_5_90           ! 24 Azimuth of surface-6
1               ! 25 Tracking mode-7
70              ! 26 Slope of surface-7
AA_S_10_70          ! 27 Azimuth of surface-7
1               ! 28 Tracking mode-8
90              ! 29 Slope of surface-8
AA_S_10_90          ! 30 Azimuth of surface-8
1               ! 31 Tracking mode-9
45              ! 32 Slope of surface-9
AA_S_15_45          ! 33 Azimuth of surface-9
1               ! 34 Tracking mode-10
30              ! 35 Slope of surface-10
AA_S_20_30          ! 36 Azimuth of surface-10
1               ! 37 Tracking mode-11
55              ! 38 Slope of surface-11
AA_S_25_55          ! 39 Azimuth of surface-11
1               ! 40 Tracking mode-12
```

65 ! 41 Slope of surface-12

AA_S_25_65 ! 42 Azimuth of surface-12

1 ! 43 Tracking mode-13

75 ! 44 Slope of surface-13

AA_S_35_75 ! 45 Azimuth of surface-13

1 ! 46 Tracking mode-14

90 ! 47 Slope of surface-14

AA_S_35_90 ! 48 Azimuth of surface-14

1 ! 49 Tracking mode-15

55 ! 50 Slope of surface-15

AA_W_45_55 ! 51 Azimuth of surface-15

1 ! 52 Tracking mode-16

30 ! 53 Slope of surface-16

AA_W_50_30 ! 54 Azimuth of surface-16

1 ! 55 Tracking mode-17

65 ! 56 Slope of surface-17

AA_W_50_65 ! 57 Azimuth of surface-17

1 ! 58 Tracking mode-18

45 ! 59 Slope of surface-18

AA_W_55_45 ! 60 Azimuth of surface-18

1 ! 61 Tracking mode-19

75 ! 62 Slope of surface-19

AA_W_60_75 ! 63 Azimuth of surface-19

1 ! 64 Tracking mode-20

90 ! 65 Slope of surface-20

AA_W_60_90 ! 66 Azimuth of surface-20

1 ! 67 Tracking mode-21

50 ! 68 Slope of surface-21

AA_W_70_50 ! 69 Azimuth of surface-21

1 ! 70 Tracking mode-22

10 ! 71 Slope of surface-22

AA_W_70_10 ! 72 Azimuth of surface-22

1 ! 73 Tracking mode-23

25 ! 74 Slope of surface-23

AA_W_70_25 ! 75 Azimuth of surface-23

1 ! 76 Tracking mode-24

65 ! 77 Slope of surface-24

AA_W_70_65 ! 78 Azimuth of surface-24

1 ! 79 Tracking mode-25

90 ! 80 Slope of surface-25

AA_W_85_90 ! 81 Azimuth of surface-25

1 ! 82 Tracking mode-26

75 ! 83 Slope of surface-26

AA_W_85_75 ! 84 Azimuth of surface-26

1 ! 85 Tracking mode-27

45 ! 86 Slope of surface-27

AA_W_90_45 ! 87 Azimuth of surface-27

1 ! 88 Tracking mode-28

30 ! 89 Slope of surface-28

AA_W_95_30 ! 90 Azimuth of surface-28

1 ! 91 Tracking mode-29

70 ! 92 Slope of surface-29

AA_W_95_70 ! 93 Azimuth of surface-29

1 ! 94 Tracking mode-30

55 ! 95 Slope of surface-30

AA_W_100_55 ! 96 Azimuth of surface-30

1 ! 97 Tracking mode-31

75 ! 98 Slope of surface-31

AA_W_110_75 ! 99 Azimuth of surface-31

1 ! 100 Tracking mode-32

90 ! 101 Slope of surface-32

AA_W_110_90 ! 102 Azimuth of surface-32

1 ! 103 Tracking mode-33

55 ! 104 Slope of surface-33

AA_W_115_55 ! 105 Azimuth of surface-33

1 ! 106 Tracking mode-34

30 ! 107 Slope of surface-34

AA_W_120_30 ! 108 Azimuth of surface-34

1 ! 109 Tracking mode-35

70 ! 110 Slope of surface-35

AA_W_120_70 ! 111 Azimuth of surface-35

1 ! 112 Tracking mode-36

45 ! 113 Slope of surface-36

AA_W_125_45 ! 114 Azimuth of surface-36

1 ! 115 Tracking mode-37

75 ! 116 Slope of surface-37

AA_W_130_75 ! 117 Azimuth of surface-37

1 ! 118 Tracking mode-38

90 ! 119 Slope of surface-38

AA_N_135_90 ! 120 Azimuth of surface-38

1 ! 121 Tracking mode-39

50 ! 122 Slope of surface-39

AA_N_145_50 ! 123 Azimuth of surface-39

1 ! 124 Tracking mode-40

25 ! 125 Slope of surface-40

AA_N_145_25 ! 126 Azimuth of surface-40

1 ! 127 Tracking mode-41

10 ! 128 Slope of surface-41

AA_N_145_10 ! 129 Azimuth of surface-41

1 ! 130 Tracking mode-42

65 ! 131 Slope of surface-42

AA_N_145_65 ! 132 Azimuth of surface-42

1 ! 133 Tracking mode-43

75 ! 134 Slope of surface-43

AA_N_155_75 ! 135 Azimuth of surface-43

1 ! 136 Tracking mode-44

90 ! 137 Slope of surface-44

AA_N_155_90 ! 138 Azimuth of surface-44

1 ! 139 Tracking mode-45

45 ! 140 Slope of surface-45

AA_N_160_45 ! 141 Azimuth of surface-45

1 ! 142 Tracking mode-46

90 ! 143 Slope of surface-46

AA_N_160_90 ! 144 Azimuth of surface-46

1 ! 145 Tracking mode-47

30 ! 146 Slope of surface-47

AA_N_165_30 ! 147 Azimuth of surface-47

1 ! 148 Tracking mode-48

70 ! 149 Slope of surface-48

AA_N_165_70 ! 150 Azimuth of surface-48

1 ! 151 Tracking mode-49

55 ! 152 Slope of surface-49

AA_N_170_55 ! 153 Azimuth of surface-49

1 ! 154 Tracking mode-50

90 ! 155 Slope of surface-50

AA_N_175_90 ! 156 Azimuth of surface-50

1 ! 157 Tracking mode-51

75 ! 158 Slope of surface-51

AA_N_180_75 ! 159 Azimuth of surface-51

1 ! 160 Tracking mode-52

90 ! 161 Slope of surface-52

AA_N_180_90 ! 162 Azimuth of surface-52

1 ! 163 Tracking mode-53

55 ! 164 Slope of surface-53

AA_N_190_55 ! 165 Azimuth of surface-53

1 ! 166 Tracking mode-54

30 ! 167 Slope of surface-54

AA_N_195_30 ! 168 Azimuth of surface-54

1 ! 169 Tracking mode-55

70 ! 170 Slope of surface-55

AA_N_195_70 ! 171 Azimuth of surface-55

1 ! 172 Tracking mode-56

45 ! 173 Slope of surface-56

AA_N_200_45 ! 174 Azimuth of surface-56

1 ! 175 Tracking mode-57

75 ! 176 Slope of surface-57

AA_N_205_75 ! 177 Azimuth of surface-57

1 ! 178 Tracking mode-58

90 ! 179 Slope of surface-58

AA_N_205_90 ! 180 Azimuth of surface-58

1 ! 181 Tracking mode-59

50 ! 182 Slope of surface-59

AA_N_215_50 ! 183 Azimuth of surface-59

1 ! 184 Tracking mode-60

25 ! 185 Slope of surface-60

AA_N_215_25 ! 186 Azimuth of surface-60

1 ! 187 Tracking mode-61

10 ! 188 Slope of surface-61

AA_N_215_10 ! 189 Azimuth of surface-61

1 ! 190 Tracking mode-62

65 ! 191 Slope of surface-62

AA_N_215_65 ! 192 Azimuth of surface-62

1 ! 193 Tracking mode-63

75 ! 194 Slope of surface-63

AA_E_230_75 ! 195 Azimuth of surface-63

1 ! 196 Tracking mode-64

90 ! 197 Slope of surface-64

AA_E_230_90 ! 198 Azimuth of surface-64

1 ! 199 Tracking mode-65

45 ! 200 Slope of surface-65

AA_E_235_45 ! 201 Azimuth of surface-65

1 ! 202 Tracking mode-66

30 ! 203 Slope of surface-66

AA_E_240_30 ! 204 Azimuth of surface-66

1 ! 205 Tracking mode-67

65 ! 206 Slope of surface-67

AA_E_250_65 ! 207 Azimuth of surface-67

1 ! 208 Tracking mode-68

90 ! 209 Slope of surface-68

AA_E_250_90 ! 210 Azimuth of surface-68

1 ! 211 Tracking mode-69

30 ! 212 Slope of surface-69

AA_E_265_30 ! 213 Azimuth of surface-69

1 ! 214 Tracking mode-70

45 ! 215 Slope of surface-70

AA_E_270_45 ! 216 Azimuth of surface-70

1 ! 217 Tracking mode-71

75 ! 218 Slope of surface-71

AA_E_275_75 ! 219 Azimuth of surface-71

1 ! 220 Tracking mode-72

90 ! 221 Slope of surface-72

AA_E_275_90 ! 222 Azimuth of surface-72

1 ! 223 Tracking mode-73

10 ! 224 Slope of surface-73

AA_E_290_10 ! 225 Azimuth of surface-73

1 ! 226 Tracking mode-74

25 ! 227 Slope of surface-74

AA_E_290_25 ! 228 Azimuth of surface-74

1 ! 229 Tracking mode-75

50 ! 230 Slope of surface-75

AA_E_290_50 ! 231 Azimuth of surface-75

1 ! 232 Tracking mode-76

65 ! 233 Slope of surface-76

AA_E_290_65 ! 234 Azimuth of surface-76

1 ! 235 Tracking mode-77

75 ! 236 Slope of surface-77

AA_E_300_75 ! 237 Azimuth of surface-77

1 ! 238 Tracking mode-78

90 ! 239 Slope of surface-78

AA_E_300_90 ! 240 Azimuth of surface-78

1 ! 241 Tracking mode-79

45 ! 242 Slope of surface-79

AA_E_305_45 ! 243 Azimuth of surface-79

1 ! 244 Tracking mode-80

30 ! 245 Slope of surface-80

AA_E_310_30 ! 246 Azimuth of surface-80

1 ! 247 Tracking mode-81

65 ! 248 Slope of surface-81

AA_E_310_65 ! 249 Azimuth of surface-81

1 ! 250 Tracking mode-82

55 ! 251 Slope of surface-82

AA_S_315_55 ! 252 Azimuth of surface-82

1 ! 253 Tracking mode-83

75 ! 254 Slope of surface-83

AA_S_325_75 ! 255 Azimuth of surface-83

1 ! 256 Tracking mode-84

90 ! 257 Slope of surface-84

AA_S_325_90 ! 258 Azimuth of surface-84

1 ! 259 Tracking mode-85

90 ! 260 Slope of surface-85

AA_S_330_90 ! 261 Azimuth of surface-85

1 ! 262 Tracking mode-86

55 ! 263 Slope of surface-86

AA_S_335_55 ! 264 Azimuth of surface-86

1 ! 265 Tracking mode-87

65 ! 266 Slope of surface-87

AA_S_335_65 ! 267 Azimuth of surface-87

1 ! 268 Tracking mode-88

30 ! 269 Slope of surface-88

AA_S_340_30 ! 270 Azimuth of surface-88

1 ! 271 Tracking mode-89

45 ! 272 Slope of surface-89

AA_S_345_45 ! 273 Azimuth of surface-89

1 ! 274 Tracking mode-90

70 ! 275 Slope of surface-90

AA_S_350_70 ! 276 Azimuth of surface-90

1 ! 277 Tracking mode-91

90 ! 278 Slope of surface-91

AA_S_350_90 ! 279 Azimuth of surface-91

*** External files

ASSIGN "C:\Users\pclau_000\Dropbox\Thesis\TRNSYS\Ottawa CWEC Data 2014-2015\CAN_ON_Ottawa.716280_CWEC.epw" 209

```
*|? Which file contains the CWEC weather data? |1000
*-------------------------------------------------------------------------------


* Model "Building" (Type 56)
*


UNIT 56 TYPE 56          Building
*$UNIT_NAME Building
*$MODEL .\Loads and Structures\Multi-Zone Building\Type56.tmf
*$POSITION 483 173
*$LAYER Main # # #
*$#
PARAMETERS 3
210             ! 1 Logical unit for building description file (.bui)
1               ! 2 Star network calculation switch
0.5             ! 3 Weighting factor for operative temperature
INPUTS 15
15,1            ! Weather data:Dry bulb temperature -> 1- TAMB
15,7            ! Weather data:Percent relative humidity -> 2- RELHUMAMB
15,4            ! Weather data:Effective sky temperature -> 3- TSKY
15,1            ! Weather data:Dry bulb temperature -> 4- TSGRD
15,16           ! Weather data:Solar zenith angle -> 5- AZEN
```

```
AAZM_TYPE56          ! AzimuthAngles:AAZM_TYPE56 -> 6- AAZM
0,0                  ! [unconnected]  7- GRDREF
0,0                  ! [unconnected]  8- TGROUND
0,0                  ! [unconnected]  9- TBOUNDARY
0,0                  ! [unconnected]  10- BRIGHT
0,0                  ! [unconnected]  11- SHADE_CLOSE
0,0                  ! [unconnected]  12- SHADE_OPEN
0,0                  ! [unconnected]  13- MAX_ISHADE
0,0                  ! [unconnected]  14- MAX_ESHADE
SOLAR_PANEL          ! Radiation:SOLAR_PANEL -> 15- SOLAR_VENT
*** INITIAL INPUT VALUES
0 0 0 0 0 0 0 0 0 0 0 0 0 0 0
*** External files
ASSIGN "July_28_E.b17" 210
*|? Building description file (*.bui) |1000
*--------------------------------------------------------------------------


* Model "Irradiation" (Type 65)
*


UNIT 65 TYPE 65         Irradiation
*$UNIT_NAME Irradiation
```

```
*$MODEL .\Output\Online Plotter\Online Plotter Without File\Type65d.tmf
*$POSITION 317 223
*$LAYER Main # # #
PARAMETERS 12
1               ! 1 Nb. of left-axis variables
1               ! 2 Nb. of right-axis variables
0               ! 3 Left axis minimum
3600            ! 4 Left axis maximum
0               ! 5 Right axis minimum
3600            ! 6 Right axis maximum
1               ! 7 Number of plots per simulation
12              ! 8 X-axis gridpoints
0               ! 9 Shut off Online w/o removing
-1              ! 10 Logical unit for output file
0               ! 11 Output file units
0               ! 12 Output file delimiter
INPUTS 2
IT_H_0_0            ! Radiation:IT_H_0_0 ->Left axis variable
IB_H_0_0            ! Radiation:IB_H_0_0 ->Right axis variable
*** INITIAL INPUT VALUES
IT_H_0_0 IB_H_0_0
LABELS  3
```

"Total Incident Solar Radition [kJ/hr m²]"

"Beam Incident Solar Radition [kJ/hr m²]"

"Irradition"

*---

* Model "Temperature" (Type 65)

*

UNIT 66 TYPE 65 Temperature

*$UNIT_NAME Temperature

*$MODEL .\Output\Online Plotter\Online Plotter Without File\Type65d.tmf

*$POSITION 449 298

*$LAYER Main # # #

PARAMETERS 12

1 ! 1 Nb. of left-axis variables

2 ! 2 Nb. of right-axis variables

-20 ! 3 Left axis minimum

35 ! 4 Left axis maximum

-20 ! 5 Right axis minimum

35 ! 6 Right axis maximum

1 ! 7 Number of plots per simulation

12 ! 8 X-axis gridpoints

0 ! 9 Shut off Online w/o removing

-1 ! 10 Logical unit for output file

```
0                ! 11 Output file units
0                ! 12 Output file delimiter
INPUTS 3
15,1             ! Weather data:Dry bulb temperature ->Left axis variable
56,16            ! Building: 16- TAIR_DOME ->Right axis variable-1
56,1             ! Building: 1- TAIR_WATER_TANK ->Right axis variable-2
*** INITIAL INPUT VALUES
Tamb DOME DOME
LABELS  3
"Temperatures    [deg C]"
"Temperatures    [deg C]"
"Temperatures"
*-------------------------------------------------------------------------------
* Model "System_Printer" (Type 25)
*
UNIT 9 TYPE 25           System_Printer
*$UNIT_NAME System_Printer
*$MODEL \Trnsys17\Studio\lib\System_Output\Type25a.tmf
*$POSITION 328 106
*$LAYER OutputSystem #
PARAMETERS 10
STEP             ! 1 Printing interval
```

```
START          ! 2 Start time
STOP           ! 3 Stop time
211            ! 4 Logical unit
2              ! 5 Units printing mode
0              ! 6 Relative or absolute start time
-1             ! 7 Overwrite or Append
-1             ! 8 Print header
0              ! 9 Delimiter
1              ! 10 Print labels
INPUTS 31
56,1           ! Building: 1- TAIR_WATER_TANK ->Input to be printed-1
56,2           ! Building: 2- TAIR_B1 ->Input to be printed-2
56,3           ! Building: 3- TAIR_B2 ->Input to be printed-3
56,4           ! Building: 4- TAIR_B3 ->Input to be printed-4
56,5           ! Building: 5- TAIR_B4 ->Input to be printed-5
56,6           ! Building: 6- TAIR_B5 ->Input to be printed-6
56,7           ! Building: 7- TAIR_B6 ->Input to be printed-7
56,8           ! Building: 8- TAIR_B7 ->Input to be printed-8
56,9           ! Building: 9- TAIR_B8 ->Input to be printed-9
56,10          ! Building: 10- TAIR_B9 ->Input to be printed-10
56,11          ! Building: 11- TAIR_B10 ->Input to be printed-11
56,12          ! Building: 12- TAIR_B11 ->Input to be printed-12
```

56,13 ! Building: 13- TAIR_B12 ->Input to be printed-13

56,14 ! Building: 14- TAIR_B13 ->Input to be printed-14

56,15 ! Building: 15- TAIR_B14 ->Input to be printed-15

56,16 ! Building: 16- TAIR_DOME ->Input to be printed-16

56,17 ! Building: 17- TAIR_DOOR_BOTTOM ->Input to be printed-17

56,18 ! Building: 18- TAIR_C6 ->Input to be printed-18

56,19 ! Building: 19- TAIR_C5 ->Input to be printed-19

56,20 ! Building: 20- TAIR_C4 ->Input to be printed-20

56,21 ! Building: 21- TAIR_C3 ->Input to be printed-21

56,22 ! Building: 22- TAIR_C2 ->Input to be printed-22

56,23 ! Building: 23- TAIR_C1 ->Input to be printed-23

56,24 ! Building: 24- TAIR_C14 ->Input to be printed-24

56,25 ! Building: 25- TAIR_C8 ->Input to be printed-25

56,26 ! Building: 26- TAIR_C9 ->Input to be printed-26

56,27 ! Building: 27- TAIR_C10 ->Input to be printed-27

56,28 ! Building: 28- TAIR_C11 ->Input to be printed-28

56,29 ! Building: 29- TAIR_C12 ->Input to be printed-29

56,30 ! Building: 30- TAIR_C13 ->Input to be printed-30

IT_S_0_50 ! Radiation:IT_S_0_50 ->Input to be printed-31

*** INITIAL INPUT VALUES

TAIR_WATER_TANK T_B1 T_B2 T_B3 T_B4 T_B5 T_B6 T_B7 T_B8 T_B9 T_B10 T_B11

T_B12 T_B13 T_B14 T_DOME T_DOOR T_C6 T_C5 T_C4 T_C3 T_C2 T_C1 T_C14 T_C8

T_C9 T_C10 T_C11 T_C12 T_C13 SOLAR_VENT_RAD

*** External files

ASSIGN "Type25a.txt" 211

*|? Which file should contain the printed results? You can use the deck filename by entering "***", e.g. "***.out", or "***.dat" |1000

*--

END

Appendix C: Arduino Program

```
/*-(Import required libraries)-*/
#include <Time.h>
#include <Wire.h>
#include <SPI.h>
#include <SD.h>
#include <OneWire.h>
#include <DallasTemperature.h>
#include <DHT.h>
#include <LowPower.h>
#include <DS3232RTC.h> //source: https://github.com/JChristensen/DS3232RTC

/*-( Declare Constants )-*/
#define ECHO_TO_SERIAL 1 // echo data to serial port for SD card reader
const int wakeUpPin = 2;
#define greenLEDpin 3
#define redLEDpin 4
#define RELAY_1 5
#define DHT1PIN 6 //DHT22 humidity and temperature sensor on digital pin 6
#define DHT2PIN 7 //DHT22 humidity and temperature sensor on digital pin 7
#define ONE_WIRE_BUS 8 // All thermocouples using 1-Wire protocol on digital pin 8
#define RELAY_2 9
const int chipSelect = 10;
#define DHTTYPE DHT22
#define RELAY_ON HIGH
#define RELAY_OFF LOW
#define resolution 5

//*-( Declare objects )-*
DHT dht1(DHT1PIN, DHTTYPE);
DHT dht2(DHT2PIN, DHTTYPE);
OneWire oneWire(ONE_WIRE_BUS);
DallasTemperature sensors(&oneWire);

//hardware address of each thermocouple
byte tc1[8] = {0x3B, 0x1A, 0x30, 0x18, 0x0, 0x0, 0x0, 0x96}; //#1
byte tc2[8] = {0x3B, 0x41, 0x2D, 0x18, 0x0, 0x0, 0x0, 0xD0}; //#2
byte tc3[8] = {0x3B, 0xF2, 0x32, 0x18, 0x0, 0x0, 0x0, 0x9D}; //#3
byte tc4[8] = {0x3B, 0x51, 0x2D, 0x18, 0x0, 0x0, 0x0, 0x8B}; //#4
byte tc5[8] = {0x3B, 0xC0, 0x27, 0x18, 0x0, 0x0, 0x0, 0xB0}; //#5
byte tc6[8] = {0x3B, 0xE0, 0x27, 0x18, 0x0, 0x0, 0x0, 0x06}; //#6
```

```
byte tc7[8] = {0x3B, 0x05, 0x2E, 0x18, 0x0, 0x0, 0x0, 0x37}; //#7
byte tc8[8] = {0x3B, 0xC4, 0x2F, 0x18, 0x0, 0x0, 0x0, 0x52}; //#8
byte tc9[8] = {0x3B, 0x07, 0x32, 0x18, 0x0, 0x0, 0x0, 0x04}; //#9
byte tc10[8] = {0x3B, 0xD3, 0x2B, 0x18, 0x0, 0x0, 0x0, 0x93}; //#10
byte tc11[8] = {0x3B, 0x47, 0x2B, 0x18, 0x0, 0x0, 0x0, 0xFE}; //#11
byte tc12[8] = {0x3B, 0xA2, 0x2B, 0x18, 0x0, 0x0, 0x0, 0x3C}; //#12
byte tc13[8] = {0x3B, 0x2F, 0x30, 0x18, 0x0, 0x0, 0x0, 0x90}; //#13
byte tc14[8] = {0x3B, 0xC7, 0x2F, 0x18, 0x0, 0x0, 0x0, 0x0B}; //#14
byte tc15[8] = {0x3B, 0x12, 0x2C, 0x18, 0x0, 0x0, 0x0, 0x6A}; //#15
byte tc16[8] = {0x3B, 0x6E, 0x6F, 0x18, 0x0, 0x0, 0x0, 0x28}; //#16
byte tc18[8] = {0x3B, 0x31, 0x76, 0x18, 0x0, 0x0, 0x0, 0xAD}; //#18
byte tc19[8] = {0x3B, 0x27, 0x32, 0x18, 0x0, 0x0, 0x0, 0xB2}; //#19
byte tc20[8] = {0x3B, 0xB2, 0x6C, 0x18, 0x0, 0x0, 0x0, 0xDF}; //#20
byte tc21[8] = {0x3B, 0x35, 0x76, 0x18, 0x0, 0x0, 0x0, 0x71}; //#21
byte tc22[8] = {0x3B, 0x19, 0x6C, 0x18, 0x0, 0x0, 0x0, 0x7B}; //#22
byte tc23[8] = {0x3B, 0x97, 0x76, 0x18, 0x0, 0x0, 0x0, 0x43}; //#23
//SD CARD
File logfile;

/*-(Declare Variables)-*/
time_t t;
int nextLoop;
int Fan_1;
int Fan_2;

/****** SETUP: RUNS ONCE ******/
void setup()
{
  Serial.begin(9600);
  Serial.println("Relays off to start");
  //(set pins as outputs )
  pinMode(RELAY_1, OUTPUT);
  pinMode(RELAY_2, OUTPUT);
  //( Initialize Pins so relays are inactive at reset)
  digitalWrite(RELAY_1, RELAY_OFF);
  digitalWrite(RELAY_2, RELAY_OFF);
  Fan_1 = 0;
  Fan_2 = 0;

  Serial.println();
  Wire.begin();
  setSyncProvider(RTC.get);
  Serial.print("Initializing SD card...");
  pinMode(10, OUTPUT);
```

```
 pinMode(wakeUpPin, INPUT);
 // see if the card is present and can be initialized:
 if (!SD.begin(chipSelect)) {
  Serial.println("Card failed, or not present");
  // don't do anything more:
  return;
 }
 Serial.println("card initialized.");
 //define filename
 char filename[] = "LOGGER00.CSV";
 for (uint8_t i = 0; i < 100; i++) {
  filename[6] = i / 10 + '0';
  filename[7] = i % 10 + '0';
  Serial.println(filename);
  if (!SD.exists(filename)) {
   // only open a new file if it doesn't exist
   logfile = SD.open(filename, FILE_WRITE);
   break;  // leave the loop!
  }
 }
 if (!logfile) {
  error("could not create file");
 }
 t = RTC.get();
  Serial.print("Logging to: ");
 Serial.println(filename);

logfile.println("date,hour,min,sec,tc-1,tc-2,tc-3,tc-4,tc-5,tc-6,tc-7,tc-8,tc-9,tc-10,tc-11,tc-
12,tc-13,tc-14,tc-15,tc-16,tc-18,tc-19,tc-20,tc-21,tc-22,tc-23,dht-1h,dht-1t,dht-2h,dht-
2t,Fan_1, Fan_2");
#if ECHO_TO_SERIAL
 Serial.println("date,hour,min,sec,tc-1,tc-2,tc-3,tc-4,tc-5,tc-6,tc-7,tc-8,tc-9,tc-10,tc-
11,tc-12,tc-13,tc-14,tc-15,tc-16,tc-18,tc-19,tc-20,tc-21,tc-22,tc-23,dht-1h,dht-1t,dht-
2h,dht-2t,Fan_1, Fan_2");
#endif

 pinMode(redLEDpin, OUTPUT);
 pinMode(greenLEDpin, OUTPUT);

 nextLoop = ((minute(RTC.get()) / resolution) + 1) * resolution;
 if (nextLoop >= 60) {
  nextLoop -= 60;
 }
 Serial.print(RTC.temperature());
```

```
  Serial.print(",");
  Serial.print(RTC.oscStopped());
  Serial.print(",");
  Serial.println(nextLoop);

  sensors.begin();
  dht1.begin();
  dht2.begin();
}

/****** LOOP: RUNS CONSTANTLY ******/
void loop()
{
  t = RTC.get();
  sensors.requestTemperatures(); // Send the command to get temperatures
  digitalWrite(greenLEDpin, HIGH);
  logfile.print(year(t), DEC);
  logfile.print("/");
  logfile.print(month(t), DEC);
  logfile.print("/");
  logfile.print(day(t), DEC);
  logfile.print(",");
  logfile.print(hour(t), DEC);
  logfile.print(",");
  logfile.print(minute(t), DEC);
  logfile.print(",");
  logfile.print(second(t), DEC);
  logfile.print(",");
  logfile.print(sensors.getTempC(tc1)); logfile.print(",");
  logfile.print(sensors.getTempC(tc2)); logfile.print(",");
  logfile.print(sensors.getTempC(tc3)); logfile.print(",");
  logfile.print(sensors.getTempC(tc4)); logfile.print(",");
  logfile.print(sensors.getTempC(tc5)); logfile.print(",");
  logfile.print(sensors.getTempC(tc6)); logfile.print(",");
  logfile.print(sensors.getTempC(tc7)); logfile.print(",");
  logfile.print(sensors.getTempC(tc8)); logfile.print(",");
  logfile.print(sensors.getTempC(tc9)); logfile.print(",");
  logfile.print(sensors.getTempC(tc10)); logfile.print(",");
  logfile.print(sensors.getTempC(tc11)); logfile.print(",");
  logfile.print(sensors.getTempC(tc12)); logfile.print(",");
  logfile.print(sensors.getTempC(tc13)); logfile.print(",");
  logfile.print(sensors.getTempC(tc14)); logfile.print(",");
  logfile.print(sensors.getTempC(tc15)); logfile.print(",");
  logfile.print(sensors.getTempC(tc16)); logfile.print(",");
```

```
  logfile.print(sensors.getTempC(tc18)); logfile.print(",");
  logfile.print(sensors.getTempC(tc19)); logfile.print(",");
  logfile.print(sensors.getTempC(tc20)); logfile.print(",");
  logfile.print(sensors.getTempC(tc21)); logfile.print(",");
  logfile.print(sensors.getTempC(tc22)); logfile.print(",");
  logfile.print(sensors.getTempC(tc23)); logfile.print(",");
  logfile.print(dht1.readHumidity()); logfile.print(",");
  logfile.print(dht1.readTemperature()); logfile.print(",");
  logfile.print(dht2.readHumidity()); logfile.print(",");
  logfile.print(dht2.readTemperature()); logfile.print(",");
  if ((sensors.getTempC(tc13)) >= 15) {
   digitalWrite(RELAY_1, RELAY_ON);
   Serial.println("Fan 1 is on");
   Fan_1 = 1;
  }
  else {
   digitalWrite(RELAY_1, RELAY_OFF);
   Serial.println("Fan 1 is off");
   Fan_1 = 0;
  }
  if ((sensors.getTempC(tc13)) >= 20) {
   digitalWrite(RELAY_2, RELAY_ON);
   Serial.println("Fan 2 is on");
   Fan_2 = 1;
  }
  else {
   digitalWrite(RELAY_2, RELAY_OFF);
   Serial.println("Fan 2 is off");
   Fan_2 = 0;
  }
  logfile.print(Fan_1, DEC);
  logfile.print(",");
  logfile.print(Fan_2, DEC);
  logfile.println();

#if ECHO_TO_SERIAL
  Serial.print(year(t), DEC);
  Serial.print("/");
  Serial.print(month(t), DEC);
  Serial.print("/");
  Serial.print(day(t), DEC);
  Serial.print(",");
  Serial.print(hour(t), DEC);
  Serial.print(",");
```

```
  Serial.print(minute(t), DEC);
  Serial.print(",");
  Serial.print(second(t), DEC);
  Serial.print(",");
  Serial.print(sensors.getTempC(tc1)); Serial.print(",");
  Serial.print(sensors.getTempC(tc2)); Serial.print(",");
  Serial.print(sensors.getTempC(tc3)); Serial.print(",");
  Serial.print(sensors.getTempC(tc4)); Serial.print(",");
  Serial.print(sensors.getTempC(tc5)); Serial.print(",");
  Serial.print(sensors.getTempC(tc6)); Serial.print(",");
  Serial.print(sensors.getTempC(tc7)); Serial.print(",");
  Serial.print(sensors.getTempC(tc8)); Serial.print(",");
  Serial.print(sensors.getTempC(tc9)); Serial.print(",");
  Serial.print(sensors.getTempC(tc10)); Serial.print(",");
  Serial.print(sensors.getTempC(tc11)); Serial.print(",");
  Serial.print(sensors.getTempC(tc12)); Serial.print(",");
  Serial.print(sensors.getTempC(tc13)); Serial.print(",");
  Serial.print(sensors.getTempC(tc14)); Serial.print(",");
  Serial.print(sensors.getTempC(tc15)); Serial.print(",");
  Serial.print(sensors.getTempC(tc16)); Serial.print(",");
  Serial.print(sensors.getTempC(tc18)); Serial.print(",");
  Serial.print(sensors.getTempC(tc19)); Serial.print(",");
  Serial.print(sensors.getTempC(tc20)); Serial.print(",");
  Serial.print(sensors.getTempC(tc21)); Serial.print(",");
  Serial.print(sensors.getTempC(tc22)); Serial.print(",");
  Serial.print(sensors.getTempC(tc23)); Serial.print(",");
  Serial.print(dht1.readHumidity()); Serial.print(",");
  Serial.print(dht1.readTemperature()); Serial.print(",");
  Serial.print(dht2.readHumidity()); Serial.print(",");
  Serial.print(dht2.readTemperature()); Serial.print(",");
  Serial.print(Fan_1, DEC);  Serial.print(",");
  Serial.print(Fan_2, DEC);
  Serial.println();
#endif //ECHO_TO_SERIAL

  digitalWrite(greenLEDpin, LOW);

  delay(1000);
  digitalWrite(redLEDpin, HIGH);
  logfile.flush();
  digitalWrite(redLEDpin, LOW);

  delay(1000);
  goToSleep();
```

```
}
void goToSleep(void) {
  RTC.setAlarm(ALM2_MATCH_MINUTES, nextLoop, 1, 1);
  RTC.alarmInterrupt(ALARM_2, true);
  attachInterrupt(0, wakeUp, LOW);

  LowPower.powerDown(SLEEP_FOREVER, ADC_OFF, BOD_OFF);
  detachInterrupt(0);
  RTC.alarm(ALARM_2);
  nextLoop += resolution;
  if (nextLoop >= 60) {
    nextLoop -= 60;
  }
}
void wakeUp()
  // Handler for the pin interrupt.
void error(char *str)
{
  Serial.print("error: ");
  Serial.println(str);
  // red LED indicates error
  digitalWrite(redLEDpin, HIGH);
  while (1);
}
```